ON COATING DURABILITY OF POLYMER COATED SHEET METAL UNDER PLASTIC DEFORMATION

A Dissertation

by

YU-HSUAN HUANG

Submitted to the Office of Graduate Studies of
Texas A&M University
in partial fulfillment of the requirements for the degree of

DOCTOR OF PHILOSOPHY

May 2010

Major Subject: Mechanical Engineering

ON COATING DURABILITY OF POLYMER COATED SHEET METAL UNDER PLASTIC DEFORMATION

A Dissertation

by

YU-HSUAN HUANG

Submitted to the Office of Graduate Studies of
Texas A&M University
in partial fulfillment of the requirements for the degree of

DOCTOR OF PHILOSOPHY

Approved by:

Chair of Committee,	Jyhwen Wang
Committee Members,	Xin-Lin Gao
	Ibrahim Karaman
	Yu Ding
Head of Department,	Dennis O'Neal

May 2010

Major Subject: Mechanical Engineering

ABSTRACT

On Coating Durability of Polymer Coated Sheet Metal Under Plastic Deformation.

(May 2010)

Yu-Hsuan Huang, B.S., Cheng-Kung University;

M.S., Tsing-Hua University

Chair of Advisory Committee: Dr. Jyhwen Wang

Polymer coated sheet metal components find diverse applications in many industries. The manufacturing of the components generally involves forming of sheet metal into the desired shape and coating of the formed part with organic coating. An alternative manufacturing route is to coat the sheet metal first before forming. The change in the manufacturing sequence can potentially improve cost and reduce environmental impact. This approach, however, requires the coating to survive the deformation process. Thus, the effect of plastic deformation on coating adhesion is of primary interest to many engineers and researchers.

This research aims at developing a methodology to predict the adhesion of coating after metal forming processes. A pull-off apparatus that measures the coating pull-off stress was used to indicate the coating adhesion strength. Several types of specimen were designed to obtain uniaxial tension, biaxial tension, and tension-compression deformation modes on pre-coated sheet by using a uniaxial tensile tester. Experimental results from two selected polymer coated sheet metals show that coating

adhesion was affected by plastic deformation. An analytical model based on a virtual interface crack concept was developed to indicate the adhesion potential of the coating-substrate interface. From interfacial fracture mechanics, the initial adhesion potential is defined as the energy release rate characterized by the virtual interface crack and the initial pull-off stress. The analytical model was used to predict coating adhesion loss after deformation in uniaxial tension mode. The analytical model predictions agreed well with experimental results. Finite element analysis tool was applied to simulate more complex deformation modes in stamping of coated sheet meals. The stress field near the interface crack tip was used to calculate the energy release rate and predict the adhesion loss under different deformation modes. The predictions obtained from numerical method are also in good agreements with the experimental results in biaxial tension and tension-compression modes.

The research has led to a better understanding of the effects of plastic deformation on coating adhesion. The developed adhesion test methods can be used to generate useful information on coating durability for diverse practical use. It is also expected that the results of the research will facilitate the development of better polymer coated sheet metal to be used in sheet metal forming processes.

DEDICATION

This dissertation is dedicated to my father, Che-Hsiung, my mother, Tsai-Yun, and my wife Chiao-Yun for their patience and unconditional support.

ACKNOWLEDGEMENTS

My very sincere gratitude goes to Dr. Jyhwen Wang, the chairman of my advisory committee, for his valuable guidance and support. I would also like to express my appreciation to committee members, Dr. Xin-Lin Gao, Dr. Ibrahim Karaman and Dr. Yu Ding for providing insightful comments on my dissertation.

I would like to show my deepest appreciation to my family, for their endless love, support, and encouragement. I would like to thank all the past and current students in our department who provided advice and encouragement.

My special thanks go to my friends and colleagues, Wei Yang, Liang Zhang, and Yu Han, for their friendship and helpful advice for this dissertation.

TABLE OF CONTENTS

Page

LIST OF FIGURES

Page

Page

Page

Page

LIST OF TABLES

1. INTRODUCTION

Each year more than 60 million tons of flat-rolled metal is consumed in North America. This sheet metal has diverse application in various industries. In the construction industry, metal sheets are used for residential doors, metal roofs, wall panels, and air-conditioning ductwork. In the automotive industry, parts such as closure panels, body-in-whites, fuel tanks, and oil filter shells are produced almost entirely from metal sheets. In the packaging industry, sheet metals are used to manufacture steel drums, tin gift boxes, and food and beverage cans. The appliance industry produces refrigerators, ovens, washers, dryers, vending machines, and foodservice equipments from sheet metals. Consumer products such as furniture (e.g. desk and cabinet) and computers (e.g. chassis) also consist of sheet metal parts.

Parts fabricated from sheet metal are generally coated with polymer coating for functional, surface protection, and decoration purposes. For example, organic coatings are required for food and beverage packaging to prevent food-metal interaction. Metal doors and roofs are coated with various colors for aesthetic purpose. Automotive parts are mostly coated with multiple layers of paint for aesthetic and corrosion protection. For all purposes, the traditional manufacturing processes for sheet metal involve the sequence of forming sheet metal into a desired shape followed by the application of coating or paint.

This dissertation follows the style of *International Journal of Adhesion and Adhesive.*

The polymer resin in coating is delivered by dissolving the polymer in a carrier fluid. After coating is applied, parts are then placed in an oven for the coating to cure. The organic solvent contains toxic substance. In many cases, gaseous volatile organic compounds (VOCs) are generated during curing. The process also produces large amount of waste water. As a result, such coating process becomes a serious environmental concern [1]. To meet the environmental standards and health regulations passed by the governments around the world, the manufacturers need to maintain and improve their in-house painting lines with increasing cost. Furthermore, issues such as parts stoppage caused by painting, drying, curing, transporting, and coating defects due to dirt and oil residue on the surface of deformed metal parts can create significant bottlenecks and quality problems.

An efficient alternative is to use pre-painted materials from sheets or coil coating for metal forming processes. The coil coating process was invented to assist the Venetian blinds manufacturers in the 1940s. Now, the coil coating process could reduce VOCs emissions and prevent the formation of hazardous wastes with its highly automated and continuous process [2, 3]. As shown in Figure 1, a typical coil coating line consists of several basic operations, including unwinding a metal coil, cleaning and treating surfaces, applying and curing primer, applying and curing of the finish coat, and rewinding the coil. Today's coil coating process is operated in a large, complex, and sophisticated fabrication line with machines costing upwards of $ 30 million US and stretching more than a mile long. The coil coating lines can operate 24 hours a day and are able to treat more than 4,500 tons of steel or 2,250 tons of aluminum per week. The

coating thickness can be accurately controlled during the process, which ensures consistent chemical and mechanical properties of the coating. Since the coil coating is a continuous process that produces materials with consistent coating quality, the products can have strong resistance against harsh weather and corrosive environments. Coil coating lines are not limited to painting, but could also be used for printing, embossing, coining, laminating and even applying lubricant on sheet metal surfaces. Compared to the batch type of post-forming painting process, the coil coating provides a higher quality of coating adhesion and a variety of coating types, while resulting less impact on the environment [4, 5].

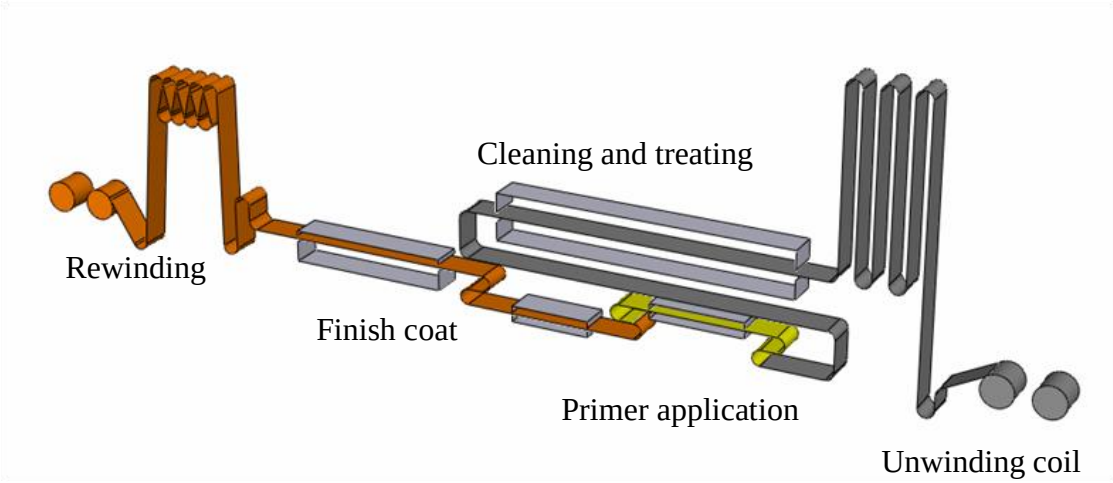

Figure 1 Schematic of a typical coil coating line [2]

Although manufacturers are converting from post-forming painting to forming pre-coated metal sheets for part fabrication, maintaining coating surface integrity and adhesive bond after forming is a major technical challenge. In forming pre-coated sheet

metal, adhesion loss along coating-substrate interface under plastic deformation can be a critical concern. Mechanics of sheet metal forming has been studied extensively. The research has led to a better understanding of the deformation processes and resulted in improved products and processes. However, the effect of plastic deformation on coating adhesion is not well understood. The aim of this research is to provide a better understanding of the interface failure mechanism under plastic deformation and to develop a methodology for predicting the adhesion loss on polymer coated metal sheet at different deformation conditions.

To summarize the state-of-art knowledge related to this research, previous work in the areas of adhesion test, characterization of deformation modes, and modeling of debonding are reviewed in Section 2. In preparation for experimental work reported in the later Sections, Section 3 describes the methods to evaluate adhesion strength and to create various deformation states. An analytical model based on virtual interfacial crack to predict coating adhesion loss after deformation is presented in Section 4. To deal with complex deformation modes, a numerical approach is investigated and reported in Section 5. Conclusions of the research and suggestions for future work are given in Section 6.

2. LITERATURE REVIEW

To provide a basis for this research, a review of previous works in three areas: adhesion measurement, deformation method, and modeling of interface adhesion are presented. Several experimental procedures related to coating adhesion evaluation will be reviewed in order to choose a suitable method for this work. To observe coating adhesion affected by deforming a polymer coated sheet metal, experimental methods producing different deformation modes are reviewed. To model the interface adhesion loss, efforts are made to assess works addressing interface adhesion problems. The Section ends with a description the present work's scope, including the experimental approach along related modeling, and experimental methodologies.

2.1 Measurements of coating adhesion

Crosshatch tape test for coating adhesion

A common method for characterizing the strength and weakness of coated materials is the ASTM D3359 crosshatch tape test [6]. This test creates crosshatching lines on coating, using a cutter with multiple edges. Each line is cut from the top layer of coating to the substrate layer, creating an area of grids for later tests. A special tape is then placed on the scratched coating surface, and peeled off at a specific angle and constant speed (Figure 2). By counting the number of coating grids removed by the tape, the adhesive strength is defined. As most polymer coatings are too strong to peel off, accelerated pre-conditioning is generally required [1, 7]. The test gives only the number

of the grids removed, and is not a quantitative measure of adhesion strength between coating and substrate.

(a)

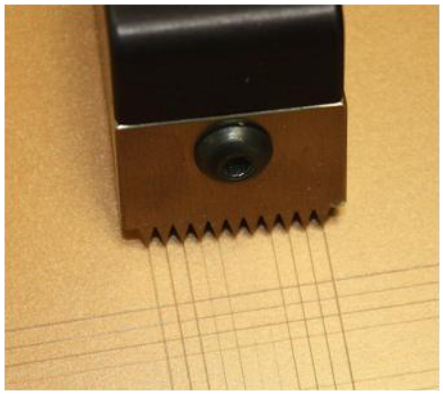

(b)

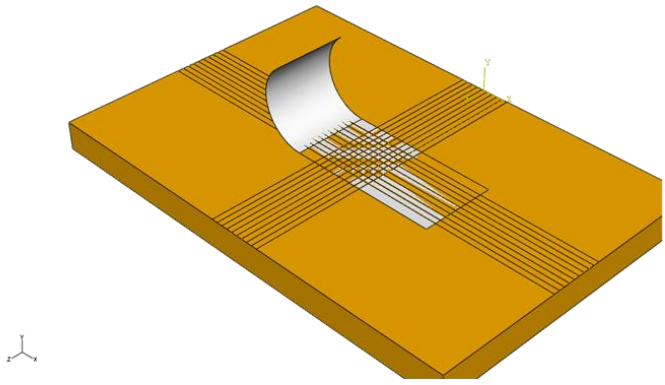

Figure 2 Crosshatch tape test. (a) crosshatch lines by cutter (b) tape placed for peeling the crosshatch area [1]

Double-cantilever beam, four point, and three point bending test

Sun et al [8] examined adhesively-bonded joints in steel sheets using the double-cantilever beam (DCB) system. Two steel sheets were bonded adhesively and loaded by

a tensile tester to study the mode-I fracture on adhesion interface. A DCB was also used in investigating the bonding strength of sandwiched materials by Ostergaard et al [9]. Laminated sheets are generally materials adhesively joined by two metal sheets; while sandwiched materials are made up of thicker core material bonded with top and bottom cover sheets. For DCB testing, the specimen is created with an initial crack in one end along the interface between the top-plate and core material. Then pulling load is applied on the pre-crack side to initiate crack propagation (Figure 3). The pulling mechanism is similar to the peel test and can be conducted using a uniaxial tensile tester. For polymer coated metal sheet, the coating adhesion is relatively strong, and thickness is less than 50um. To investigate the coating adhesion of polymer coated metal sheets produced from a continuous process, it is difficult to make a pre-crack and to initiate crack propagation.

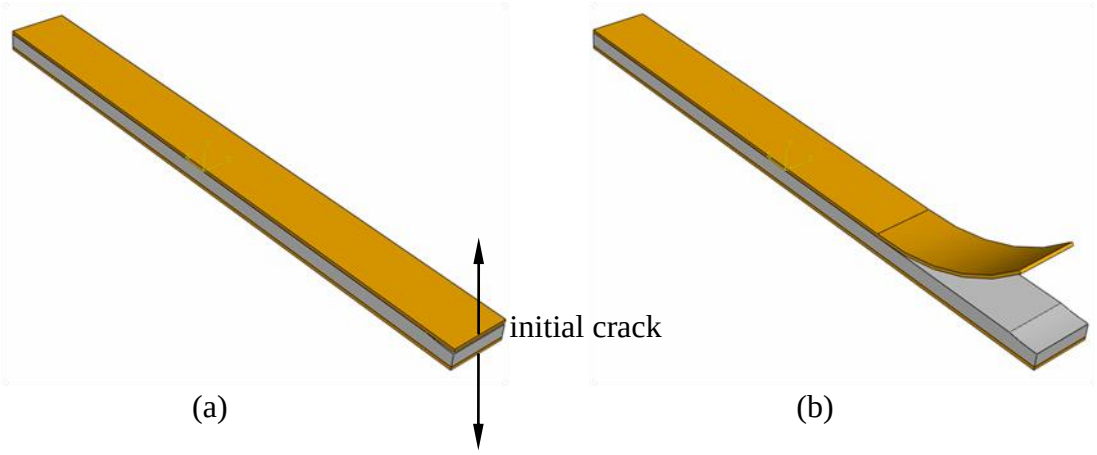

Figure 3 An adhesion measurement on sandwich specimen. (a) an initial crack is made and peeled by uniaxial tensile tester with special fixture (b) one of the crack opening and propagation modes

For polymer coated materials, Charalambides et al [10] devised a test specimen to measure the fracture resistance of bimaterial interface using a four-point-bending mechanism. A polymer-coated metal sheet was made into a four-point-bending specimen. A pre-crack area and a notch in the coating layer were generated in the center of specimen (Figure 4). The four-point-bending mechanism has the ability to introduce moment on both ends and force the center pre-crack to propagate along the interface. Using the four-point-bending method, Guan et al [11] examined the ceramic coating on aluminum alloy specimen without pre-crack. The crack initiate was observed by scanning electron microscope (SEM). Thouless [12], Yang et al [13] and Sun et al [14], used an end-notched flexure specimen bonded by adhesive and loaded by a three point bending fixture (Figure 5). This test is mainly used to study the mode II fracture problem of two steel plates jointed by adhesive with elastic-plastic material behavior. Through this test, it can be observed that evaluating adhesion by a peeling or bending mechanism involves initial crack preparation on the specimen. These evaluation methods are time consuming and do not directly measure the adhesion strength.

Indentation, impression test on coating adhesion

An indentation test can also be used to characterize coating adhesive (Figure 6). Testing of brittle coatings on ductile substrates were presented in [15, 16]. To perform indentation tests on coated materials, a wedge indenter is impressed through the coating and into the ductile substrate. The plastic deformation of the substrate can then induce interfacial crack propagation. By obtaining the crack size as a function of the impression

force, the interfacial fracture toughness can be measured. The size of delaminated area can be observed by optical microscope or scanning electron microscope (SEM). Impression heads can be sphere, cone, and wedge in geometry. The wedges have several advantages as it can produce larger force to create interfacial crack. Long wedge shape can be assumed as plane-strain condition for analytical calculation. This technique is used to obtain interfacial toughness by measuring impression force and crack area for thin brittle elastic coating on ductile substrates. It is not a suitable method to measure polymer coating adhesion on metal substrates.

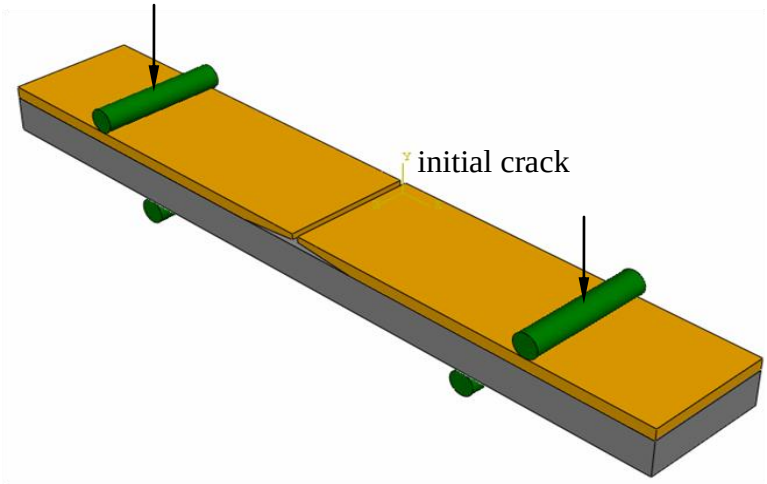

Figure 4 Four-point bending

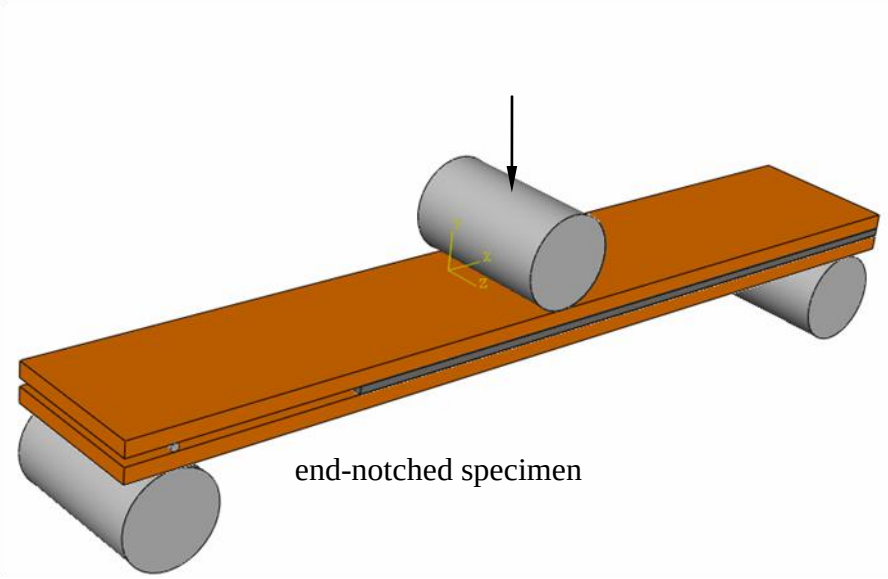

Figure 5 Three point bending test on end-notched-flexure specimen [13]

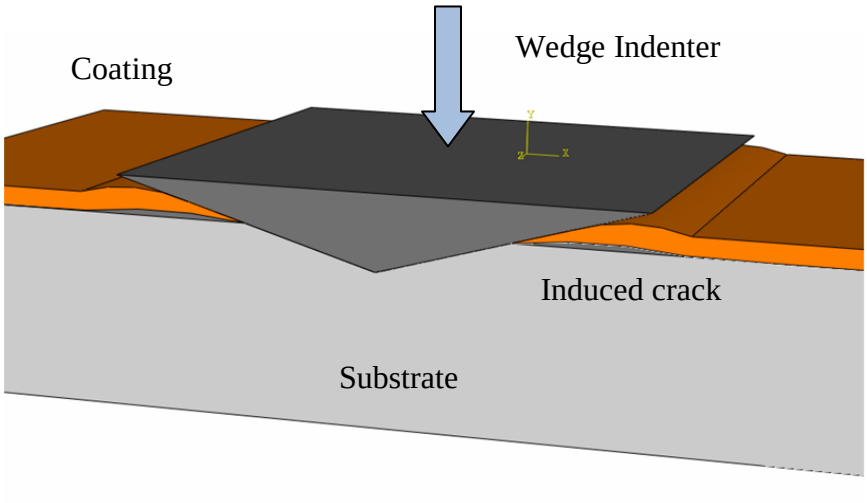

Figure 6 Coating adhesion test by wedge indenter

Spiral notch torsion test

A novel spiral notch torsion test (SNTT) was proposed to measure interface fracture toughness [17, 18]. SNTT specimen was a cylindrical bar with a 45 degree spiral groove as shown in Figure 7. The groove width and depth was about 254μm (0.01in), and the coating material was applied about 10~15μm thickness. Pure torsion was loaded on the top and bottom sides of the specimen. The pure shear along the groove line became tensile loading (Mode I crack opening). Two acoustic emission (AE) detection sensors were attached on both ends of specimen to observe the onset of crack open. The computer recorded the torque load and the time AE reached a peak value. SEM was used to exam the crack size on the spiral groove. The interface fracture toughness was then obtained. The technique is only suitable for bar specimens and requires significant sample preparation.

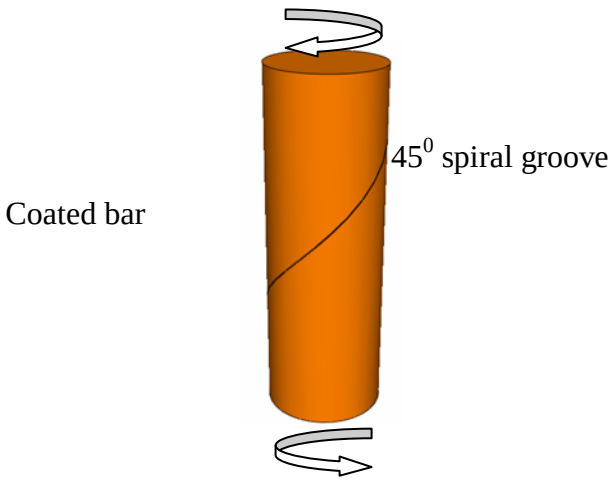

Figure 7 Spiral notch torsion test [17]

Laser spallation

A high energy laser-induced acoustic pulse loading is used to determine the thin film adhesion. The compressive stress pulse is created in the substrate by a laser pulse. As it propagates and reflects from free surface, the tensile loading spalls the film from the substrate (Figure 8). Kandula et al [19] conducted an interfacial strength test on coatings using the laser-induced spallation technique, and developed an analytical relationship to calculate the interfacial stress by measuring the free surface (coating) displacement. Although no mechanical contact occurs on either coating or substrate during laser spallation, the technique is mainly suitable for film thickness less than 1μm. It is not suitable for coating adhesion evaluation on polymer coated sheets due to thicker coating, thermal effect, and the intensive equipment setup required by laser spallation.

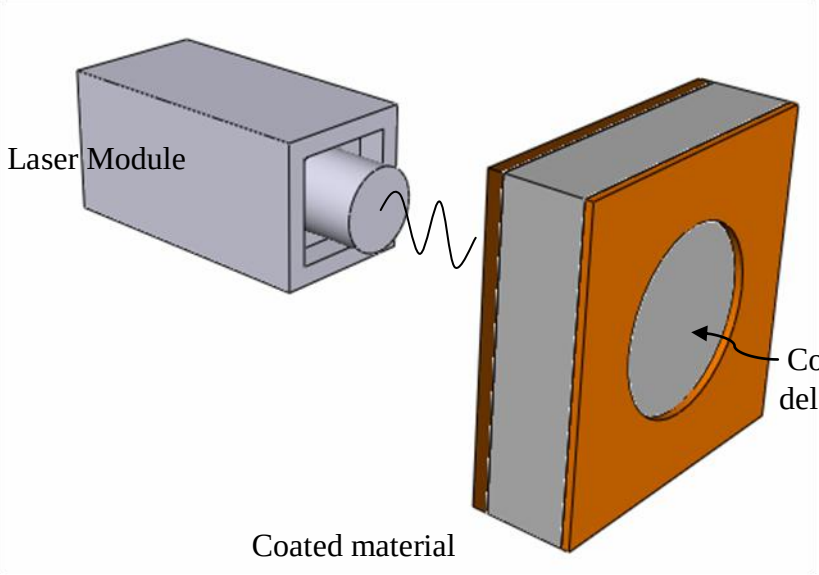

Figure 8 Laser spallation on measuring coating adhesion

Lap shear

ASTM D1002 lap shear test [20, 21] is commonly used to test adhesive joint structures. Figure 9a shows a test performed on two metal plates bonded adhesively. Another modified test that separates adhesive jointed specimens in shear manner is shearing test by Takiguchi and Yoshida [22] . It investigated the interface adhesion of laminated sheets under V-bending effect. The deformed V-shape area of laminated sheets subjected to different degree of plastically deformation, several sections of deformed laminated sheets were cut and test by shearing test fixture (Figure 9b). The test examined the interface adhesion of laminated sheets under plastic deformation. To investigate coating adhesion of polymer coated sheet, it is difficult to prepare specimens for lap shear tests.

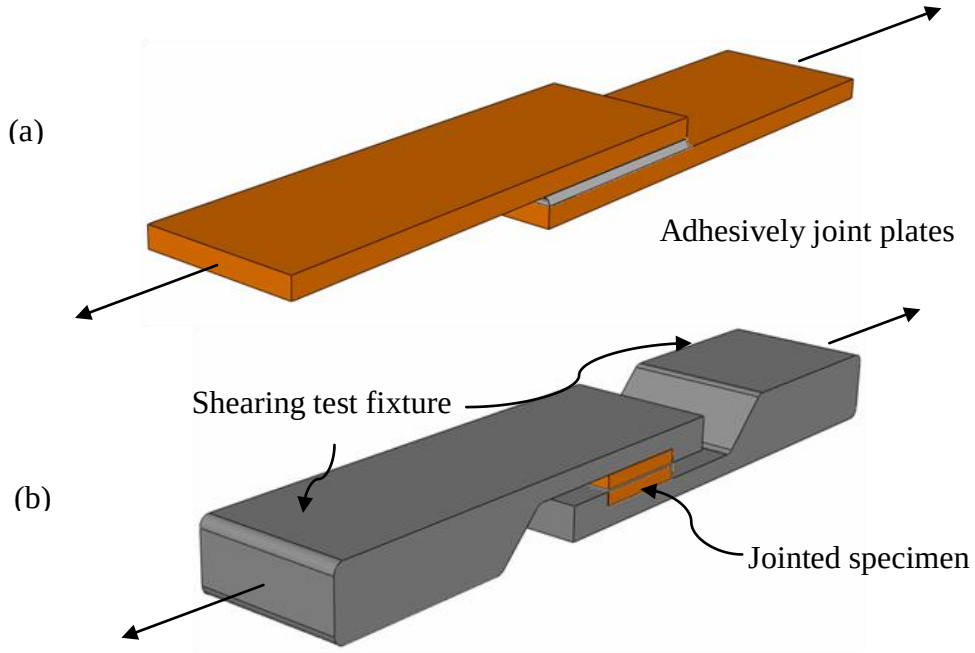

Figure 9 Lap shear test. (a) diagram of ASTM D1002 lap shear specimen [20] (b) the shearing test on selected adhesively joint section [22]

Tensile test on adhesive bond

Tensile tests on adhesive bonds are mainly for measuring the adhesive strength by uniaxial tensile tester. ASTM D2095 [20, 23] is designed for adhesive tensile strength test. Two metal rods bonded adhesively are made to obtain the adhesive strength in tensile load (Figure 10a). Spray coating adhesion also can be obtained by ASTM C633 [24] using a similar tensile load mechanism. Watanabe et al. and Babu et al. [25, 26] prepared specimens to examine coating adhesion by tensile test.

Similar to the tensile bond test, but easier in specimen preparation is the ASTM D4541 pull-off test [27, 28] (Figure 10b). A metal stud or dolly is adhesively bonded on the coating. A force normal to the coating is then applied on the stud to pull the coating off. The method measures the maximum force separating the coating from the substrate. The technique can be used in polymer coated materials and can obtain a quantitative coating adhesive strength. Dai Gil and Byung Chul [29] used a pull-off test to examine coating adhesive strength. An automated system [30] for adhesion test was proposed by using array of pull-off studs and automatically pulled to improve the accuracy of the test results.

There are many other experimental methods [31, 32] for measuring the interface fracture toughness. These methods, however, require extensive specimen preparation and post processing to obtain the adhesion properties.

Therefore, it can be concluded that, to study adhesion of polymer coated metal sheet under plastic deformation, the pull-off (stud-pull) test is the most suitable due to the simplicity of specimen preparation and the directness of measuring quantitative

adhesive strength. However, it should be noted that flat specimen is required for metal stud attachment.

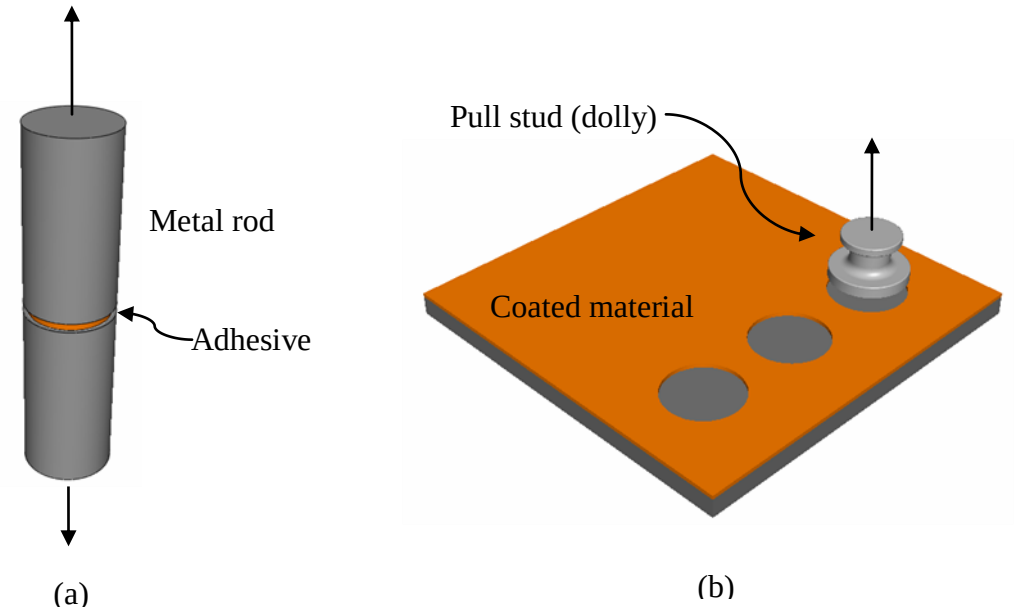

Figure 10 Tensile testing of adhesive bonding. (a) standard tensile testing specimen (b) pull-off test on coated materials by metal stud (dolly)

2.2 Deformation modes

In sheet metal forming research, a forming limit diagram (FLD) [33, 34] is typically generated to demonstrate the failure limit of metal sheets at various deformation conditions (strain states). This research focuses on the degree of adhesion loss in different deformation conditions. These deformation conditions can be shown in a diagram similar to FLD and the deformation modes can be obtained by different forming processes (Figure 11).

Modified uniaxial tensile test

The coated material loaded in tension to investigate the coating adhesion is less specimen preparation compared to other forming processes in Figure 11. Dillard et al. [35] analyzed the notched coating adhesion (NCA) test with pre-conditioned samples loaded in tension. The effect of the applied strain on the adhesion strength of coated-sheet was observed. Schaufler et al [36] also loaded a diamond-like carbon coated material in tension and observed the crack on coating by SEM, focused ion beam and transmission electron microscope. The results indicated that cracks were initiated when larger strain was applied on the substrate. Vayeda and Wang [1] used a modified uniaxial tensile test, and rectangular stretch bend test combining with crosshatch tape test to characterize coating durability. Base on the results, the durability limit diagram (DLD) similar to FLD was constructed for the complex forming operation.

Uniaxial tensile test is commonly used for characterizing material properties. Sheet type tensile test specimens are suitable for pull-off adhesion test as specimen remain flat (for metal stud attachment) after deformation.

Biaxial tension mode

For biaxial tension mode, dome height tester with sphere shape punch head can create biaxial tension mode on sheet metal [33]. The dome shaped coated sheet is not suitable for metal stud (dolly) attaching unless the metal stud is relatively smaller than the dome's diameter. A novel mechanism for biaxial tension testing with uniaxial tensile tester is available [37, 38]. The specimen can be result in a flat type after biaxial

stretching. The geometry for flat biaxial tension specimen is a cross shape with fillets on the corner and thinner at the center area (Figure 12). The polymer coated metal sheet obtained from continuous process is difficult to make a thickness reduction at the center area.

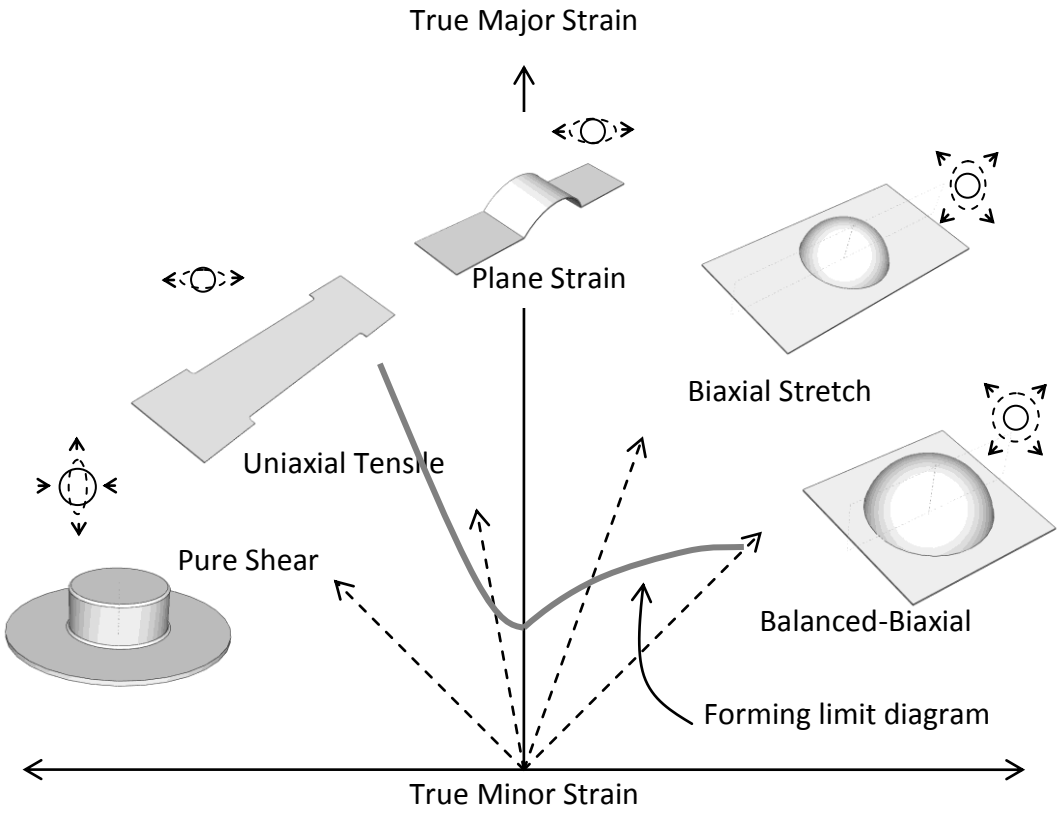

Figure 11 Forming limit diagram and forming processes for related deformation modes[33]

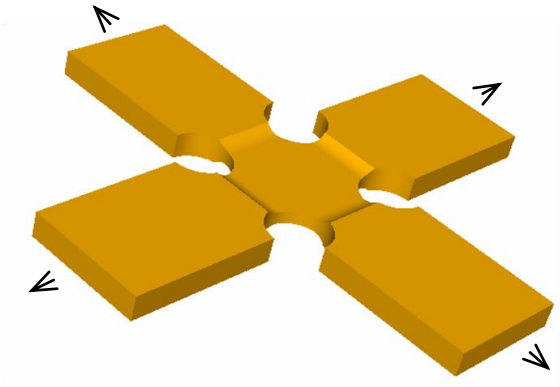

Figure 12 Cross shape specimen for biaxial stretching test with reduced thickness at center area

Tension-compression test

Cup-drawing process [33] can create tension-compression deformation mode on the flange. With proper specimen width, the dome height tester could also create this deformation mode. Another method to create tension-compression loading on metal sheet is draw-compression test presented by Cao et al [39]. It was a wedge strip of sheet metal with boundary constraints created the wrinkling on sheet metal. By adjusting constraint width and wedge geometry of specimen; the tension-compression deformation mode is created by uniaxial tensile tester. Although specimens deformed by these methods are suitable for pull-off test, care must be taken to avoid damage on the coating during materials flow though the gap of die and holder or constraint fixtures. Another novel specimen design that creates pure shear deformation mode by using a tensile tester is proposed by Shouler and Allwood [40]. The design consists of a sheet metal with a special geometrical opening that allows a pure shear mode deformed at certain area (Figure 13a). The strains were observed from the laser marked circles before and after

deformation. It can be observed that the created pure shear area on the specimen is too small for conducting pull-off test. Yosida buckling test [41] was first developed to provide wrinkling-resistant properties for different metal sheets. The test involves loading a square sheet along one of the diagonals in tension (Figure 13b). The numerical works conducted by Wang et al [42] indicated that a tension-compression deformation mode was created on the specimen. It is a suitable method to conduct the pull-off stress at tension-compression condition.

After considering the available and the results of previous studies, the experimental approach of this research is endeavored to measure pull-off stress change on polymer-coated metal sheet subjected to various plastic deformation modes. In this research, experiments are designed to obtain uniaxial tension, biaxial tension, and tension-compression deformation modes on coated sheet metal by using a uniaxial tensile tester.

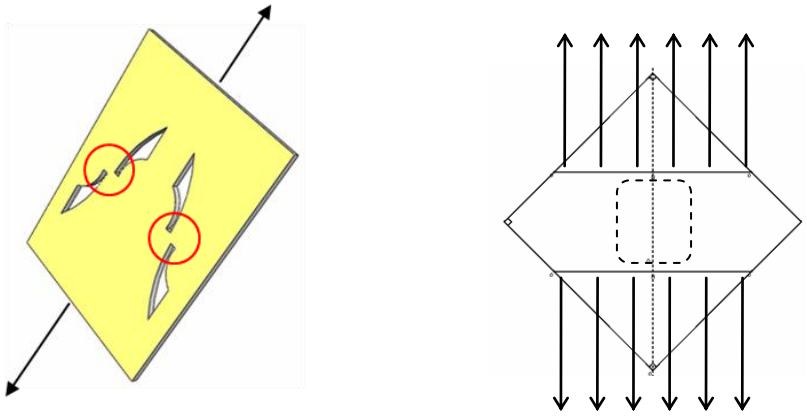

(a) (b)

Figure 13 (a) Specimen for creating pure shear at circle area [40] (b) Yosida buckling test [42]

2.3 Modeling of interface debonding

Kim and Yu[43] presented a review of forming and failure behavior of coated, laminated and sandwiched sheet metal. The work defined the major failure mechanism on forming laminated and sandwiched sheets under static and dynamic loading. The mechanism of coating adhesion related to deformation process was little discussed.

The mechanics of interface fracture drew much attention in the investigation of delamination due to thermal expansion on highly mismatch layered materials in consumer electronic products [44]. The earlier research on interface fracture mechanics was first focused on interface crack of layered linear elastic solids. Williams[45] and Erdogan [46] investigated the stress around a crack along interface of a dissimilar media. The work was expanded into linear elastic interface fracture mechanics for interfacial crack problems by Rice and Dundurs [47-49]. Suo and Hutchinson [50] presented interface crack as a bimaterial under general loading conditions. The analytical model was based on a semi-infinite interface crack model where normal force and bending loads were applied on the top and bottom layers. The stress intensity factor and energy release rate at the interface were calculated. The analytical solution was then applied for a four point bending test on bimaterial specimen with a center pre-crack. The method was used for determining the interface fracture resistance under bending loads. A paper that collects major theories and works before 1992 on fracture mechanics of layered materials was published by Hutchison and Suo [51].

The interface fracture mechanics was used to study interface fracture behavior under combined loading. Wang [52] proposed a fracture criterion to correlate the theory

with experimental works. The investigation included mixed mode I and mode II loading by scarf joint test (adjustable mixed-mode ratio) on brittle epoxy adhesive material. Banks-Sills et al [53, 54] examined glass/epoxy interface by Brazilian test. The test was conducted on a specimen composed of two materials in a half disk with an initial interface crack. The specimen was then loaded in compression to obtain the critical fracture load at different mixed-mode angles. By a numerical procedure, the critical interface energy release rate for adhesion was obtained. The predictions were in agreement with previous experimental results. Although this method had a good predictive capability, the initial interface crack size was required as an input to the model.

In the traction separation method proposed by Tvergarrd and Hutchison [55-57] , the cohesive zone was modeled on interface. In this method, crack growth between elastic-plastic solids could be analyzed. Although it considered materials in the elastic-plastic range, an assumed separation stress along the interface was needed for the computation.

Tijum et al [58] recently examined the interface adhesion of polymer coated metal sheet during plastic deformation. The proposed method included the use of the cohesive zone method to define the interface properties and the numerical simulation of the deformation process. The work emphasized on the evolution of roughness of the metal that influence adhesion and evolution of polymer behavior. Bosch et al [59, 60] also applied cohesive zone method to modeling the interface on deformation of polymer coated metal sheet. The techniques were used in deep-drawing simulation of a polymer coated steel. Coating delamination was observed during cup drawing simulation.

Although cohesive zone method is a powerful tool to model delamination problems, the separation parameters are required before the simulation and the computation cost to include the analysis in numerical simulation of complex stamping is significant.

2.4 Proposed method

This research aims to develop a methodology for determining the possible effects of plastic deformation on coating adhesion and how adhesion loss can be predicted. To accomplish this objective, several tasks will be performed.

1. Establish pull-off testing procedure and conduct tests to measure coating adhesion (bonding) strength on polymer coated metal sheets.
2. For coated sheet metal specimens into different deformed conditions (strain states). The experiments should include major deformation modes such as plane strain, bi-axial tension, and deep drawing modes.
3. Measure the coating adhesion strength of the deformed specimen and observe the adhesion loss.
4. Develop analytical and/or numerical models to predict coating adhesion loss due to plastic deformation.

The pull-off test was chosen for this study to measure the coating adhesion before and after deformation. The pull-off stress of coating is an indication of coating adhesion strength which could be affected by plastic deformation. To use a tensile tester to obtain various strain states on specimens, several specimen geometry and fixtures are designed

such that uniaxial tension, biaxial tension, and tension-compression modes can be attained.

The proposed method to predict adhesion loss due to plastic deformation is based on the concept of *adhesion potential*. By evaluating the amount of adhesion potential "consumed" by plastic deformation, the adhesion loss can be predicted.

For a given coated sheet metal, there could be insignificant defects or micro scale cracks along the coating-substrate interface. The details of the coating-substrate interface are not generally known. During the deformation process, micro-scale cracks could initiate and propagate [61]. As such, it is assumed that there is an initial "equivalent" or "virtual" crack along interface. The adhesion potential of the un-deformed materials is then defined by the energy release rate due to debonding (fracture). Thus the adhesion potential is a function of the material properties, the virtual crack length, and the pull-off stress (applied stress that can cause debonding). While subjected to plastic deformation, the force and moment acting on the interface are induced by the coating-substrate property mismatch. As a result, a stress that is lower than pull-off stress can cause the coating to be separated from the substrate. In the following Sections, the experimental work along with the developed analytical models and numerical methods are presented.

3. EXPERIMENTAL SET-UP AND RESULTS

To observe the adhesion loss of coated-sheets after deformation, this study will conduct experiments measuring pull-off stresses on specimens before and after applied deformation. This Section describes the set-up and procedure of experimental works. First, the device used for measuring adhesion stress by up-lifting coating from a substrate is introduced. Second, a description of the procedure for attaching a metal stud on the coating for successful separation is provied. Finally, several specimen shapes are then designed to obtain different deformation mode on flat surface. The experiments conducted on the deformed samples are able to produce the major portions of deformation modes (Figure 11) commonly observed in sheet metal forming processes. Adhesion test results on samples involving uniaxial tension, biaxial tension, and tension-compression loading are also included in this Section.

3.1 Pull-off Test

Introduction of Pull-off Tester

The ‘pull-off’ tester shown in Figure 14 is a portable device used to measure adhesive strength [27, 28] . The testing procedure involves attaching a metal stud (or dolly) to the coating surface with glue and up-lifting the metal stud by a hydraulic pump. The lifting rate can be adjusted and recorded during the pulling process. A maximum stress is shown on the stress indicator. The “metal stud” is produced in several sizes (10, 14, 20, and 50mm diameter) for variety of coating adhesion strength. Metal studs are

created in different sizes because the compact hydraulic pump has a limited force capability, leading to the necessity of varying sizes to compensate for force. Smaller metal stud size is suitable for higher quality coating with good adhesion strength. Lower quality coating with weak adhesion strength would therefore require larger metal studs. It should be noted that metal studs can only be attached on a flat area to obtain a valid adhesion strength measurement.

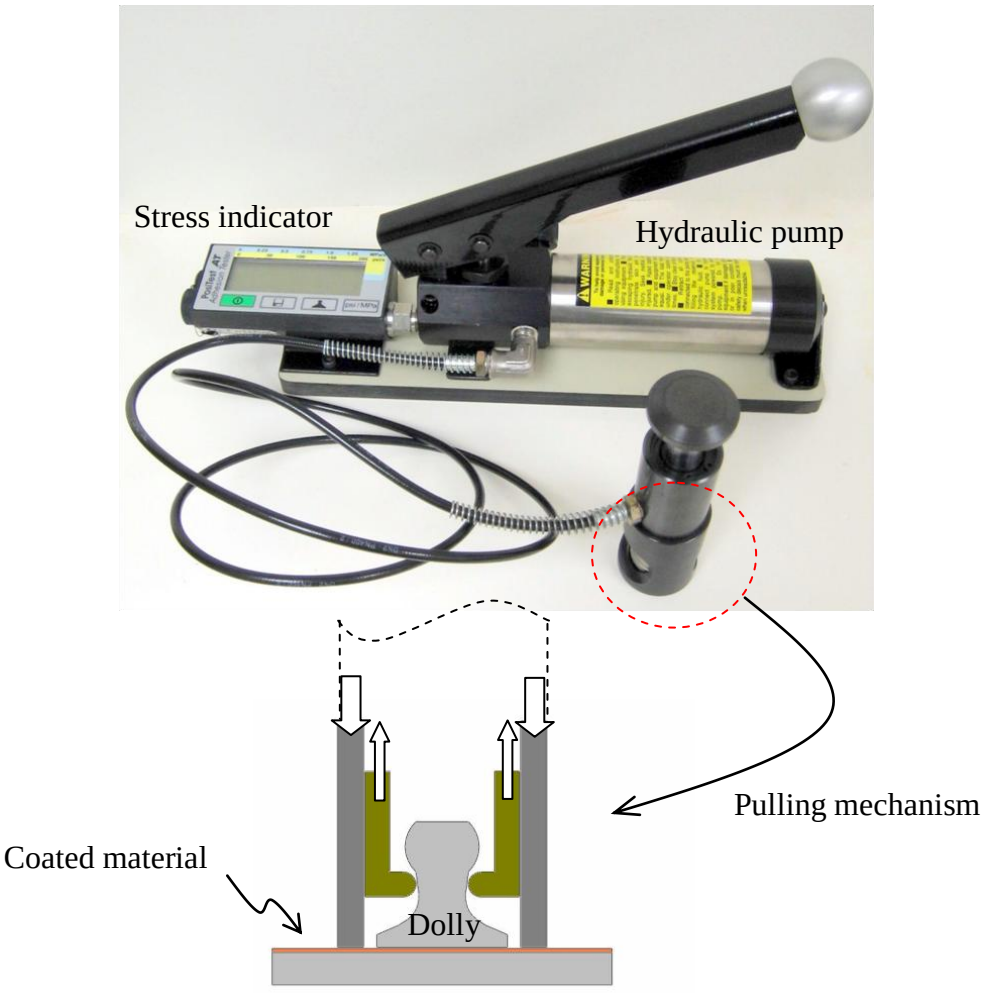

Figure 14 Pull-off tester. Manual hydraulic pump with specially designed self aliment head [28]

To successfully obtain a valid coating adhesive value, the delamination modes must be examined after each pulling. Possible delamination modes include adhesive failure between metal stud and coating, cohesive failure of coating, and adhesive failure between coating and substrate. These modes depend on the strength of the interfaces (stud/coating or coating/substrate) and the strength of coating (Figure 15). The glue must be chosen carefully to achieve strong adhesion between dolly and coating such that the coating can be pulled off completely.

Figure 15 Delamination modes on coating/substrate. (a) failure at stud-coating interface (b) failure at coating (c) failure at coating-substrate

Metal stud Attachment

To ensure the complete removal of coating, the metal stud attachment procedure and glue selection are important. Both the metal stud and the coating surface must be prepared carefully before applying adhesive. The procedure is detailed as follows,

- Clean the coating surface with alcohol (or degreaser) and wipe dry with a cloth.
- Scratch the dolly surface several times with 400 grit paper.

- Clean the metal stud with alcohol (or degreaser) and wipe dry with cloth, ensuring the surface is free from particles. Apply the glue immediately after drying.
- Apply one or two drops of glue to the metal stud surface and allow it to spread over the surface.
- Gently place the metal stud on the coating surface and adjust to the desired position.
- Hold for 30 seconds with light pressure and leave the metal stud to cure for 48hours at room temperature (~21 Celsius) under 60% relative humility.

3.2 Deformation modes and specimen design

Sheet metal is usually formed into complex geometrical shapes for wide application. The forming limit information of sheet metal is important for designers. This research will not examine the formability of coated-sheet, but will observe the adhesion loss of coating under different deformation conditions. Three particular deformation modes, shown in Figure 16, cover the strain conditions in the major and minor strain space in forming limit diagram. With large specimen width, the uniaxial tension load will create a strain state close to the plane strain condition. With biaxial tension, the strain path and final strain state will be located on the right hand side of the strain space. The third deformation mode is most commonly observed in the cup-drawing process. In the flange area, the material is subjected to radial-tension and hoop-

compression. The strain path and the final strain state will be on the left hand side of the strain space.

To measure the pull-off stress after plastic deformation of the coated-sheet, the deformed specimen must have a flat area for metal stud to attach. Therefore, a major task in the experimental work is to design specimens, to be deformed using a uniaxial tensile tester, that can result in various strain states in uniaxial tension, biaxial tension, and deep drawing modes.

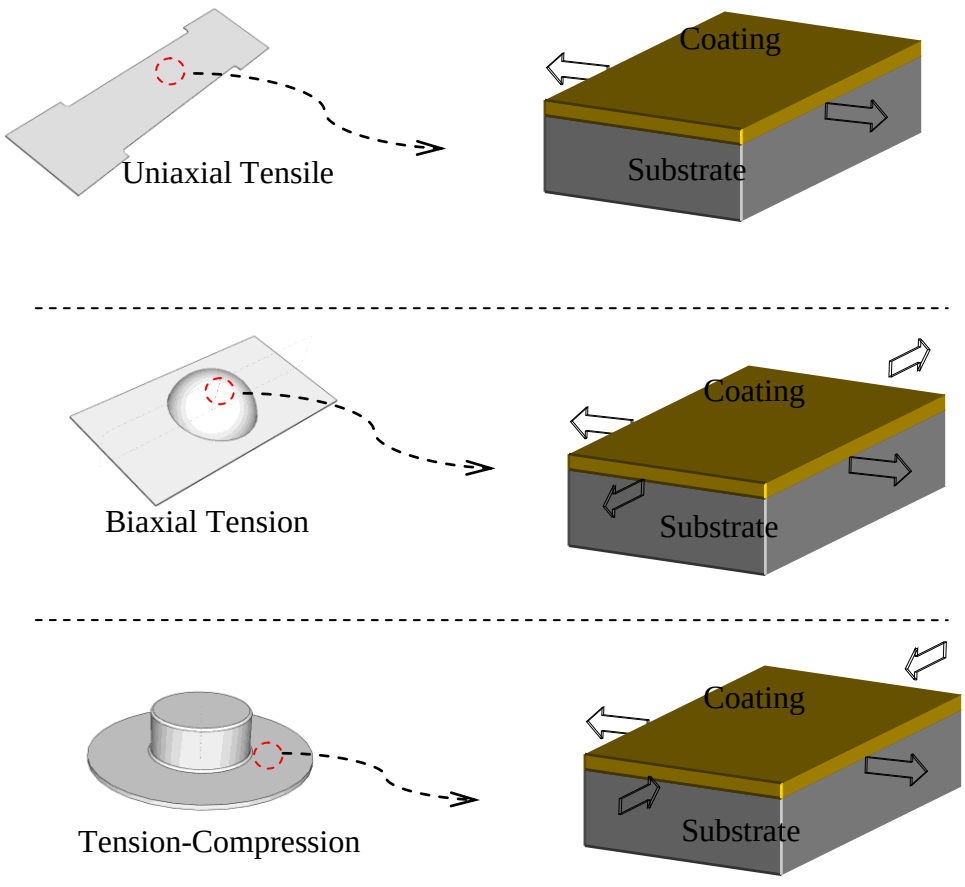

Figure 16 Three forming modes that create different applied strain combination

Uniaxial mode

Specimens for uniaxial tension mode are modified from a standard tensile specimen. The geometry and loading direction are depicted in Figure 17. The center area is designed to hold two 10mm metal studs. The specimens can be stretched to various strain levels while the maximum strain attained before fracture depends on the mechanical property of the substrate.

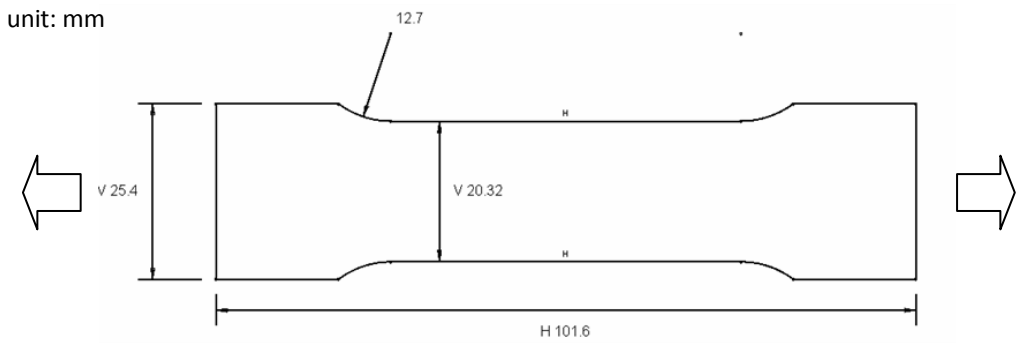

Figure 17 Specimen shape for uniaxial tension mode

Biaxial tension mode

Sheet metal forming limit on biaxial tension mode can be obtained from the limiting dome height test. However, it is difficult to conduct pull-off test on a curved surface. Another choice for performing biaxial stretching test on flat sheet is to use cross shape specimen with a reduced thickness in the center area (Figure 12). As the thickness of a polymer coated metal sheet is constant, the geometry of the specimen has to be redesigned. Finite element forming simulation was used to facilitate specimen design. As shown in Figure 18a, the present biaxial tension specimen has reduced widths in both

planar directions. To obtain biaxial tensile strain, sequential stretching loads are applied as shown in Figure 18b. The final strain state at the center of the specimen depends on the amount of the deformation during sequential stretching. After forming, a metal stud is then attached at the center of the specimen to conduct pull-off adhesion test. With this experimental procedure, the effect of strain path on coating adhesion loss is not considered.

(a)

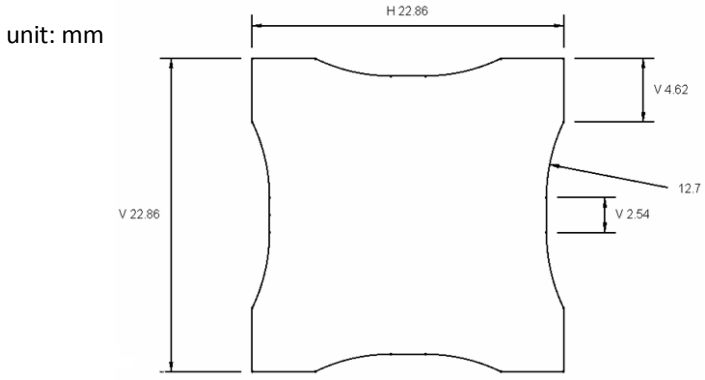

(b)

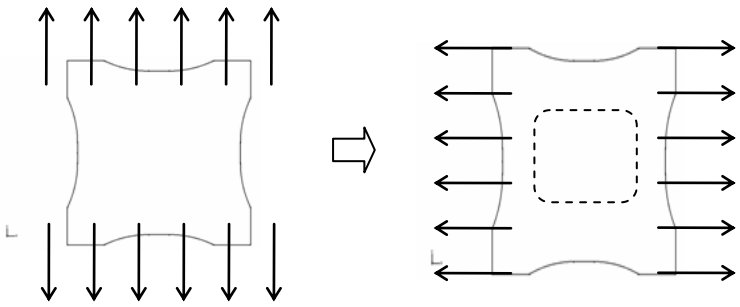

Figure 18 Biaxial tension specimen for this research. (a) the sketch of biaxial tension specimen (b) the sequence stretch by uniaxial tensile tester

Tension-compression mode

The Yosida buckling test was modified into suitable size for tension-compression mode in this research. The polymer coated metal sheets were cut into 25.4 mm by 25.4 mm square to fit the jaw width of tensile tester. The detail geometry is presented in Figure 19. While subjected to tensile loading in the longitudinal direction, the strain in the transverse direction is in compression. As the width gradually increases in the middle, necking and fracture can be prevented or delayed. The final tension-compression strain states depend on the amount of stretching on the specimen. After the deformation, a metal stud is attached at the center for the coating pull-off test. It should be noted that specimens with different rhombus shapes can also be used to obtain a wide range of tension-compression strain states.

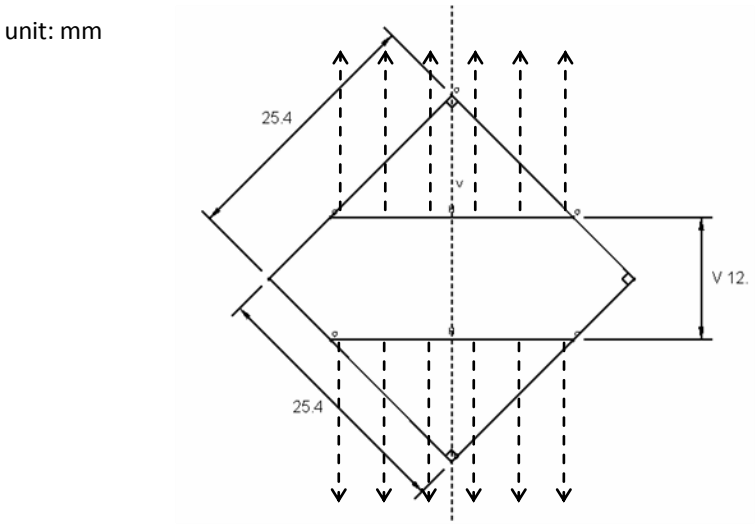

Figure 19 Modified Yosida buckling test specimen, and loading position and direction

For all specimens, deformation is conducted by using a uniaxial tensile tester (Figure 20). The boundary condition is displacement control and the strains after unloading are measured. As shown in Figure 21, square grids are created on the back side of the area where the pull-off adhesion strength is evaluated. An optical microscope with an X-Y table is used to measure the grid size, and the major and minor strains are calculated from the changes in grid size.

Figure 20 Uniaxial Tensile Tester

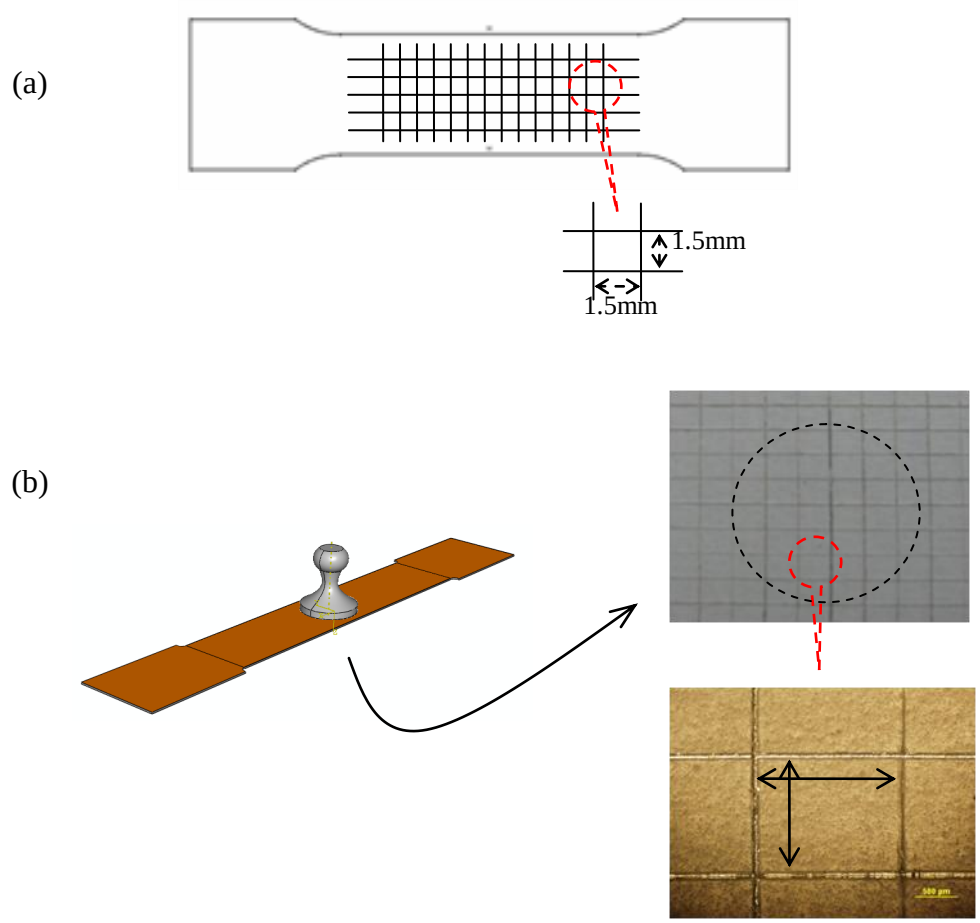

Figure 21 Strain measurement. a) make 1.5 by 1.5mm grid on the back side of substrate, b) after deformation, measure the grid size change was measured by an optical microscope

3.3 Experimental Results

Two types of polyvinylidene fluoride (PVDF) coated-sheet metal were chosen to determine the coating durability. The differences are in the primer and the color of the

PVDF. The coating in gray color is with polyester primer and the brown coating is with polyurethane primer (Table 1).

Table 1 Two types of Coated sheets

Name	Color	Coating	Primer	Substrate
Material I	Gray	PVDF	Polyester	Steel sheet
Material II	Brown	PVDF	Polyurethane	Steel sheet

Initial Pull-off Test

The initial pull-off stress obtained from these polymer coated metal sheets is valid if the coating can be separated from substrate successfully as depicted in Figure 22a. Figure 22b indicates that both PVDF coating with different primers can be pulled off by using CA40 (from 3M®), a high strength cyano-acrylate adhesive with low viscosity and short setting-time, to attach the metal stud on the coating surface. Test was conducted on five specimens for each type of coated-sheet. The adhesion stress in Table 2 showed that Material II had stronger adhesion strength (~4MPa) than Material I (~2.75MPa) initially. The information was used to compare the coating adhesion measured after plastic deformation.

(a) (b)

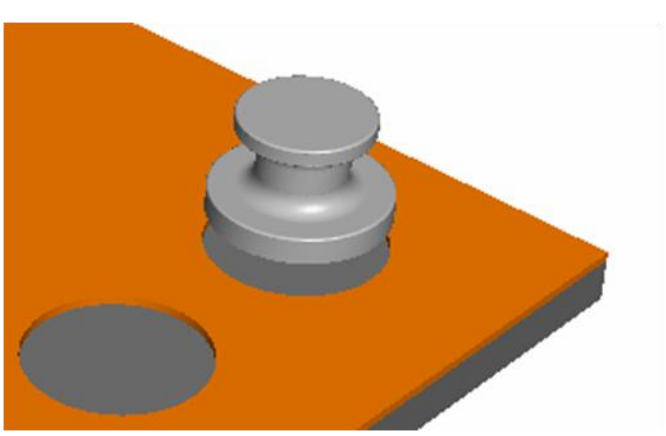

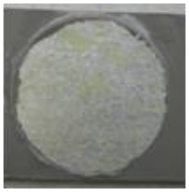

Material I (Gray)

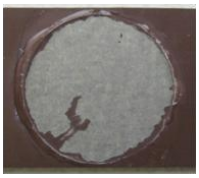

Material II (Brown)

Figure 22 (a) Metal stud attached on the coating surface, and successfully separated the coating from surface (b) coating delaminated from substrate; initial pull-off test on two types of coated-sheet

Table 2 Initial Pull-off stress of coated-sheets

Name	Material I (Gray)	Material II (Brown)
Average	2.75 MPa	4.00MPa
#1	2.93	4.59
#2	2.85	4.09
#3	2.85	3.91
#4	2.62	3.79
#5	2.48	3.63

Uniaxial tension mode

The uniaxial tension loads were applied by displacement control. The 3mm, 6mm, 9mm, and 12mm axial displacement were prescribed on the specimens in order to create different strain states. The deformed specimens with several strain values were shown in Figure 23. The actual strain for each metal stud area was measured by optical microscope. The maximum applied strain was near 20% at 12mm applied displacement. There was a crack initiated at the edge in the mid length of the specimen when applied displacement reached the 12mm (circled area at Figure 17).

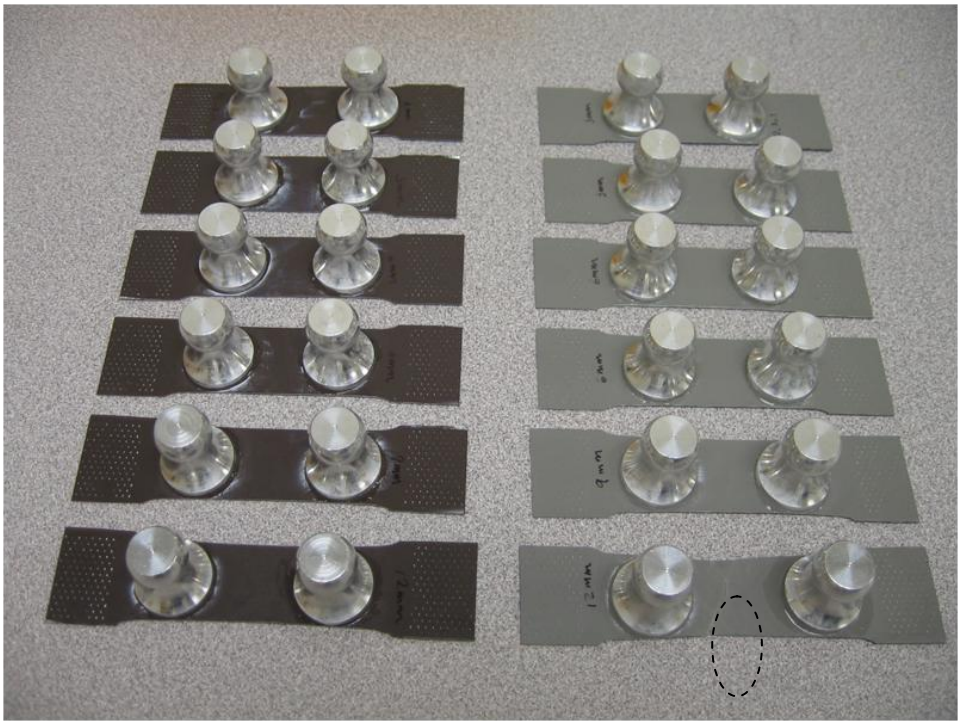

Figure 23 Specimen deformed into different tension strain value, note that failure induced while applied strain reach the coated sheet meet the forming limit

Sample pull-off test specimen after loaded in uniaxial tension is shown in Figure 24. It demonstrated that coating was delaminated completely from substrate by metal stud, and the pull-off stresses were valid for adhesion measurements. For Material I coated sheet in uniaxial tension (Figure 25), the pull-off stress decreases as the applied uniaxial tension strain increases. The same trend was also observed in Figure 26 for Material II coated sheet, the coating adhesion strength of both materials was affected by the plastic deformation in uniaxial tension mode.

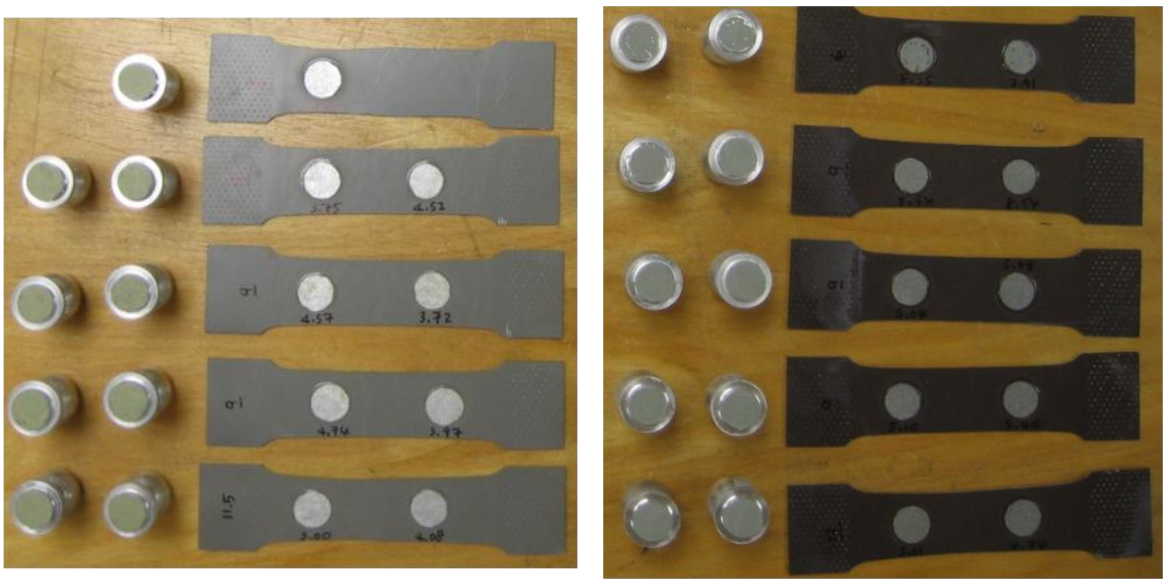

Figure 24 Selected specimens on Pull-off test after subjected to uniaxial tension load. (Left: Material I coated sheet, PVDF topcoat with polyester primer; Right: Material II coated sheet, PVDF topcoat with polyurethane primer)

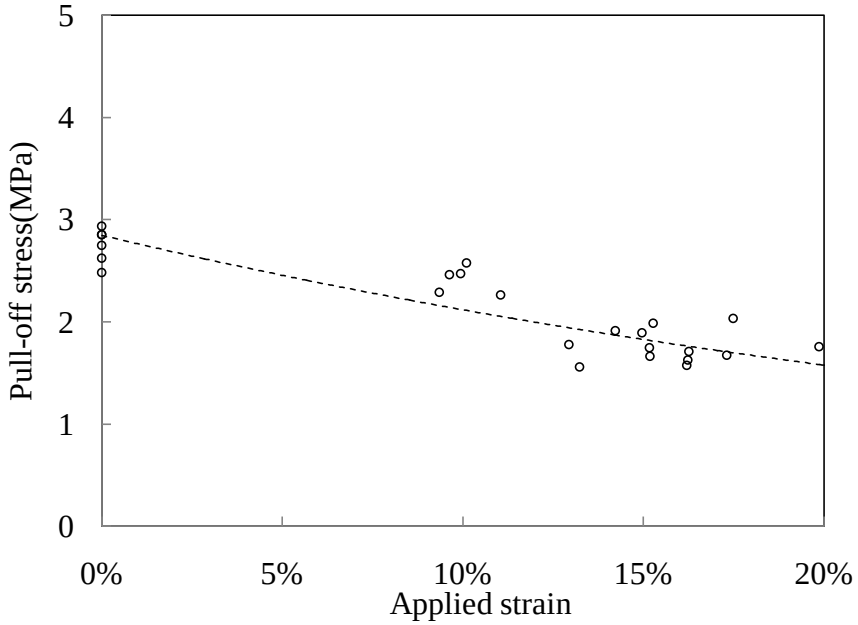

Figure 25 Adhesion loss on Material I coating under uniaxial tension mode

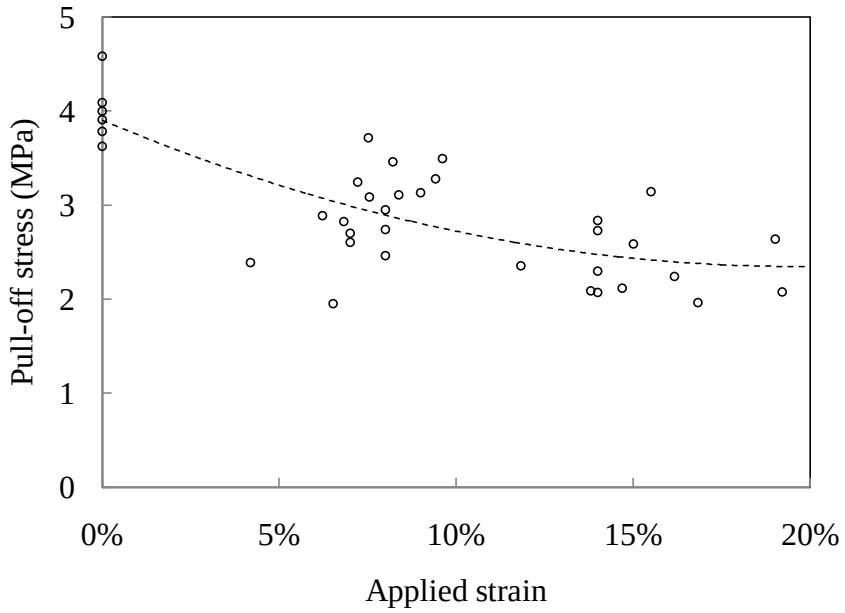

Figure 26 Adhesion loss on Material II coating under uniaxial tension mode

Biaxial tension mode

Before observing the adhesion loss under biaxial tension loading, the specimen for sequence biaxial stretching was examined to ensure that there is no fracture in the center area of the specimens subjected. Results in Figure 27 showed that with excessive stretching (~3.8mm, 3.6mm), failure can occur at the center area.

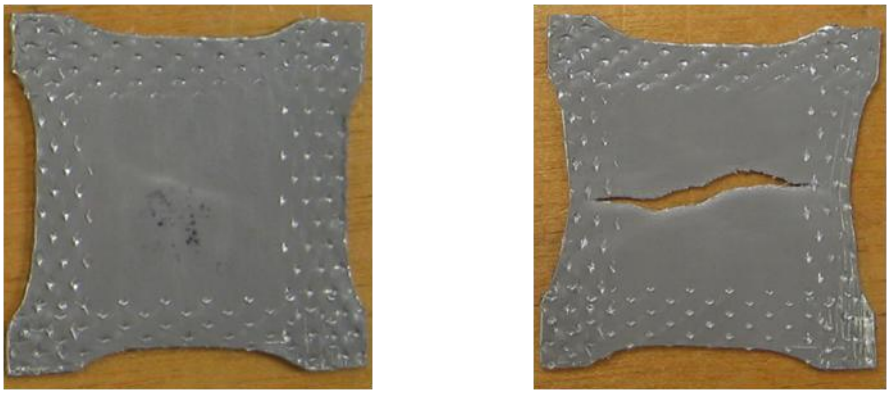

(a) (b)

Figure 27 Applied strains over the sheet metal forming limit on biaxial tension mode. (a) crack initiate at the central area (b) crack forming and propagate (Material I coated sheet, PVDF topcoat with polyester primer)

The sequence stretching on biaxial tension mode was conducted by displacement control. Two displacement loading conditions, (2.9mm, 2.7mm) and (3.5mm, 3.3mm), resulting in (5%, 5%) and (10%, 10%) strains, were applied for biaxial stretching on both Material I and Material II coated sheet. There were 6 specimens for each applied

strain condition. The center area (stud attached) was maintained square shape after sequential stretching by a tensile tester. The deformed specimens were subjected to pull-off test and the results of the test were shown in Figure 28. It can be observed that the coating was delaminated completely from substrate by metal stud, and the pull-off stresses were valid for adhesion measurements. From Figure 29, it can be seen that for Material I coated sheet, the pull-off stress decreases as applied biaxial tension strain increases. The trend is more prominent as shown Figure 30, for Material II coated sheet. It can be concluded that the coating adhesion strength was affected by the plastic deformation in biaxial tension mode.

Figure 28 Pull-off test results of biaxial tension specimens. (Left: Material I coated sheet, PVDF topcoat with polyester primer; Right: Material II coated sheet, PVDF topcoat with polyurethane primer)

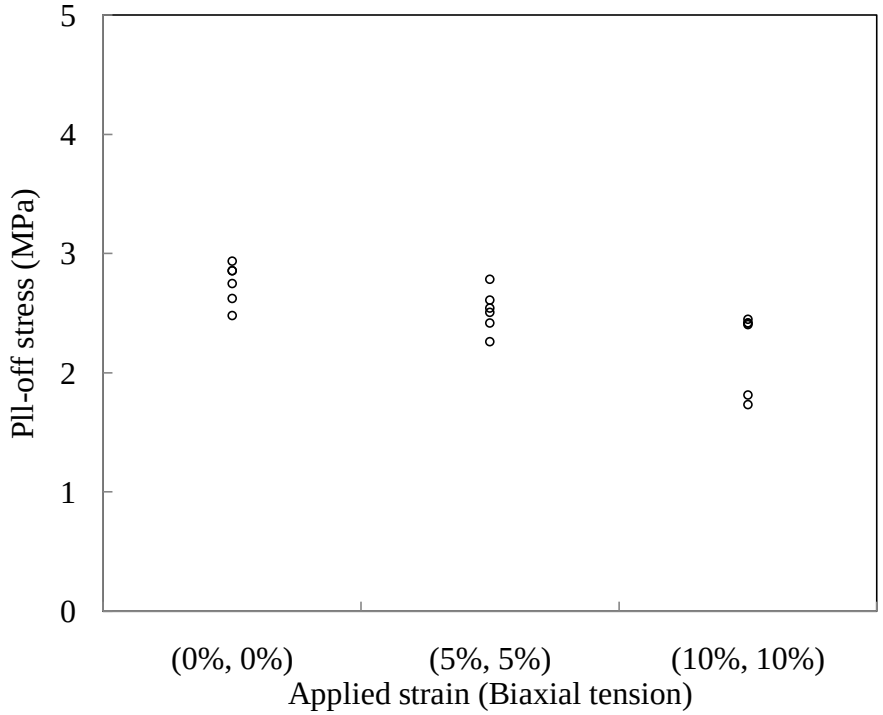

Figure 29 Adhesion loss on Material I coating under biaxial tension mode

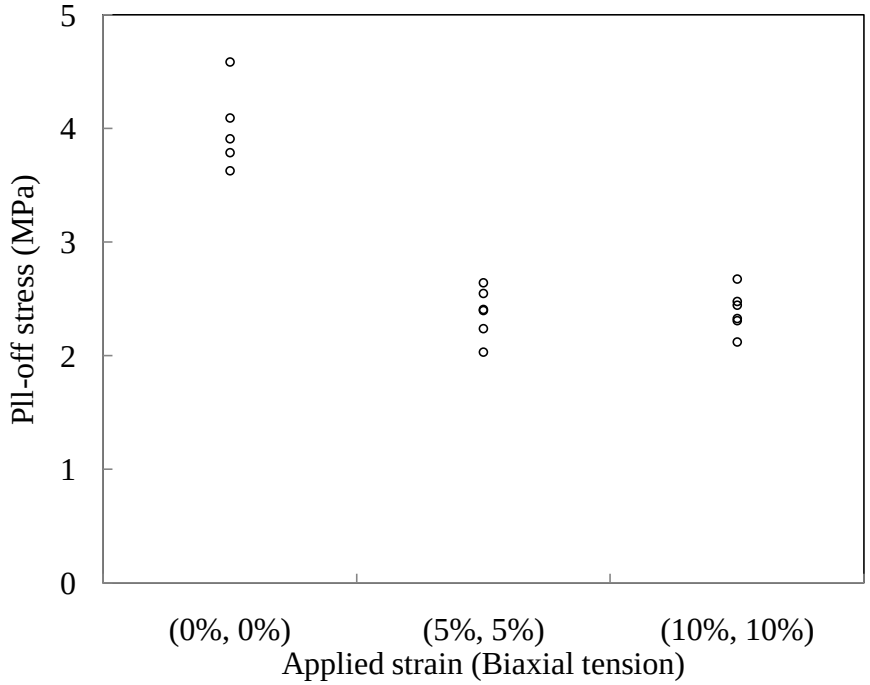

Figure 30 Adhesion loss on Material II coating under biaxial tension mode

Tension-compression mode

Modified Yosida buckling test was also loaded by uniaxial tensile tester and one of the plastically deformed specimens was shown in Figure 31.

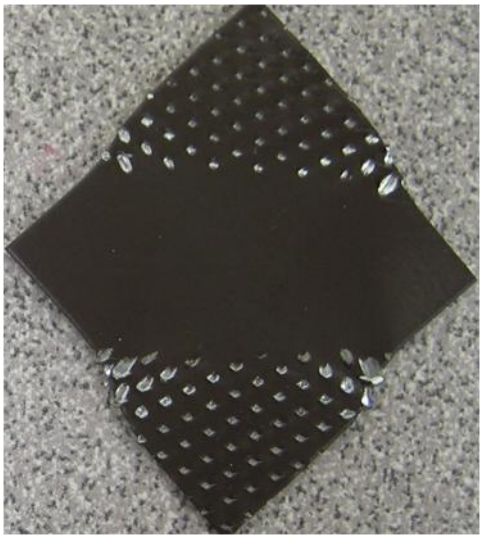

Figure 31 Modified Yosida buckling test specimen after unload by tensile tester (Material II coated sheet, PVDF topcoat with polyurethane primer)

Two loading conditions, axial stretching of 3mm and 4mm, were applied on both Material I and Material II coated sheet. Examples of specimens after deformation and pull-off test were shown in Figure 32. It is shown that the coating was delaminated completely from substrate by metal stud and the pull-off strength measurements were valid. The strain at center area (where metal stud was attached) was measured by optical microscope. The strain measurement results indicated that Material I coated sheet

specimens reached tension-compression strain states (5%, -5%) and (15%, -10%) while Material II coated sheet attained strain states of (10%, -5%) and (15%, -10%) in the tension-compression mode. From Figures 33 and 34, it can be observed that both coated sheets have a reduced pull-off stresses. The experimental data indicate that the coating adhesion strength was affected by tension-compression deformation mode.

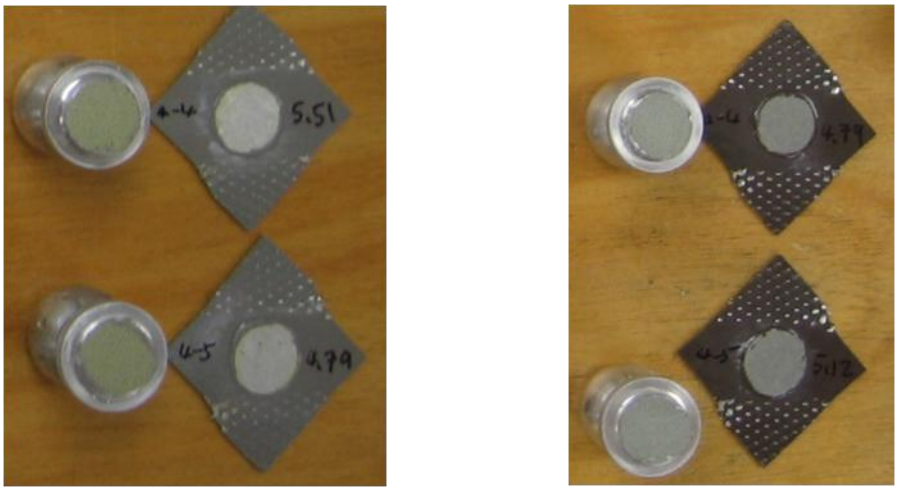

Figure 32 Selected specimens on Pull-off test after subjected to tension-compression load. (Left: Material I coated sheet, PVDF topcoat with polyester primer; Right: Material II coated sheet, PVDF topcoat with polyurethane primer)

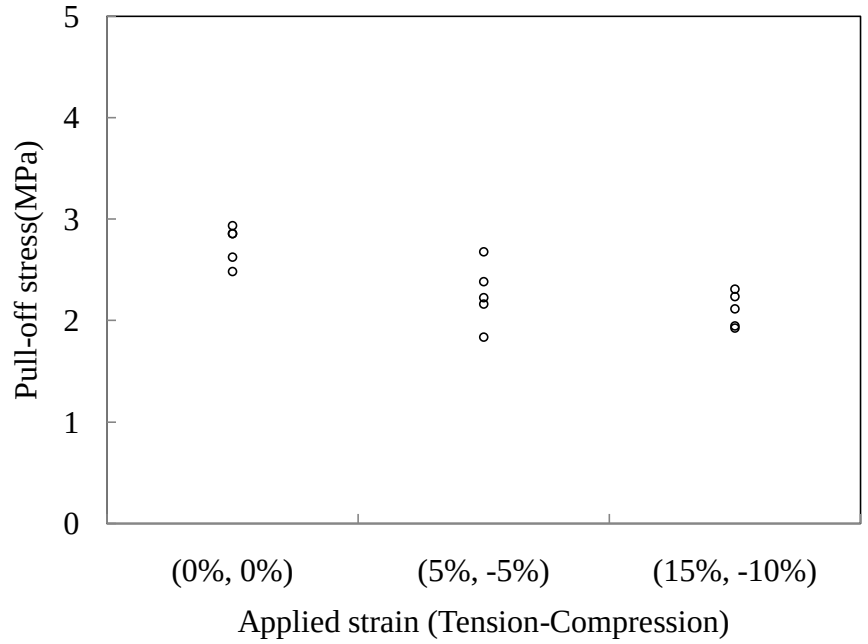

Figure 33 Adhesion loss on Material I coating under tension-compression mode (Modified Yosida Test)

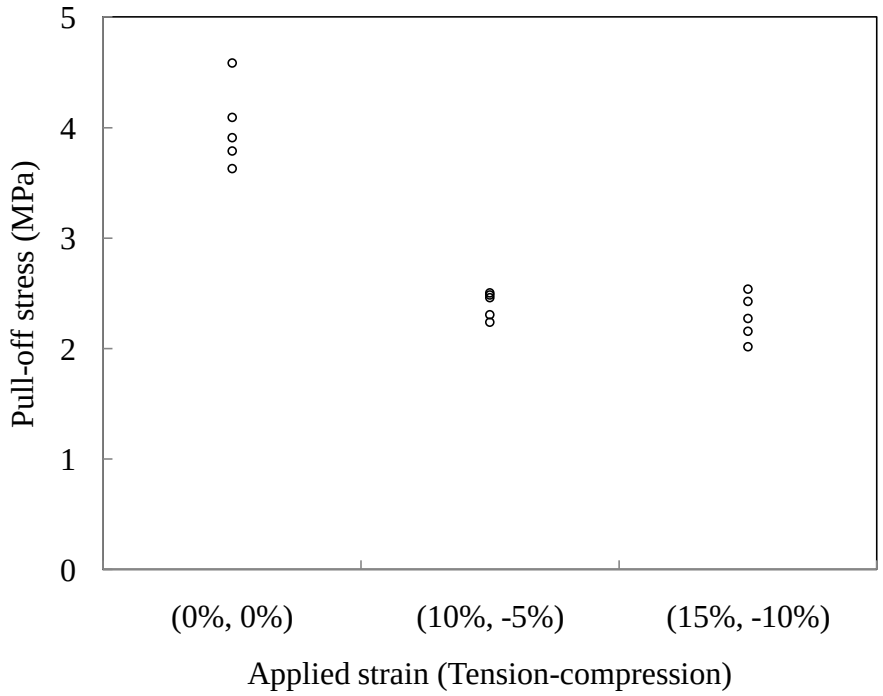

Figure 34 Adhesion loss on Material II coating under tension-compression mode (Modified Yosida Test)

4. ANALYTICAL METHOD

The approach to predict adhesion loss of a polymer coated sheet metal due to plastic deformation was briefly discussed at the end of Section 2. This Section introduces the concept of *adhesion potential* and virtual crack. Based on the concept, the development of the theoretical model for adhesion loss prediction is presented. An analytical model is built to demonstrate the methodology for specimens subjected to plane strain deformation. A parametric study is included to investigate the effect of coating and substrate parameters on coating adhesion loss.

4.1 Virtual interface crack model

For a given coated material, the detail of polymer-metal interface is not precisely known. As the polymer coating can be separated from the metal substrate during the pull-off test, it is assumed that there is an initial “equivalent” or “virtual” crack along the interface. The adhesion potential of the un-deformed materials is then defined by the energy release rate due to debonding (fracture). Thus the adhesion potential is a function of the material properties, the virtual crack length, and the pull-off stress (applied stress that can cause debonding). While subjected to plastic deformation coating-substrate property mismatch can result in force and moment acting on the interface. Assuming the adhesion potential is constant, a stress that is lower than the initial pull-off stress can cause the coating to be separated from the substrate.

To predict coating adhesion loss due to uniaxial tensile loading, an analytical plane-strain model was developed. As shown in Figure 35, the energy release rate of semi-infinite interface crack ($G_{semi\_infinite}$) with general boundary conditions can be derived as [51]:

$$G_{semi\_infinite} = \frac{1}{2\bar{E}_1}\left(\frac{P_1^2}{h} + 12\frac{M_1^2}{h^3}\right) + \frac{1}{2\bar{E}_2}\left(\frac{P_2^2}{H} + 12\frac{M_2^2}{H^3} - \frac{P_3^2}{Ah} - \frac{M_3^2}{Ih^3}\right) \quad (4\text{-}1)$$

where $\bar{E}_i = E_i/(1-\nu_i^2), i = 1,2$. E and ν are Young's modulus and Poisson's ratio, respectively. P_i and M_i (i=1, 2, 3) are axial forces and moments per unit width. H is the substrate thickness while h is the coating thickness. Dimensionless cross-section A is $A = 1/\eta + \Sigma$, $\eta = h/H$, $\Sigma = \bar{E}_1/\bar{E}_2$; and moment of inertia I is $I = \Sigma[(\Delta - 1/\eta)^2 - (\Delta - 1/\eta) + 1/3] + \Delta/\eta\,(\Delta - 1/\eta) + 1/(3\eta^3)$. The Δh is the neutral axis distance above the bottom of coated-sheet, $\Delta = (1 + 2\Sigma\eta + \Sigma\eta^2)/(2\eta(1+\Sigma\eta))$.

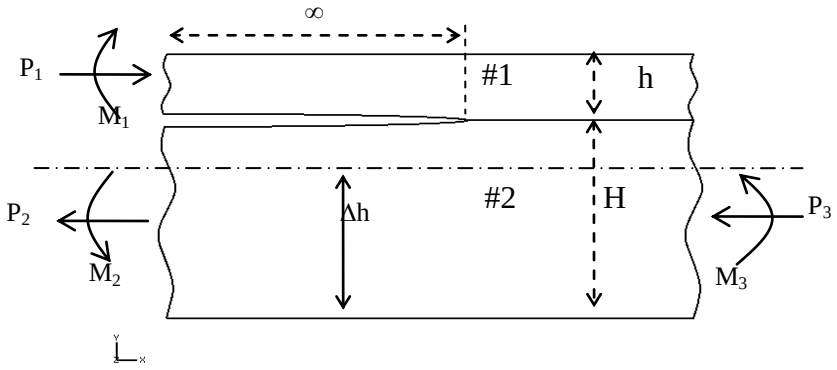

Figure 35 Semi-infinite interface crack problem [50]

In the present work, the coated-sheet is modeled as a bi-layered material system consists of coating and substrate, with an initial crack length $2a_0$ shown as Figure 36a. While the coated sheet is deformed, a large strain (ε_x) can be observed. The pull-off test conducted after plastic deformation results in an up-lifting stress, σ_{22}, normal to the coating surface. Based on the virtual crack assumption, the boundary conditions of coated-sheet subjected to plane strain deformation and pull-off test can be divided into two parts: the applied strain on the coated specimen shown in Figure 36b and the uplifting stress on the coating in Figure 36c.

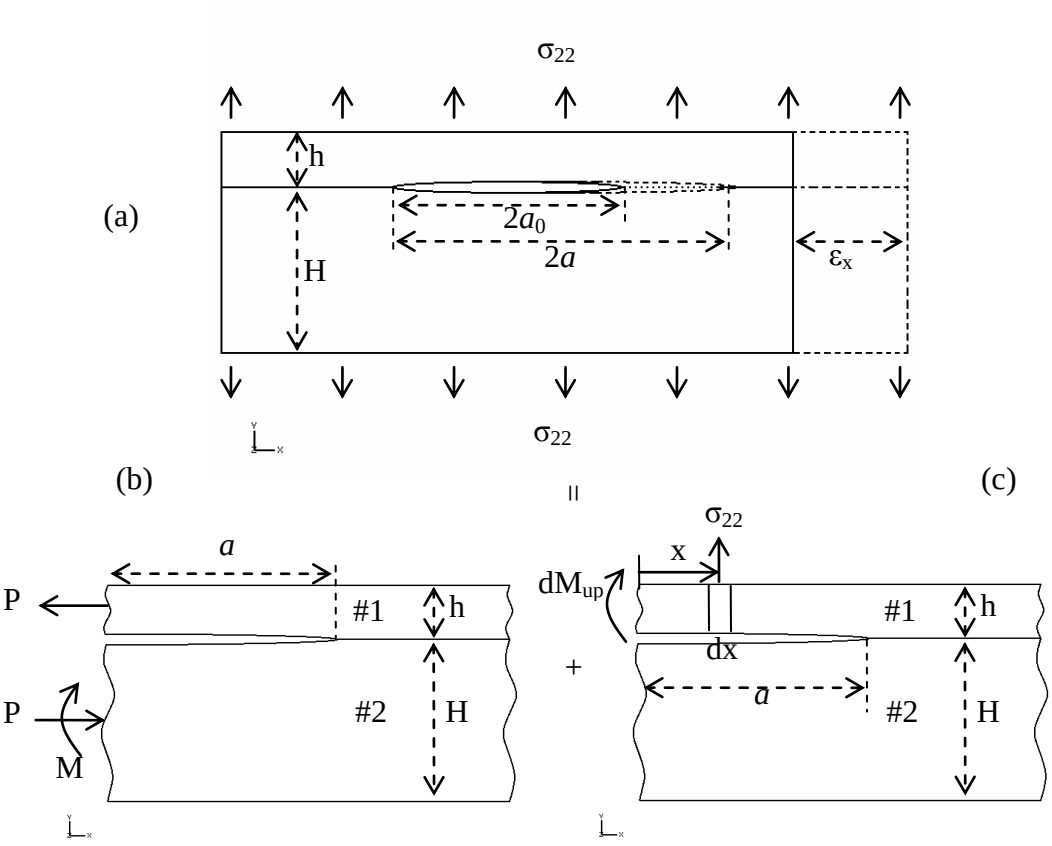

Figure 36 Boundary conditions of coated sheet under uniaxial tensile mode

The induced force and moment due to applied strain are based on the material properties of coatings and can be obtained by,

$$\mathrm{P} = \sigma_{coating}\,\mathrm{h} \tag{4-2}$$

where P is the force applied in x-direction; σ_{coating} is due to the coating material properties after unloading (layer #1).

$$\mathrm{M} = \mathrm{P}\left(\frac{\mathrm{h}+\mathrm{H}}{2}\right) \tag{4-3}$$

where M is the moment due to force P.

Another moment created by the uplift stress (σ_{22}) can be approximated as:

$$\mathrm{dM_{up}} = \sigma_{22}\mathrm{dx}(a - \mathrm{x}) \tag{4-4}$$

Integrating Equation (4-4) from x = 0 to x = *a*, the moment due to uplift stress at coating becomes,

$$\mathrm{M_{up}} = \int_0^{\mathrm{a}} \sigma_{22}(a - \mathrm{x})\mathrm{dx} = \frac{1}{2}\sigma_{22}a^2 \tag{4-5}$$

where crack length $a = a_0\exp(\varepsilon_{\mathrm{x}})$, a_0 is the initial virtual interface crack length. Substituting Equations (4-2) to (4-5) into Equation (4-1), with $\mathrm{P_1} = \mathrm{P_2} = -\mathrm{P}$, $\mathrm{M_1} = \mathrm{M_{up}} = 0.5a^2\sigma_{22}$, $\mathrm{M_2} = -\mathrm{M} = -\mathrm{P(h + H)}/2$, $\mathrm{P_3} = \mathrm{M_3} = 0$, the energy release rate, G, due to applied strain and uplifting stress can be expressed as:

$$\mathrm{G} = \frac{1}{2\bar{\mathrm{E}}_1}\left(\frac{[-\mathrm{P}]^2}{\mathrm{h}} + 12\frac{\left[0.5a^2\sigma_{22}\right]^2}{\mathrm{h}^3}\right) + \frac{1}{2\bar{\mathrm{E}}_2}\left(\frac{[-\mathrm{P}]^2}{\mathrm{H}} + 12\frac{[-\mathrm{M}]^2}{\mathrm{H}^3}\right) \tag{4-6}$$

Substituting $\varepsilon_{\mathrm{x}} = 0$ and $\sigma_{22} = \sigma_{22\_\text{initial}}$ (the initial pull-off stress) into Equation (4-6) as the boundary condition for conducting pull-off test on un-deformed specimen, the initial adhesion potential becomes:

$$G_{\text{initial}} = \frac{1}{2\bar{E}_1}\left(12\frac{[0.5a_0{}^2\sigma_{22\_\text{initial}}]^2}{h^3}\right) \quad (4\text{-}7)$$

Similarly, after plastic deformation of ε_x, a new pull-off stress, σ_{22_new}, may be reduced and which is an unknown value. But the new energy release rate (G_{new}) can be calculated from:

$$G_{new} = \frac{1}{2\bar{E}_1}\left(\frac{(-P)^2}{h} + 12\frac{[0.5a^2\sigma_{22\_\text{new}}]^2}{h^3}\right) + \frac{1}{2\bar{E}_2}\left(\frac{(-P)^2}{H} + 12\frac{(-M)^2}{H^3}\right) \quad (4\text{-}8)$$

As the adhesion potential is constant and the applied force and moment causes the pull-off stress to change, by equating (4-7) and (4-8), the new pull-off stress can be expressed as a function of the geometry and material parameters, the initial pull-off stress, and the applied strain:

$$\sigma_{22\_\text{new}} = \{\left(\frac{a_0}{a}\right)^4 \sigma_{22-\text{ini}}{}^2 - \frac{1}{3a^4}(\frac{P^2h^2}{3a^4} + \left(\frac{\bar{E}_1}{\bar{E}_2}\right)\left[P^2H + 12M^2\left(\frac{h}{H}\right)^3\right])\}^{1/2} \quad (4\text{-}9)$$

In Section 3, the adhesion loss of two types of polymer coated metal sheets subjected to tension deformation load were observed. Although the top coat of these two coated sheet are the same, the different primers have different initial coating adhesion. Table 3 shows the different modulus of top coat, primer, and substrate. Material I (Table 1) consists of PVDF and polyester (with similar elastic modulus) while the Material II consists of a lower modulus primer. To obtain an analytical solution, the top coat/primer/substrate system is simplified as a bi-layer system with an interfacial virtual crack. In the present model, a modified polymer coating material behavior is introduced.

The classical concepts of plasticity [62, 63] can be used for polymer in certain given conditions. Polymers are normally affected by time and temperature in both elastic and plastic regions. Parabolically and conically modified von Mises criteria are used to

consider the difference of polymer yield surface in compression and tension. The modification can cause changes in yield surface. Significant efforts have also been made to model polymers as visco-elastic-plastic solid. In the present study, the actual mechanical properties of the coating materials (both top coat and primer) are difficult to measure. As such, the approach is to approximate the material properties of the top coat and primer. Since the deformation rate is constant (~0.2mm/second) and the experiments are performed in room temperature, the polymer coating in this study is considered as a Mises solid. Figure 37 shows the stress-strain curve of substrate and two approximated coating material properties. App-I is for PVDF and polyester (with similar Young's modulus); while App-II is a combination of PVDF and polyurethane (with different modulus). Table 4 lists material properties for the prediction of coating adhesion loss in uniaxial tension loading.

Table 3 Young's modulus of polymer coated sheet [64]

Name		Young's Modulus (MPa)
Top Coat	PVDF	1030~1380
Primer	Polyester	1100
	Polyurethane	25
Substrate	Steel	210000

With the described material properties, an assumed virtual crack length a_0 = 5h (coating thickness h is 45μm), and the initial pull-off stress from the experiments (for

specimen with no plastic deformation), the initial adhesion potential can be calculated from Equation (4-7). The proposed analytical model is then used to predict the new pull-off strengths of specimens with various plastic strains. The results of coating adhesion loss predictions for both types of polymer coated sheet metals are shown in Figures 38 and 39. It can be observed that for the coated material with polyester primer (Material I), the prediction of adhesion loss is in good agreement with the experimental results. For coating with polyurethane, the experimental data is sporadic and the model seems over-predicting the coating pull-off stress after deformation.

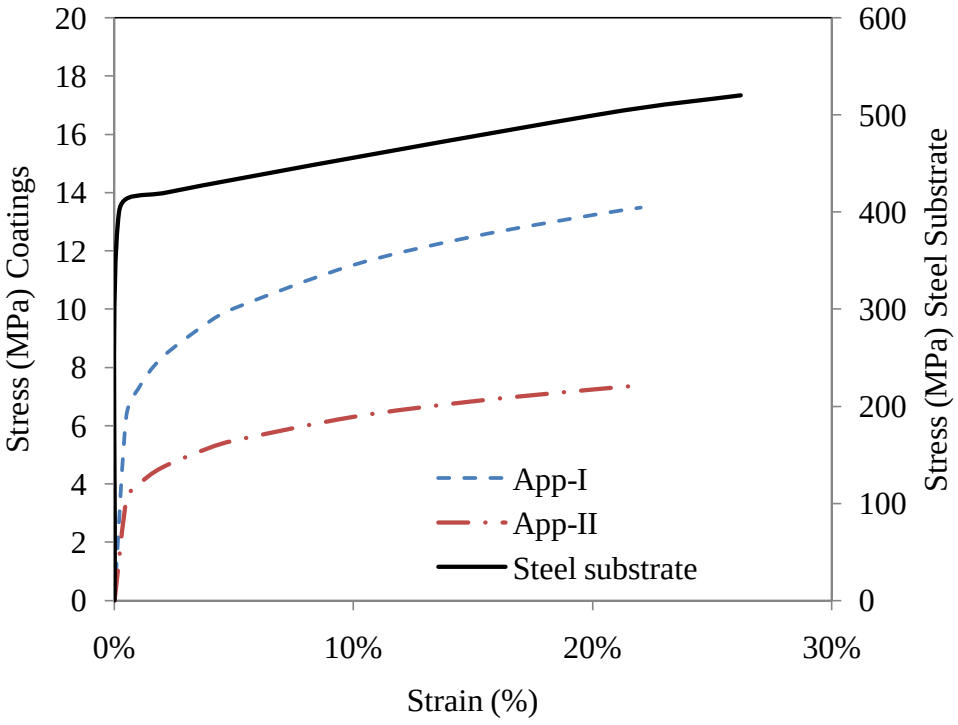

Figure 37 Stress strain curves for materials of coated-sheets

Table 4 Material laws for adhesion loss prediction in uniaxial tension load

Name	App-I	App-II
Combination	PVDF + Polyester (E=1264, ν=0.37)	PVDF + Polyurethane (E=694, ν=0.37)
Mises Solid	$\sigma=18.25(\varepsilon)^{0.2}$	$\sigma=10(\varepsilon)^{0.2}$

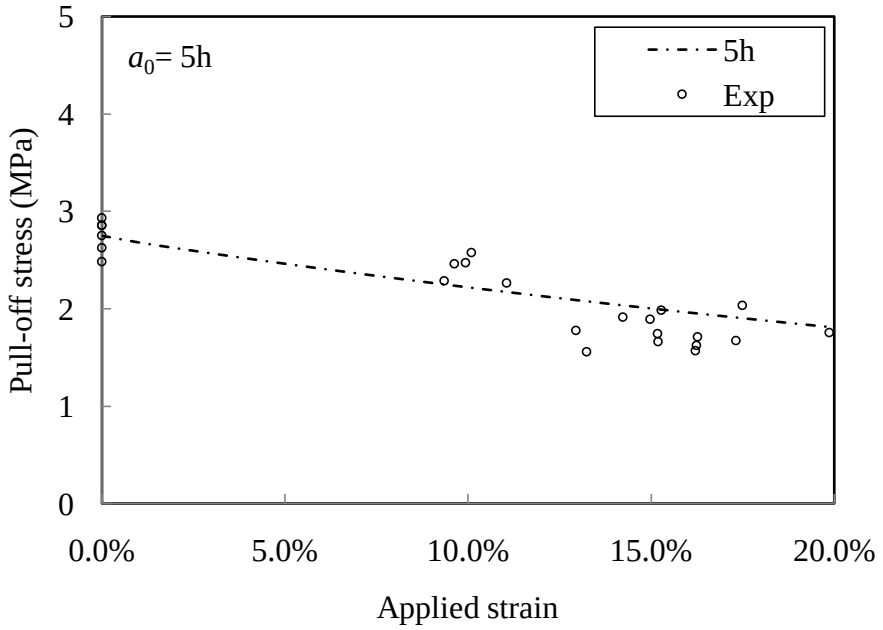

Figure 38 Coating adhesion loss prediction for Material I coated-sheet by analytical method in uniaxial tension load (Coating: App-I, a_0=5h)

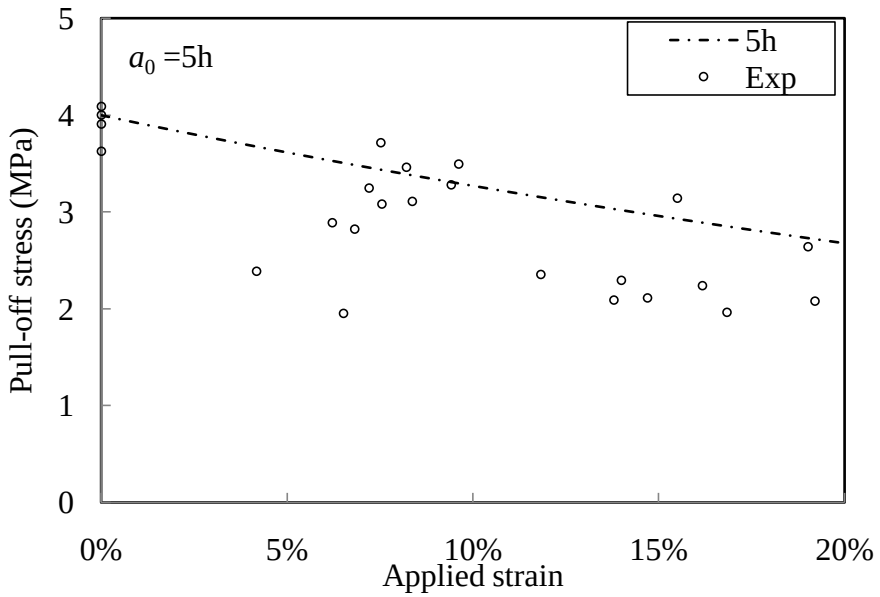

Figure 39 Coating adhesion loss prediction for Material II coated-sheet by analytical method in uniaxial tension load (Coating: App-II, a_0=5h)

4.2 Parametrical study on uniaxial tension mode

To understand how the material properties, coating/substrate thicknesses, and virtual crack length affect the adhesion after deformation, a parametrical study is presented. The investigation is based on a simple model with a virtual crack between a polymer coating and a metal substrate.

In the proposed model, the virtual crack length is one of the parameters used to determine adhesion potential. The adhesion loss shown in Figures 38 and 39 is then calculated based on the assumption of constant adhesion potential. A small virtual crack leads to a small adhesion potential that can be easily disturbed by applied strain. As a

result, the pull-off stress can decrease significantly. The effect of virtual crack length selection is shown in Figures 40 and 41. In addition to the assumed crack length of 5h (5 times the coating thickness and h = 45μm) that was used previously, the virtual crack lengths are specified as a_0 = 2h, 3h, 5h, 10h, and 100h. It can be found that with the exception of a_0 = 2h for Material I, the virtual crack length does not influence the adhesion loss prediction. As the adhesion strength of most industry coatings is high, it is reasonable to assume the virtual crack length a_0 > 3h that lead to a realistic representation of the adhesion potential.

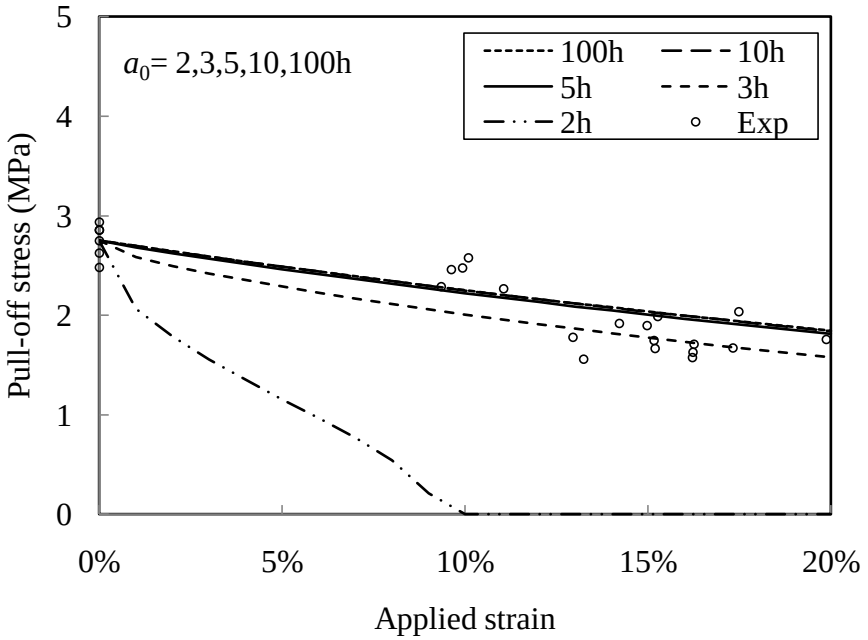

Figure 40 Coating adhesion loss prediction for Material I coated-sheet by analytical method in uniaxial tension load (Coating: App-I)

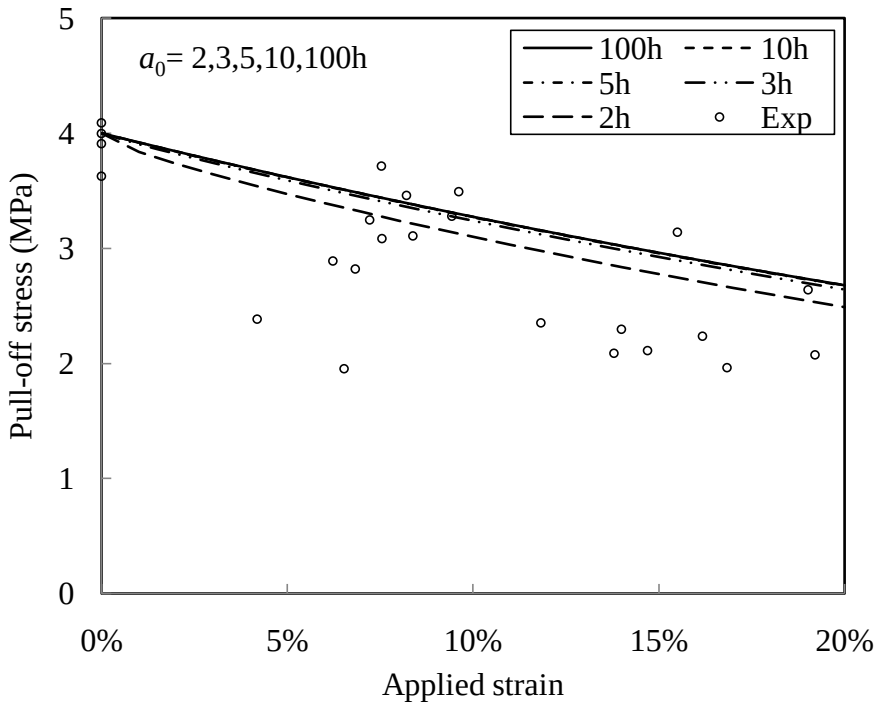

Figure 41 Coating adhesion loss prediction for Material II coated-sheet by analytical method in uniaxial tension load (Coating: App-II)

Parametric study on linear elastic coating/metal substrate

A systematic study is conducted to further investigate the percentage drop of adhesion, in terms of $\sigma_{22\_new}/\sigma_{22\_initial}$, versus applied strain (ε_x) to indicate the coating durability under uniaxial tensile deformation condition. Since the force and moment build up in coated-sheet is caused by the material properties mismatch, the parametric study first focuses on the linear elastic coating on metal substrate. The ratios of Young's Modulus (E_2/E_1,), coating-substrate thickness ratio (h/H), and the virtual crack length (a_0) are considered. In the study, the substrate is steel (E_2 = 210GPa) and the coating

thickness is specified as h = 45μm. Table 5 shows the ratios and values used in the study. The comparisons of the results are shown in Figures 42 to 44.

Table 5 The parametric studies of linear elastic coating on substrates

h/H	E_2/E_1	a_0
1	100	2h
1/10	1000	10h
1/100	10000	100h

h=45μm, E_2=210GPa

From Figure 42, it can be observed that with a small virtual crack length (a_0 = 2h) and higher modulus coating (small E_2/E_1), the adhesion strength drops rapidly after deformation. This is due to a large stress build-up for coating with large elastic modulus. It can also be observed that the adhesion loss is not very sensitive to the coating-substrate thickness ratio (h/H). Figure 43 shows that, with medium virtual crack length (a_0 = 10h), the effect of elastic modulus ratio becomes less prominent. Note that there is no difference in the trend of adhesion loss between E_2/E_1 = 1000 and E_2/E_1 = 10000. The results also show that coating-substrate thickness ratio play a more significant role with increased crack length. For long virtual crack (a_0 = 100h), the adhesion loss prediction is no longer affected by the elastic modulus ratio and the coating-substrate thickness ratio as shown in Figure 44.

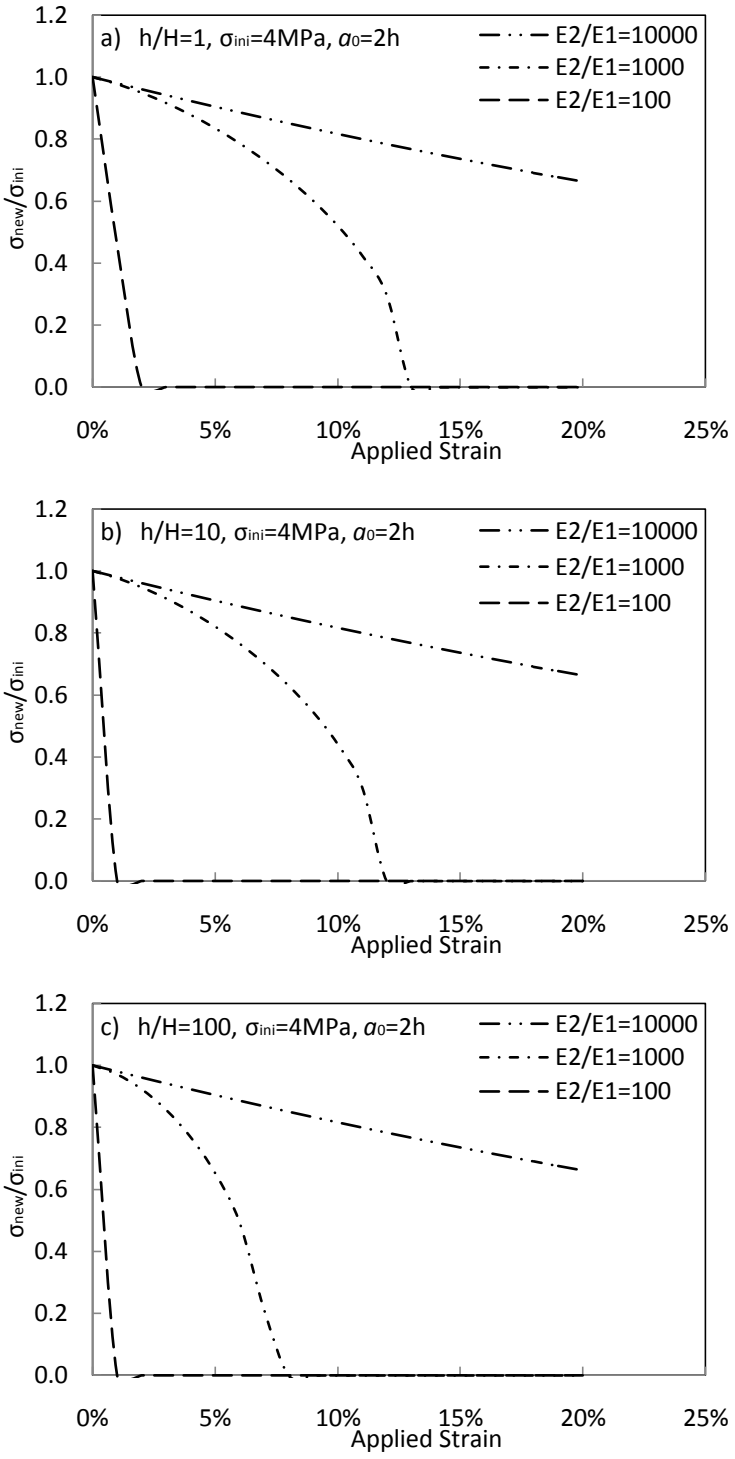

Figure 42 With short virtual crack (a_0=2h) and 4MPa initial pull-off stress, the comparisons of thickness and modulus

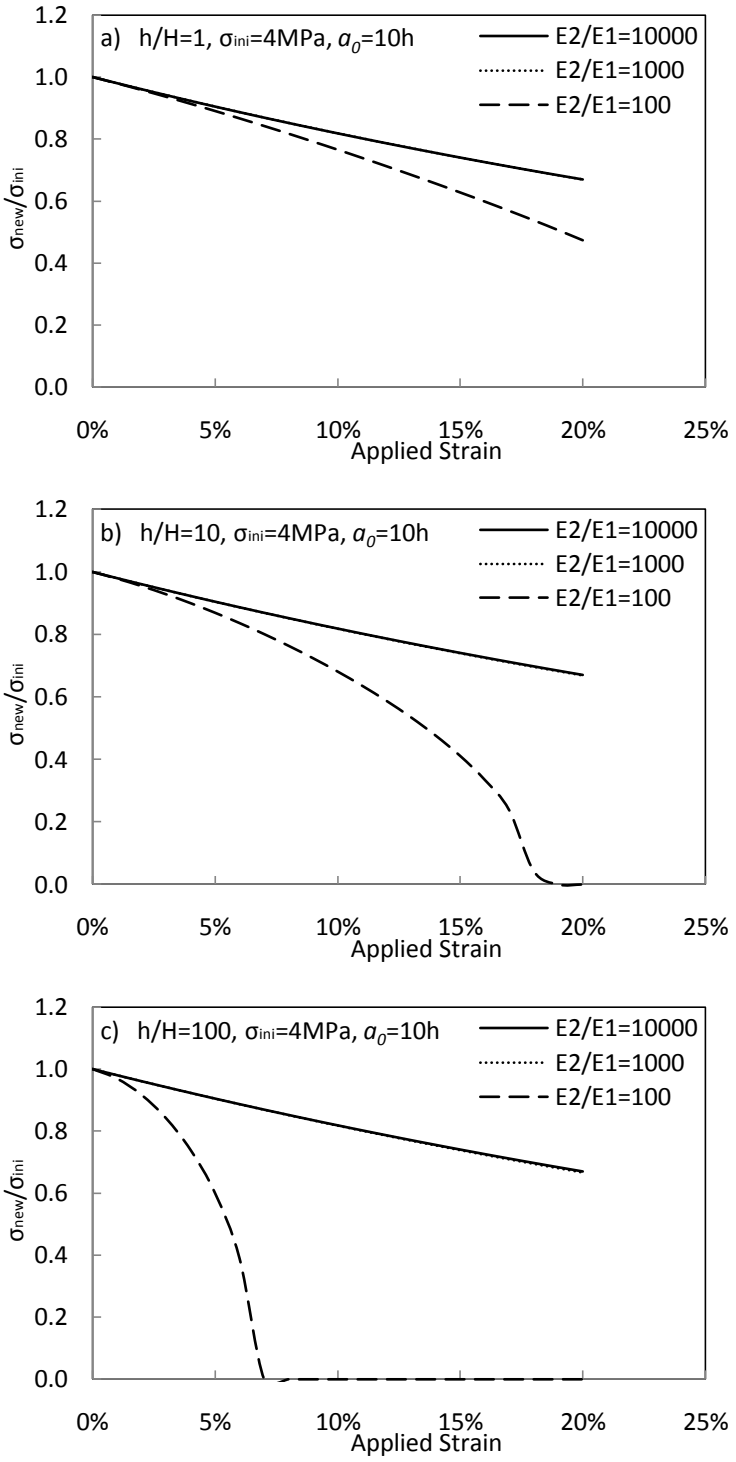

Figure 43 With medium virtual crack (a_0=10h) and 4MPa initial pull-off stress, the comparisons of thickness and modulus

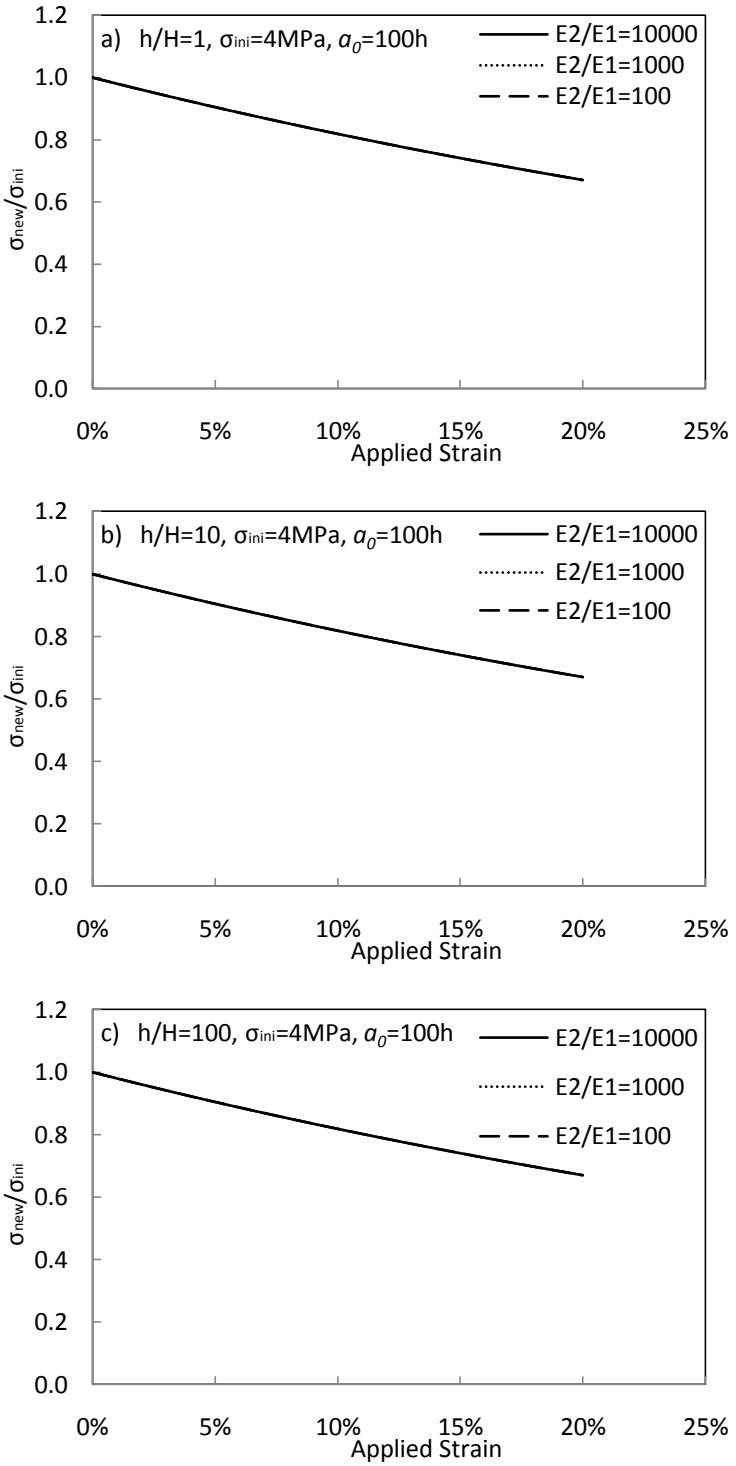

Figure 44 With long virtual crack (a_0=100h) and 4MPa initial pull-off stress, the comparisons of thickness and modulus

Parametric study on coating with Mises solid properties

The results of coating adhesion loss predictions for Material I and II by using approximate Mises solids are shown in Figures 38 and 39. The interfacial virtual crack length effect is also discussed in Figures 40 and 41. Although the primer thickness (~5μm) is relatively small compared to coating (40μm), a further investigation on effects of low primer's modulus is needed.

Three different approximate Mises solid coatings are considered (Figure 45) for second part of parametric study. E_1=1200MPa is a high strain energy coating for App-I (PVDF and polyester); E_1=700MPa is a medium strain energy coating for App-II (PVDF and polyurethane); while E_1=25MPa is a very low strain energy coating (polyurethane only). The coating-substrate thickness ratio (h/H) and the virtual crack length (a_0) are also considered. The substrate is remain the same as steel (E_2 = 210GPa) and the coating thickness is specified as h = 45μm. The comparisons of the results are shown in Figures 46 and 47.

From Figure 46, it indicates that with a small virtual crack length (a_0 = 2h) and higher strain energy coating (E_1=1200MPa, E_2/E_1=175), the adhesion strength drops faster than lower strain energy coating (E_1=25MPa, E_2/E_1=8400) after deformation. This is due to a large stress build-up for coating with higher strain energy. It can also be observed that the adhesion loss is sensitive to the coating-substrate thickness ratio (h/H) with higher strain energy coating (E_2/E_1=175). Figure 47 shows that, with medium virtual crack length (a_0 = 10h), the effect of different Mises solid polymer becomes less prominent. Due to the trend of adhesion loss is not disturbed by the considered

parameters in medium virtual crack (a_0 = 10h), the study of longer virtual crack (a_0 = 100h) is not presented.

Due to Material I and II are coated sheets with coating/substrate ratio around 10 and the results from Figure 47, the parametric study on Mises solid polymer coating are then focused on the following parameters. They are virtual crack length in 2h, 3h, and 5h; three approximate polymer coatings (Figure 45); and two initial pull-off stresses for coated sheets for Material I and Material II.

From Figure 48, it can be observed that for Material I with a smaller initial pull-off stress (2.75MPa), the adhesion strength prediction trends are not disturbed by different Mises solids in 5h crack assumption. When using a smaller interface crack in 3h, those Mises solids give differences in prediction. There is a rapidly drop by interface crack in 2h with higher strain energy solid. This is due to a short interface crack and low initial pull-off stress leads a small adhesion potential, a coating with higher strain energy consumes large amount of adhesion potential when coated sheet subjected to tension deformation load. Material I is polymer coated sheet with PVDF and polyester primer. It concludes that except using very small virtual interface crack (2h), the Mises solid with higher modulus (App-I in Figure 37) has a good prediction in tension deformation load.

Figure 49 indicates that by virtual interface crack in 5h and higher initial pull-off stress (4MPa for Material II), the effect among three approximate properties is less prominent. Only little disturbed is observed at prediction result by 3h interface crack. The prediction by App-II (E_1=700MPa) with crack in 5h and 3h is little over predicting.

It can be observed that strain energy coating property is sensitive to the prediction results by very small interface crack (2h).

It concludes that by only consider coating as PVDF only for both Material I and II with 3h virtual interface crack length, the predictions of adhesion loss are in good agreement for both types of polymer coated sheet under tension deformation load.

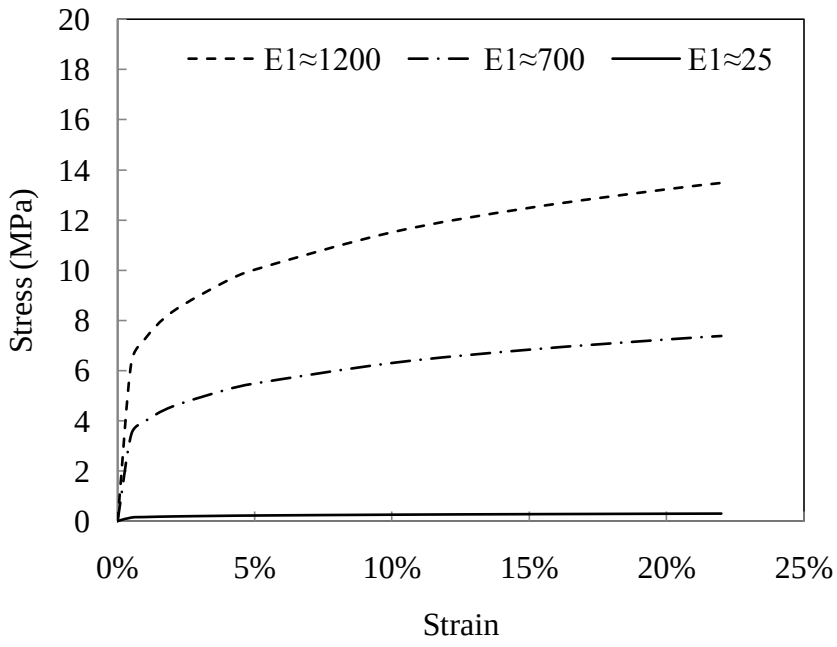

Figure 45 Stress-strain curves for three approximate Mises solid polymer coating. E_1=1200MPa is similar to PVDF and polyester, E_1=25MPa is for elastomeric material (polyurethane), E_1=700MPa is for coating consists of PVDF and polyurethane

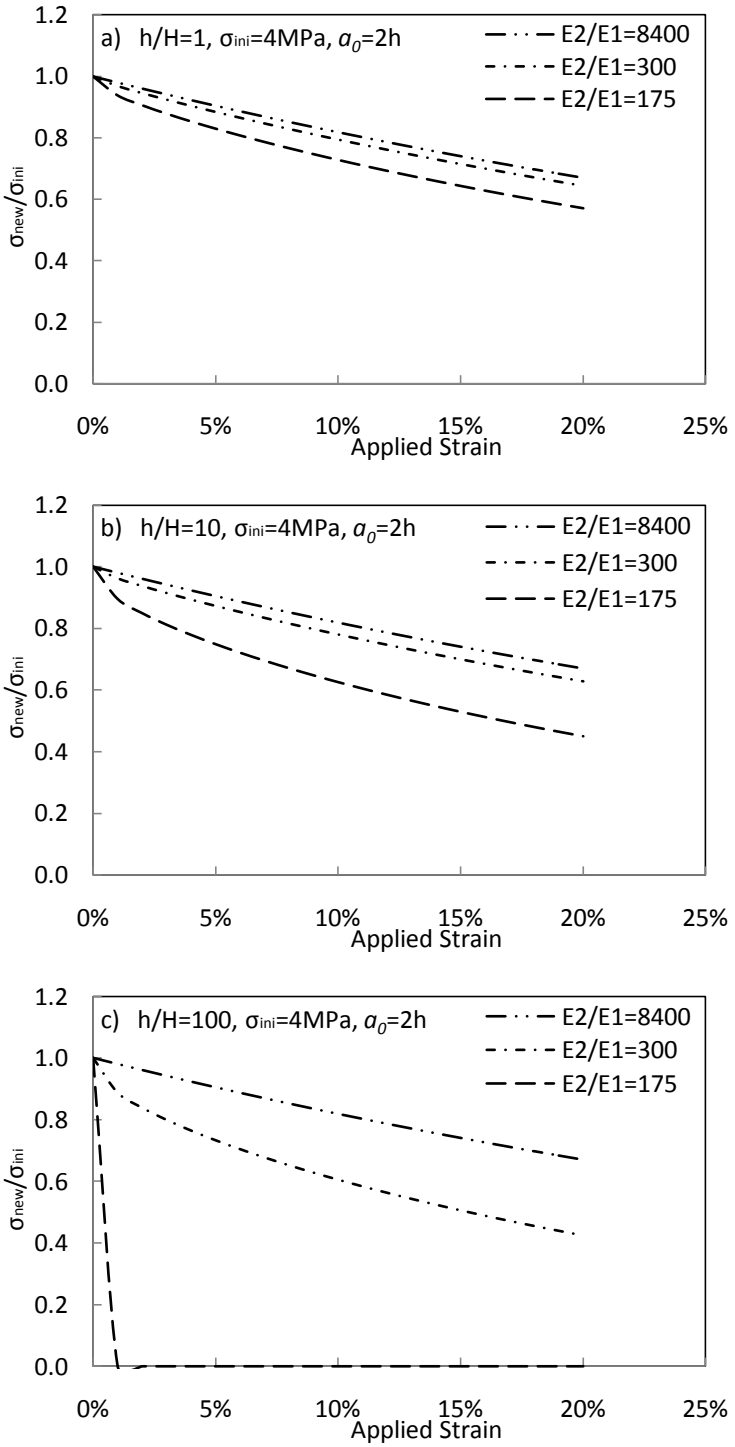

Figure 46 With short virtual crack (a_0=2h) and 4MPa initial pull-off stress, the comparisons of thickness and modulus for approximate Mises solid polymer coating

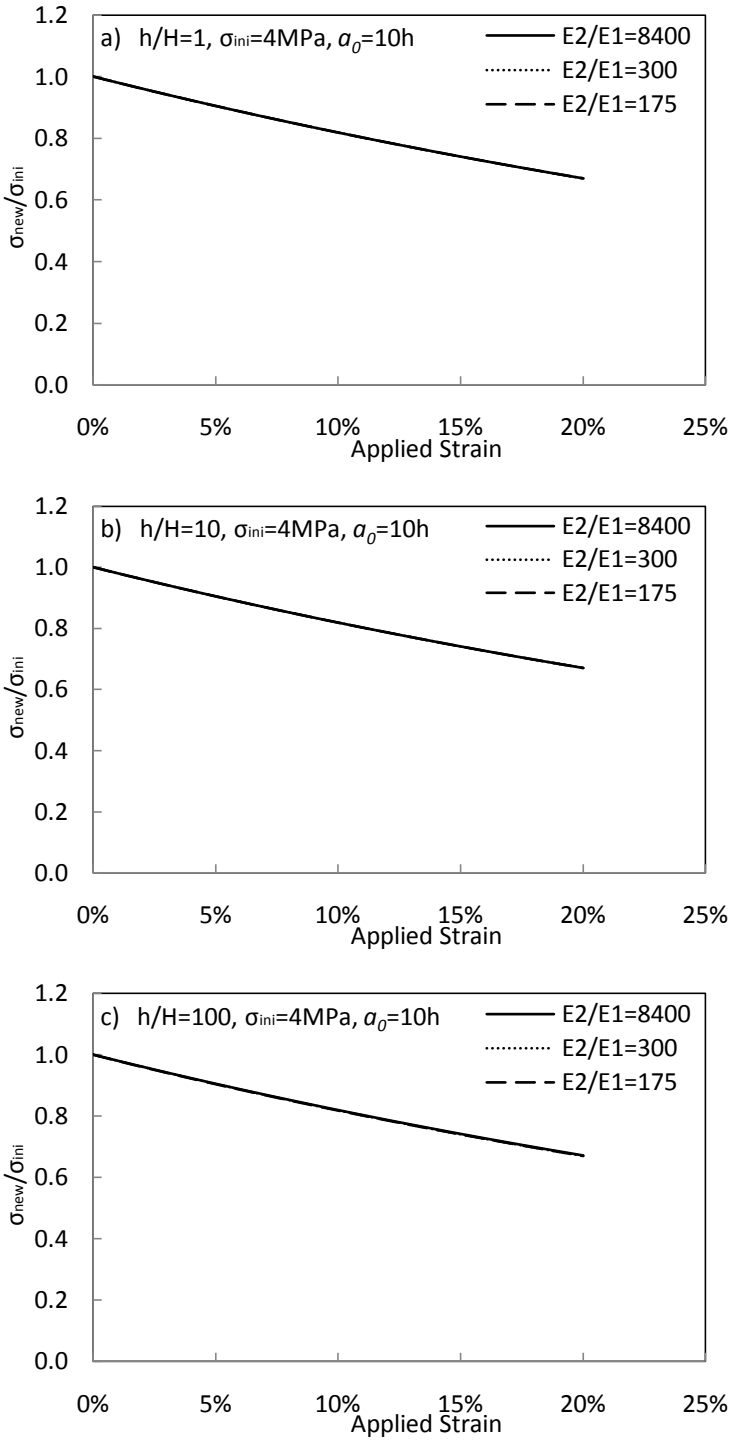

Figure 47 With medium virtual crack (a_0=10h) and 4MPa initial pull-off stress, the comparisons of thickness and modulus for approximate Mises solid polymer coating

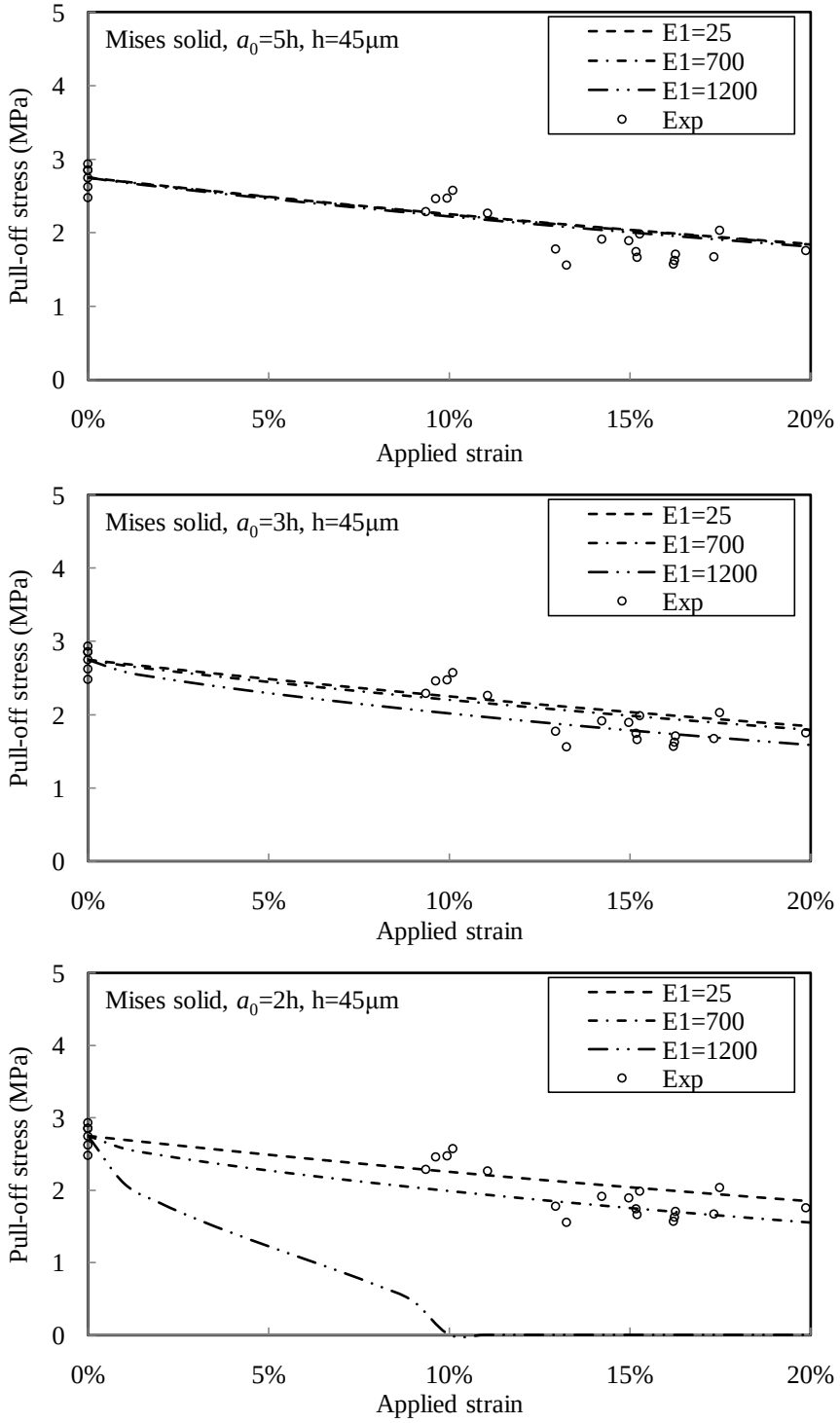

Figure 48 With 2.75MPa initial pull-off stress, the comparisons of virtual crack length and approximate Mises solid polymer coating

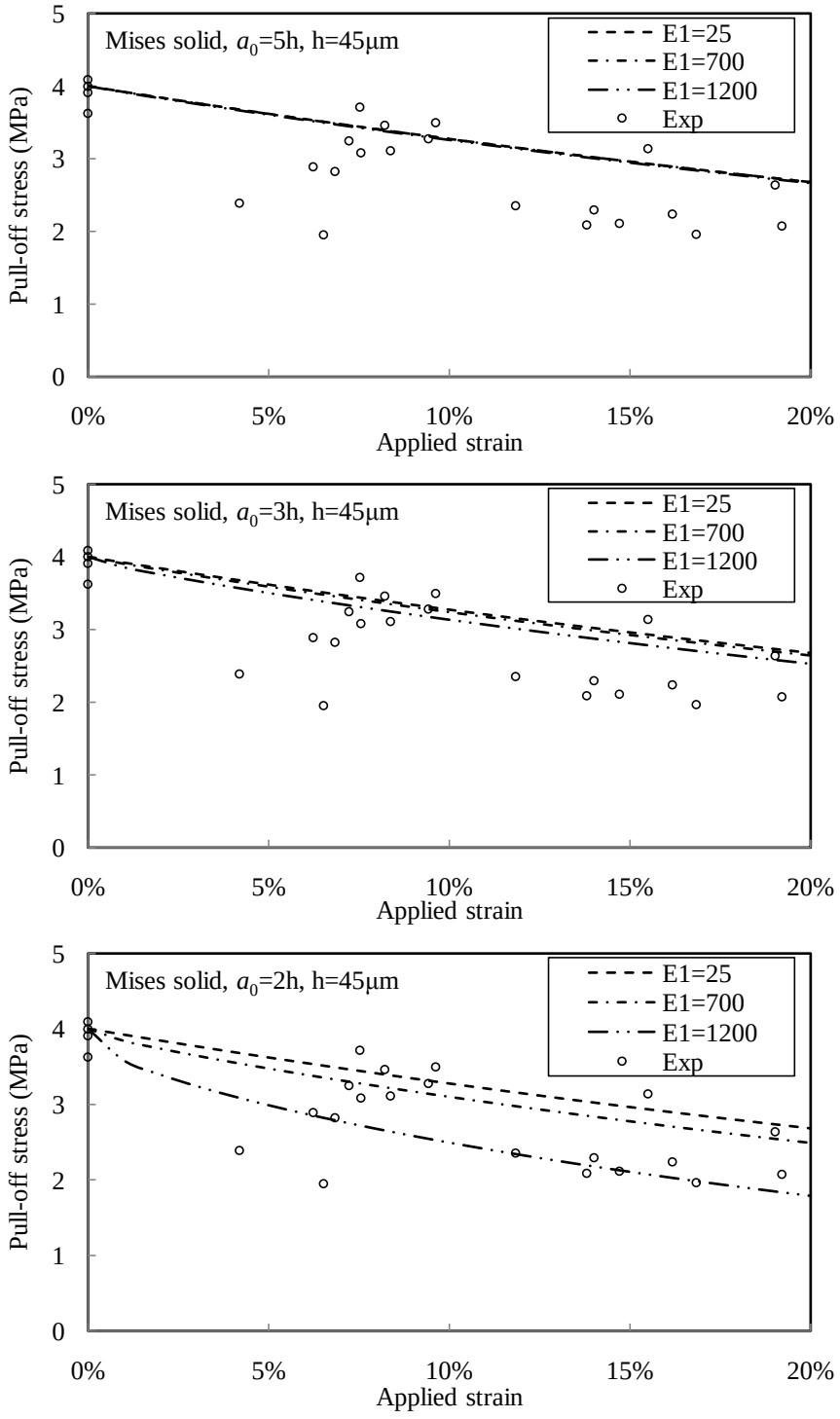

Figure 49 With 4MPa initial pull-off stress, the comparisons of virtual crack length and approximate Mises solid polymer coating

4.3 Discussions

For analytical model predictions, the initial pull-off stress was fixed at 2.75 MPa for Material I coated-sheet and 4.00MPa for Material II coated-sheet. The analytical model predicted an almost linear downward trend for both coated-sheets by using 3h virtual crack and App-I coating property. Both predictions were in a good agreement with the experimental results. Although the analytical method achieved a relatively good prediction in the present study, limitations are also observed.

- The proposed method uses a virtual crack to represent the entire defect along the interface. The approach does not consider any void nuclear nor crack propagation during the deformation process.
- Stress calculation is based on plane-strain condition that is not the exact condition obtained from the uniaxial tensile loading in the experiments.

5. NUMERICAL METHOD

In Section 4, an analytical method was presented to predict the adhesion loss in uniaxial tension deformation mode. The mathematical model was in plane-strain assumption and can only describe the specimens subjected to tensile strain parallel to the interface crack and up-lifting stress normal to the coating surface. In a practical sheet metal forming process, the material is subjected to various deformation modes including bi-axial tension and tension-compression (deep drawing). In this Section, the proposed virtual crack model is combined with numerical methods to describe the complex loading condition and coating adhesion loss. The model predictions are compared to the experimental results presented in Section 3.

5.1 Mathematical model of single interface crack problem

An interface crack model under plane-strain assumption [47] is first considered. As shown in Figure 50, the σ_{22}^{∞} and σ_{12}^{∞} are far away from the interface crack, while σ_{22} and σ_{12} are stress field at distance "*r*" from the interface crack tip.

Based on the works of Rice [47], the energy release rate G induced by interface crack "2*a*", two-layered material, with applied stress fields can be obtained by:

$$G = 0.5(1-\beta^2)[(1-{\nu_1}^2)/E_1 + (1-{\nu_2}^2)/E_2]({K_I}^2 + {K_{II}}^2) \qquad (5\text{-}1)$$

where E_i and υ_i (i=1,2) are young's modulus and Poisson's ratio, respectively. $\beta = 0.5\{[\mu_1(1-2\nu_2) - \mu_2(1-2\nu_1)]/[\mu_1(1-\nu_2) + \mu_2(1-\nu_1)]\}$, K_I and K_{II} are the real and imaginary part of the stress intensity factor, respectively. The stress intensity factor

can be calculated either by the faraway stress field, σ_{22}^{∞} and σ_{12}^{∞}; or the near tip stress field σ_{22} and σ_{12}. They are

$$K_I + iK_{II} = (\sigma_{22}^{\infty} + i\sigma_{12}^{\infty})(1 + 2i\varepsilon)(\pi a)^{0.5}(2a)^{-i\epsilon} \tag{5-2}$$

$$K_I + iK_{II} = (\sigma_{22} + i\sigma_{12})/[(2\pi r)^{-0.5}(r^{i\epsilon})] \tag{5-3}$$

where, $\epsilon = (1/2\pi)\ln[(1-\beta)/(1+\beta)]$, $i = \sqrt{-1}$, and 'r' is the distance from crack tip.

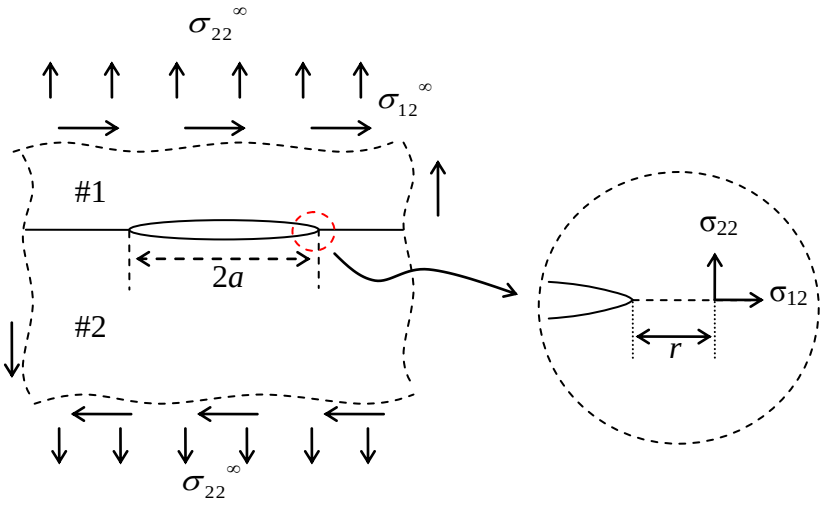

Figure 50 Interface crack model for energy release rate calculation [47, 50, 51]

In the Pull-off test, an up-lift stress normal to the coating surface is applied, and the maximum pull-off stress is recorded after the coating is completely separated from the substrate. The adhesion potential of a certain type of coating-substrate system is defined as the energy release rate G that a virtual interface crack length, $2a$, subjected to only

maximum pull-off stress. In Figure 50, the faraway stress σ_{22}^{∞} is the maximum pull-off stress obtained experimentally. By assuming a virtual interface crack "$2a$", the adhesion potential (or $G_{initial}$) of this two-layered materials can be expressed by modifying Equation (5-1) and (5-2).

$$G_{initial} = 0.5(1-\beta^2)[(1-\nu_1{}^2)/E_1 + (1-\nu_2{}^2)/E_2](K_I{}^2 + K_{II}{}^2) \qquad (5\text{-}4)$$

where $K_I + iK_{II} = (\sigma_{22}{}^{\infty})(1+2i\varepsilon)(\pi a)^{0.5}(2a)^{-i\varepsilon}$, and σ_{22}^{∞} is the initial pull-off stress obtained experimentally.

When coated-sheet subjected to a particular deformation mode, for example, the uniaxial tensile mode (Figure 51a), there will be a stress discontinuity near interface. As such a stress discontinuity can cause the coating adhesion to deteriorate, it is believed that, after deformation, a lower stress (compared to the initially measured stress) will be needed to pull-off the coating.

Figure 51c illustrated that pull-off test conducted on the coated-sheet with applied deformation. The energy release rate of the specimen shown in Figure 51c can be obtained by the method proposed in Section 4. Alternatively, the energy release rate G_{temp} for the case shown in Figure 51c can be evaluated by using stress intensity factors. According to Equation (5-3), stress intensity factor (K) can be obtained by the near crack tip stress field, σ_{22} and σ_{12}. This near tip stress fields are dominated by the new pull-off stress, $\sigma_{22\_new}^{\infty}$, and force and moment created by applied strain, ε_x. The energy release rate G_{temp} due to $\sigma_{22\_new}^{\infty}$ and ε_x is,

$$G_{temp} = 0.5(1-\beta^2)[(1-\nu_1{}^2)/E_1 + (1-\nu_2{}^2)/E_2](K_I{}^2 + K_{II}{}^2) \qquad (5\text{-}5)$$

where $K_I + iK_{II} = (\sigma_{22} + i\sigma_{22})/[(2\pi r)^{-0.5}(r^{i\epsilon})]$, and σ_{22} and σ_{12} are the near tip stress.

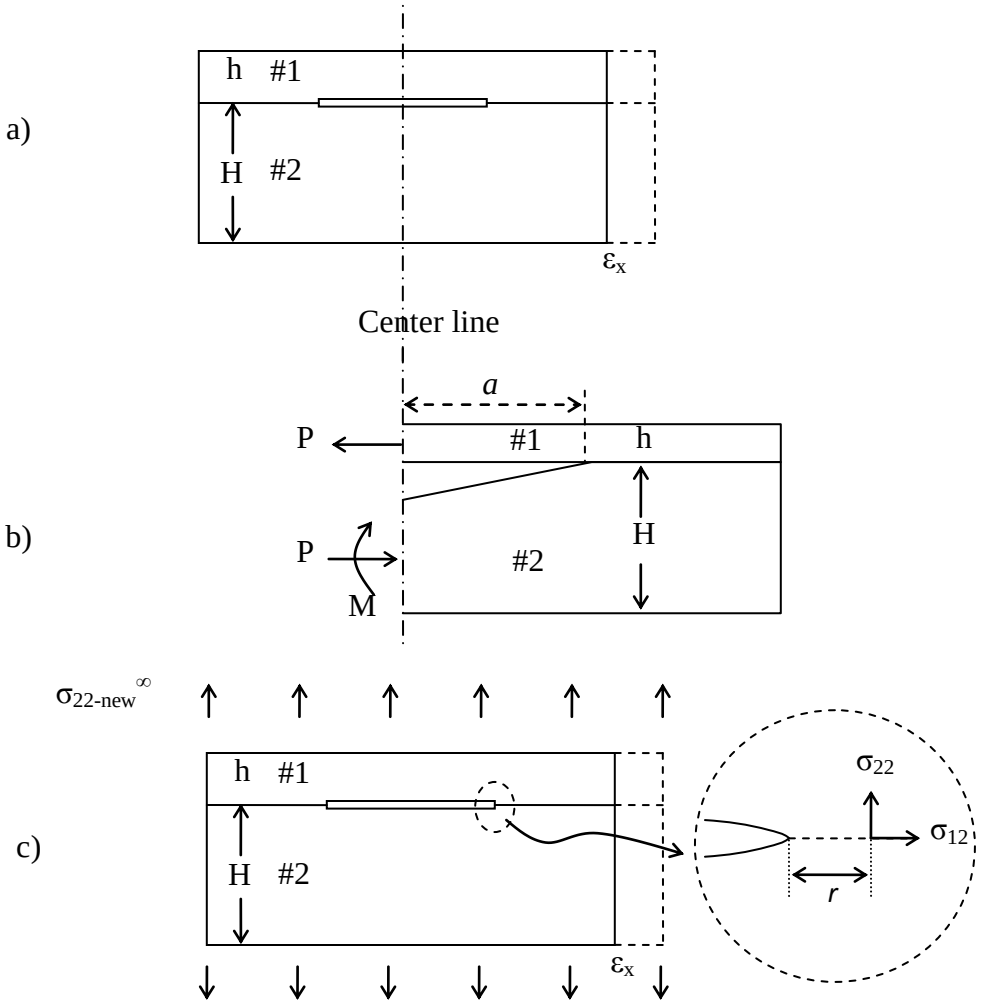

Figure 51 Tensile deformation mode. a) the coated-sheet with a permanent deformation b) residual force and moment caused by material mismatch

This near tip stress in Figure 50 can be obtained by equalizing Equation 5-2 and 5-3. However, the near tip stress field in Figure 51c, or complicated deformation condition is difficult to compute analytically. Therefore, the approach proposed here is to obtain these near tip stress fields numerically. For coated material subjected to different

deformation modes, the complex boundary conditions can be modeled and the near tip stress field can be calculated by using a commercial finite element analysis tool such as ABAQUS®.

The proposed numerical method for adhesion loss prediction is summarized in the flow chart shown in Figure 52. Step #1 is to acquire the initial pull-off stress (σ_{22}^{∞}) of a coating on the coated sheet metal with no plastic deformation. In Step #2, a finite element model with virtual interface crack is built. The details of finite element analysis are described in next section. The initial pull-off stress (σ_{22}^{∞}) is used as the boundary condition to up-lift the coating. The near tip stress field (σ_{22}, σ_{12}, and σ_{23}) at distance "*r*" are obtained by numerical method, and the stress intensity factor can be found by Equation (5-3) and (5-6). By Equation (5-7), the initial energy release rate $G_{initial}$ (which is the adhesion potential) can be obtained and can be used for later calculation. In Step #3, a certain deformation boundary conditions are applied on the initial finite element model (the same model used in Step #2). The deformed model obtained in Step #3 is then subjected to an assumed "new pull-off stress" ($\sigma_{22\text{-}new}^{\infty}$). The "new" near tip stress field is then calculated numerically in Step #5; and by Equations (5-3), (5-6), and (5-7), the temporary energy release rate G_{temp} can be determined. Compare the calculated G_{temp} with the initial adhesion potential $G_{initial}$, the accuracy of the assumed "new pull-off stress" can be evaluated. If the difference between G_{temp} and $G_{initial}$ is within a certain tolerance, the " new pull-off stress" is consider as a good estimate of the coating pull-off stress for the deformed coated sheet. Otherwise, another "new pull-off stress" is assumed for a new iteration to start from Step #4.

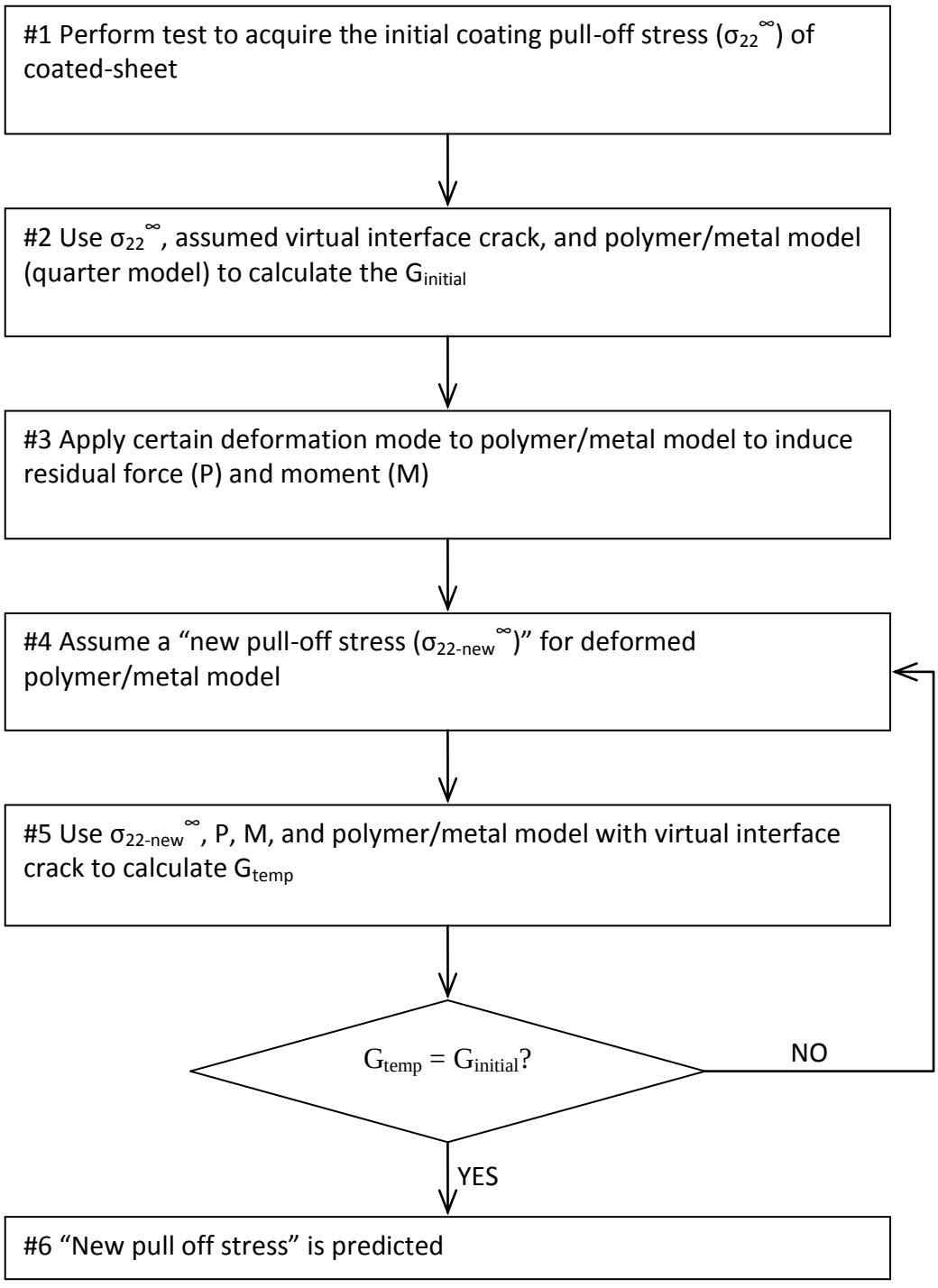

Figure 52 Numerical method flow chart

In Section 4, the analytical model is able to predict the adhesion loss under uniaxial tension mode. There are two parts in predicting the adhesion loss due to uniaxial tension deformation mode. Figure 36b shows the loading of force and moment due to material properties mismatch, while Figure 36c shows the loading of another moment (M_{up}) resulting from the up-lifting stress acting on top of the coating.

To compare the analytical and numerical model predictions, the numerical procedure is used to analyze a model similar to Figure 36b and Figure 36c. The simulation process is shown in Figures 53 and 54. As shown in Figure 53a, uniaxial tension loading is first applied. As a result, stress discontinuity can be observed as shown in Figure 53b. The up-lifting stress is then converted into another moment, M_{up}, acting at the end of coating (Figure 54). The entire stress field is simulated by finite element method, and the energy release rate is calculated by Equation (5-1), and (5-3) with the near tip stress field obtained from FEA as shown in Figure 55.

The comparison of predicted coating adhesion loss under uniaxial tension loading, based on analytical approach and numerical procedure, is presented in Figure 56. The numerical result has the same linear downward trend compare to the analytical method.

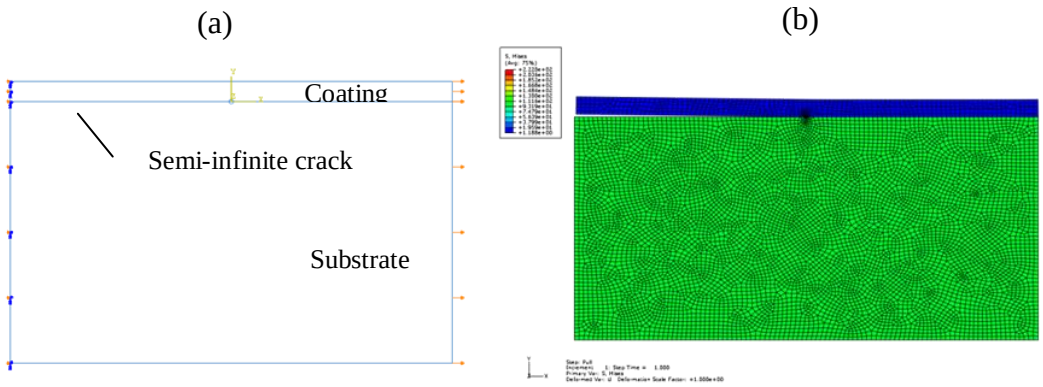

Figure 53 Semi-infinite interface crack model under applied uniaxial tension loading

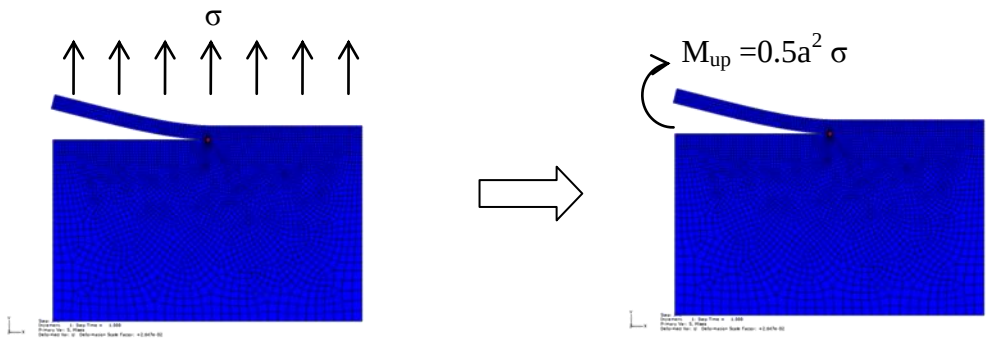

Figure 54 Up-lifting stress converted into moment M_{up} acting on the coating

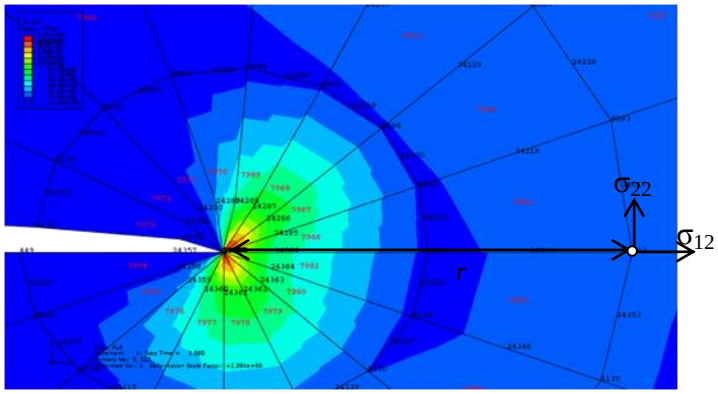

Figure 55 Detail mesh view near crack tip and the position of near tip stress field

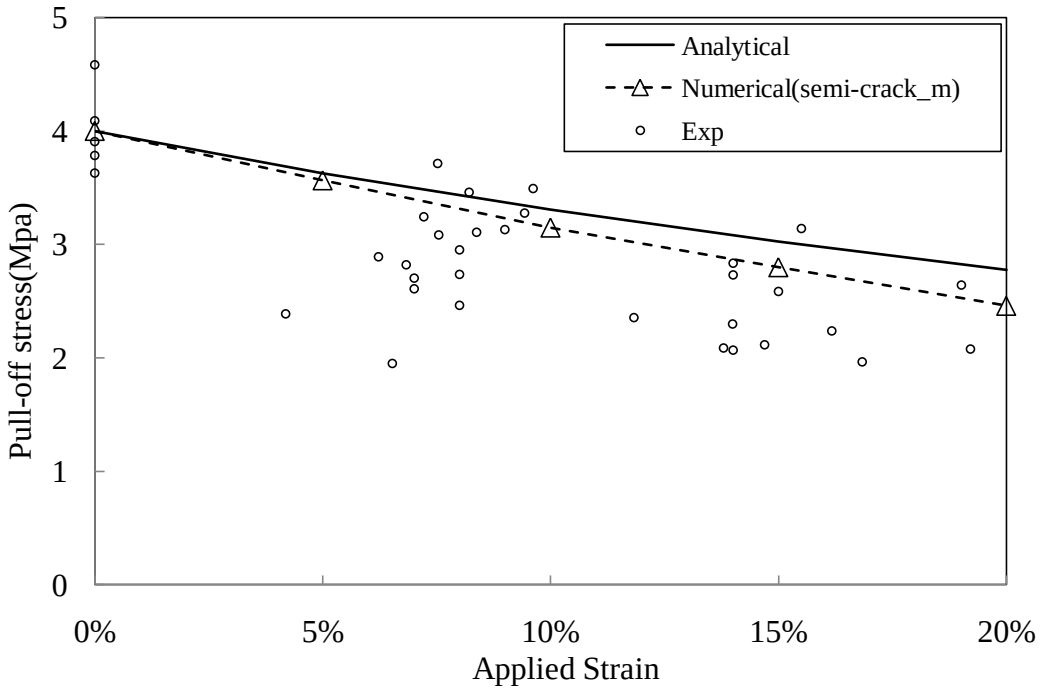

Figure 56 Comparison of coating adhesion loss predicted by analytical and numerical methods

In a practical sheet metal forming process, the material is subjected to complex deformation modes. An example of the interface crack model is shown in Figure 57. The coated material is subjected to in-plane strains and an up-lift stress is applied on the top surface. The energy release rate for the three-dimensional model cannot be expressed by the stress intensity factor in Equation 5-3 alone, and there must be a third stress intensity factor term, K_{III} [65-69].

$$K_{III} = \sigma_{23}(2\pi r)^{0.5} \tag{5-6}$$

Thus, the energy release rate G for three dimensional model is

$$G = [(1-\beta^2)/E^*]\left(K_I{}^2 + K_{II}{}^2\right) + (1/2\mu)K_{III}{}^2 \tag{5-7}$$

where $1/E^* = 1/2\ (1/\bar{E}_1 + 1/\bar{E}_2\ )$, $\bar{E}_i = E_i/(1-\nu_i{}^2)$, i=1,2. $1/\mu = 1/2\ (1/\mu_1 + \mu_2\ )$

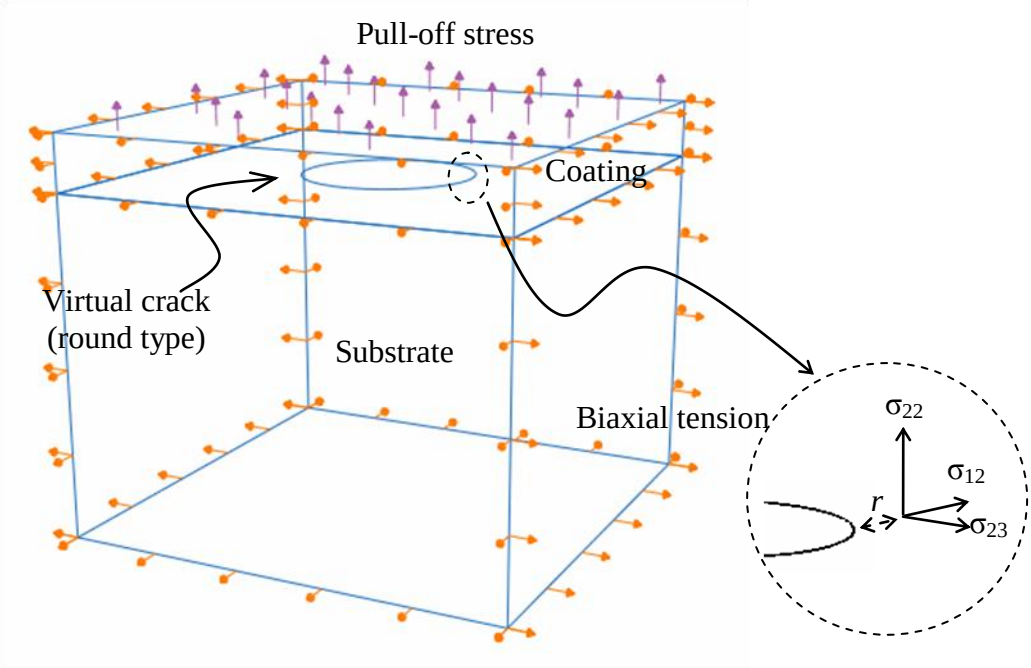

Figure 57 Three dimensional model of interface crack problem

5.2 Finite Element Model

Geometry, mesh and element type

The metal stud used in pull-off test is 10mm in diameter. To describe the problem more realistically, a quarter size finite element model is then built with the dimension of 500μm (length) by 500μm (width) by 629μm (45μm in coating and 584μm in substrate thickness). A round type crack with 45μm radius is chosen as depicted in Figure 58. The crack area is partitioned into several areas to get a finer mesh near crack tip (Figure 59). A detailed mesh view, including part of coating and substrate is shown in Figure 60.

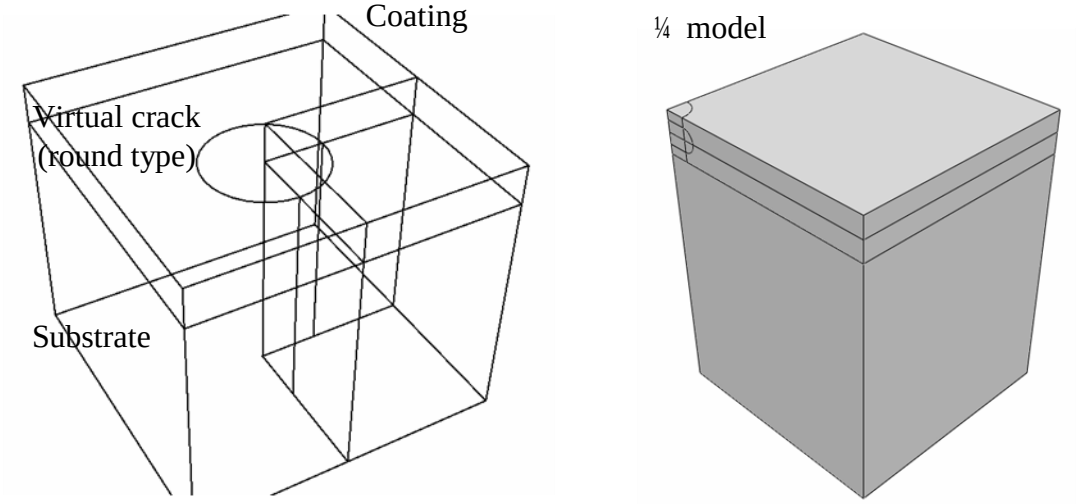

Figure 58 Round type virtual interface crack in 3D model and 1/4 size of model

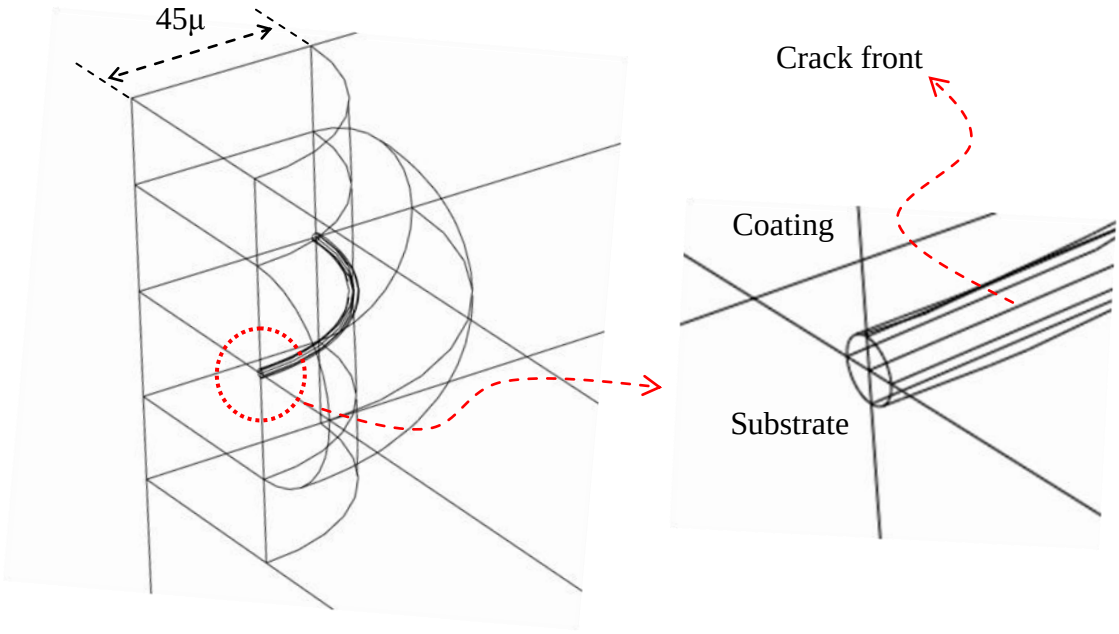

Figure 59 Interface crack and near crack tip partition

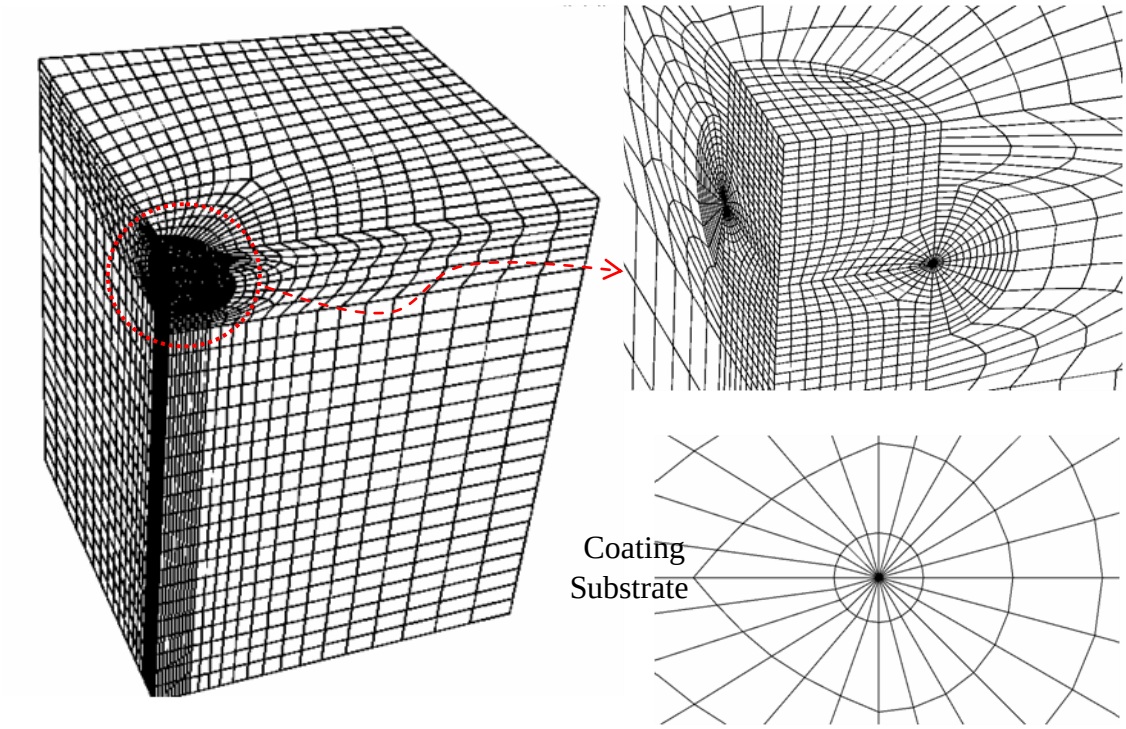

Figure 60 Detail mesh views of 1/4 model

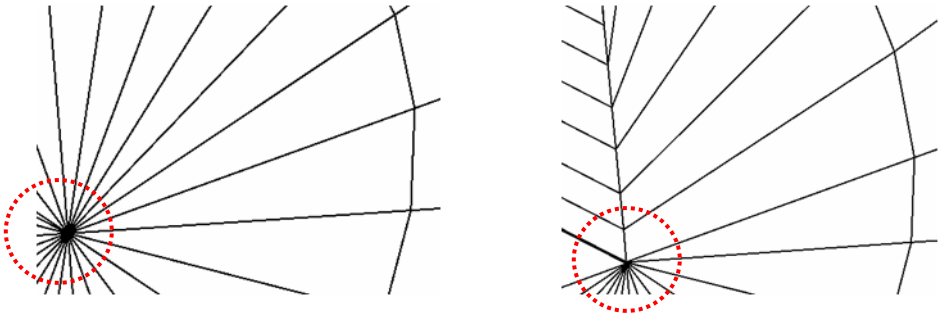

a) Before deformation b) After deformation

Figure 61 Duplicate nodes at crack tip and collapse into crack front. a) nodes at tip edge were collapsed into same point b) the tip nodes separated when crack opened

Shared nodes are used to describe the interface. The element type is C3D8R, which is an 8-node 3D element with reduce integration point. At crack tip, the edges of elements were collapsed into the same position (Figure 61). Elements around the crack tip also had 8 nodes, only two of the edges were collapsed into same position (Figure 61a), the nodes at tip edge separated when crack was opened (Figure 62b).

Material laws and analysis steps

In the numerical investigation, Material I and Material II (two different coated-sheets tested in Section 3) are used. The polymer coatings are modeled as Mises solid. To simplified the problem and shorten the computation time, both coatings and substrate are assumed isotropic. Table 6 shows the material properties for finite element analysis.

Table 6 Mechanical properties of Coating Material I, Material II and steel substrate

Material	Material I (Gray)		Material II (Brown)		Steel	
Elastic	E_1 (MPa)	ν_1	E_2 (MPa)	ν_2	Es (MPa)	ν_s
	1264	0.37	694	0.37	210000	0.30
Plastic	Stress (MPa)	Strain	Stress (MPa)	strain	Stress (MPa)	strain
	6.32	0	3.47	0	400	0
	7.27	0.005	3.98	0.005	420	0.02
	8.35	0.015	4.57	0.015	500	0.20
	9.59	0.035	5.25	0.035	520	0.26
	10.02	0.045	5.49	0.045		
	11.51	0.095	6.31	0.095		
	12.49	0.145	6.84	0.145		
	13.23	0.195	7.25	0.195		
	13.48	0.215	7.39	0.215		

H=584μm, h=45μm; *Initial adhesion*: Gray=2.75MPa, Brown=4.00MPa

Boundary conditions

Boundary conditions are applied to surfaces of the model as shown in Figure 62. To reduce simulation time, a quarter model with prescribed symmetry condition in two surfaces is shown in Figure 62. To describe the applied deformation modes, displacement loading condition for uniaxial tension, biaxial tension, or tension-compression modes can be specified. An example of biaxial tension and pull-off stress

loading is shown in Figure 63. The analysis module used is ABAQUS standard static, and the boundary condition and the loading steps are described in Table 7.

Table 7 Analysis steps for simulating the stress fields under deformation modes

STEP	XY-sym.	YZ-sym.	YZ-disp.	XY-disp.	XZ-bot.	Coating Top
INITIAL	v	V				
LOAD	v	V	v*	v*		
UNLOAD	v	V	x	x		
PULL-OFF	v	V	x	x	v	v

v: create and propagate, x: inactive, *: depends on the deformation modes

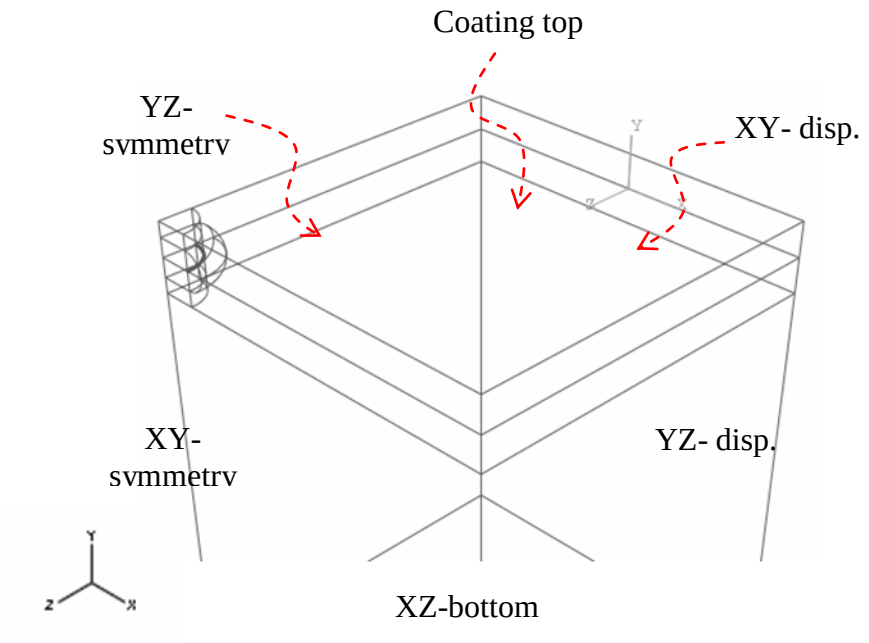

Figure 62 Boundary condition surfaces

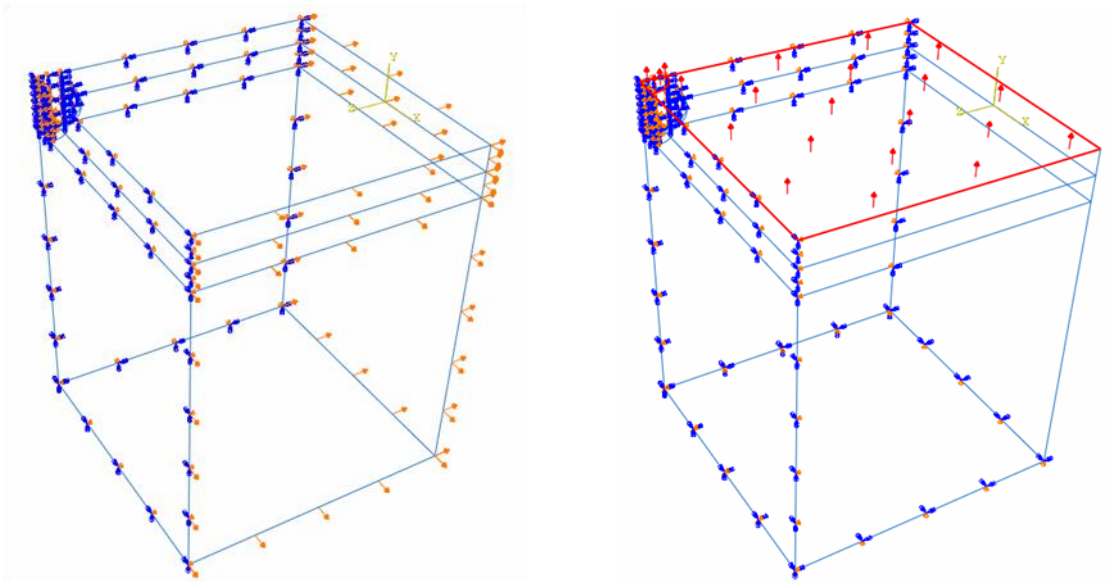

a) Applied biaxial tension b) Pull-off stress

Figure 63 Examples of applied boundary conditions. a) apply biaxial tension strain, b) apply pull-off stress on coating surface

Stress field at near tip position and energy release rate computation

Simulation results of an initial pull-off loading are shown in Figure 64. The crack is opened due to the up-lift stress (Figure 64a). A large gradient in the stress field near the crack front area can be observed. The energy release rate G is computed from the stress field at the 45^{0} position, 0.001mm away from the round type crack front (Figure 64b).

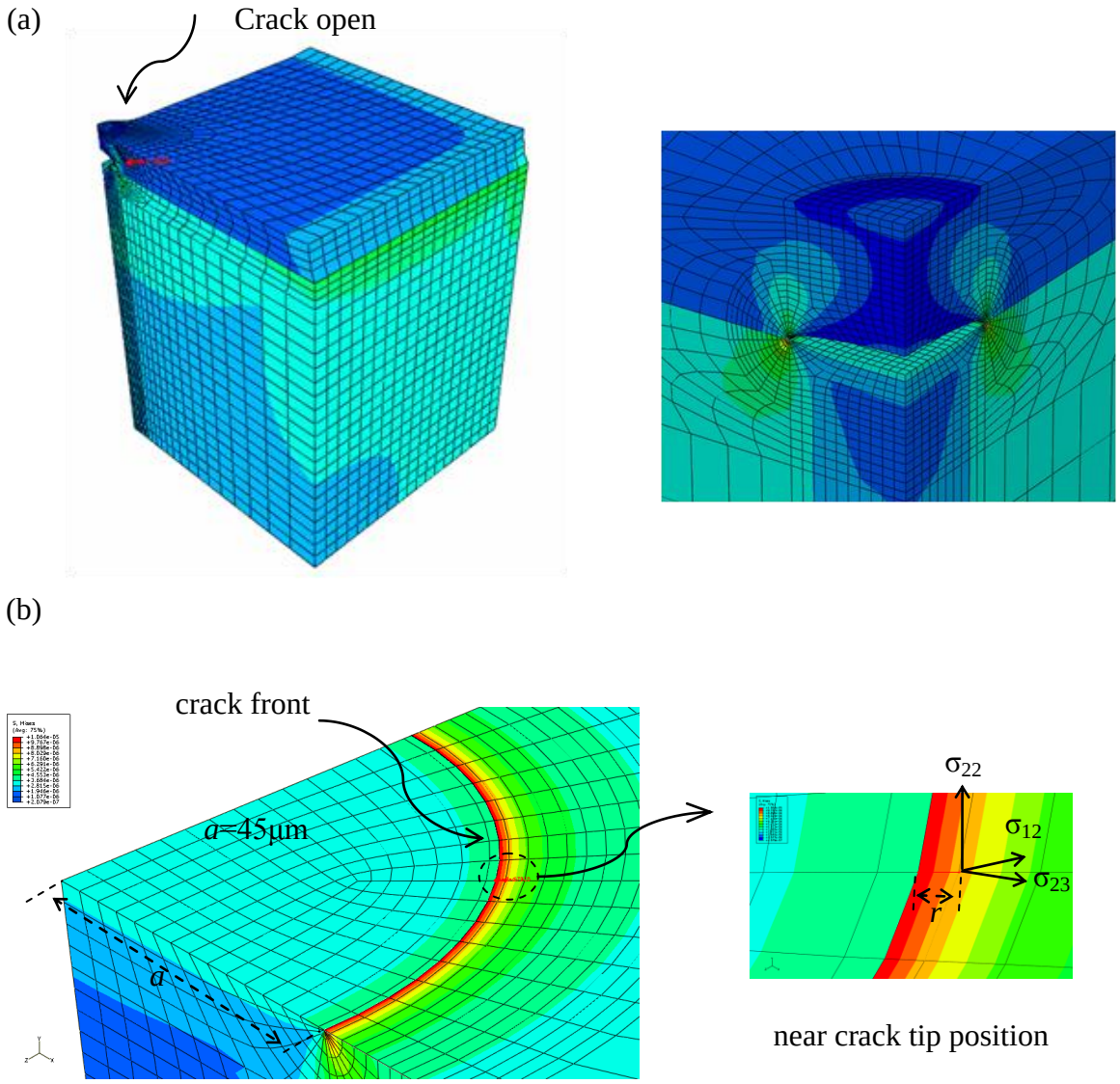

Figure 64 Near tip stress-field for energy-release rate computation. a) crack opened by up-lift stress and internal stress b) near tip stress field point for computation of the energy release rate G

5.3 Results of numerical analysis

Experiments conducted in Section 3 were in three major deformation modes. To predict coating adhesion loss in those modes successfully, iterative search for the "new

pull-off stresses" for each applied strain condition is performed. Figure 61 illustrate the different stress fields obtained from three applied strain condition. For uniaxial tension modes, 5, 10, 15, and 20% strains are applied on both Material I and II. The result of 10% applied strain in uniaxial tension mode is shown in Figure 65a. A stress discontinuity along the interface and a stress concentration near the crack tip can be observed. For biaxial tension mode, the stress field result of 10% and 5% applied major and minor strain is shown in Figure 65b. For tension-compression mode, an example of 10% tension strain on one direction and 10% compression strain on the other is shown in Figure 65c.

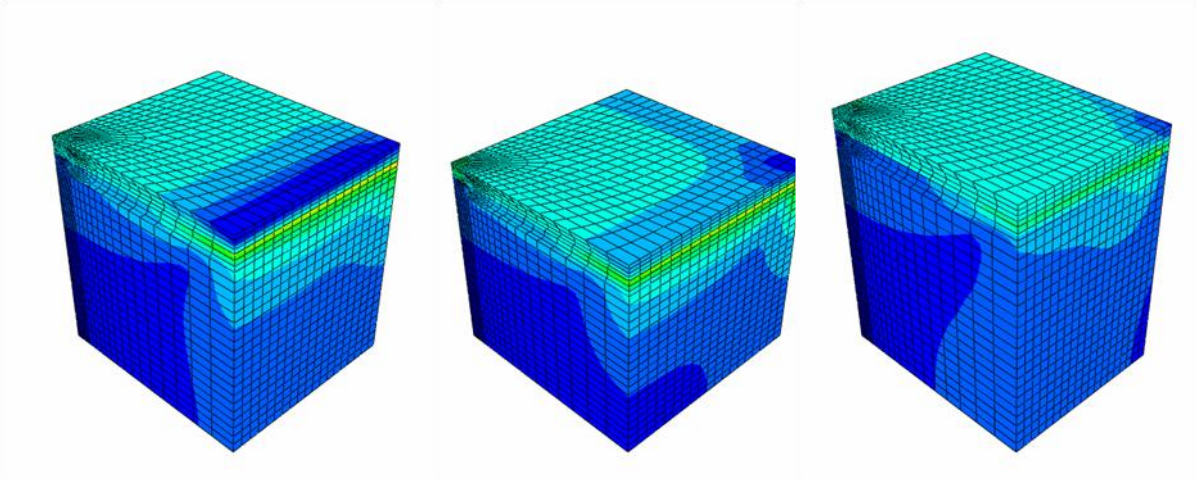

(a) Uniaxial Tension (10%) (b) Biaxial Tension (10%, 10%) (c) Tension-Compression (10%, -10%)

Figure 65 Stress field distribution and shapes of three types of deformation modes. a) apply 10% tension strain on one direction b) apply 10% tension strain on both directions c) apply 10% tension strain on one direction and 10% compression strain on another direction

The proposed numerical model is then used to predict the new pull-off strengths of specimens with various plastic strains including uniaxial tension, biaxial tension, and tension-compression modes. The results of coating adhesion loss predictions for both coated sheets are shown in Figures 66 to 71 and compared with experimental results.

In Figure 66, it can be observed that for the coated material with polyester primer (Material I), the three dimensional (3D) prediction of adhesion loss under uniaxial tension mode has a drop at applied strain of less than 5% and the adhesion stress remains almost undisturbed at higher applied strain. The 3D prediction is in good agreement with the experimental results around 10% applied strains; and the 3D model over-predicts the adhesion stress for specimen with larger than 15% applied strain. In comparing with analytical model, both 3D and analytical models have similar results within 5% applied strain. The analytical model prediction is closer to the experimental results at applied strain larger than 15%. For coating with polyurethane (Figure 67), the 3D numerical model predicts a large drop at small applied strain (less than 5%) and then a liner downward trend for larger applied strain. The large initial drop can be attributed to the large material property mismatch. In comparing with analytical model, the 3D numerical approach predicts a larger adhesion loss. It can be observed that the experimental data is sporadic with a downward trend. The 3D numerical approach agrees well with experimental results in general and very well at applied strain larger than 10%. It is also indicated that there is difference in prediction by analytical method and 3D numerical method in uniaxial tension loading. The analytical and 3D numerical methods were developed based on different assumptions and different calculation routes. The analytical

method obtains the energy release rate (adhesion potential) from force and moment due to plastic deformation and additional moment due to up-lift stress normal to the coating surface; while 3D numerical method calculates the energy release rate (adhesion potential) from the near tip stress field resulted from applied strain and up-lift stress. The analytical model uses interface crack in plane-strain assumption; while a round type crack along the interface plane is assumed in the 3D numerical model.

The 3D numerical method is built to predict the coating adhesion loss under complex deformation mode. The virtual crack is a single coin type crack along the interface plane. It should be noted that, for uniaxial tension loading, a single virtual crack can also be represented in a 2D plane strain model (Figure 72). Using the same procedure shown in the flow chart in Figure 52, the adhesion loss predictions for Material I and II based on plane strain model are shown in Figures 66 and 67 (legend marked as 2D numerical). It can be observed that while the 2D plane strain model predicted a larger adhesion loss, the overall trends are in good agreement.

Numerical prediction under biaxial tension mode is shown in Figures 68 and 69. It is shown that the predictions are in good agreements with experimental results for both Material I and II. For both coated materials, the adhesion loss is relatively large when stretched to (5%, 5%) biaxial strain. And it can be observed that there is no significant change in adhesion stress between (5%, 5%) and (10%, 10%) applied biaxial strain. This phenomenon was successfully predicted with proposed numerical approach.

In Figure 70, two applied strain conditions are used to demonstrate the coating adhesion loss under tension-compression mode. The prediction results for Material I at

(5%, -5%) and (15%, -10%) applied strain are slightly above the experimental measurement. As shown in Figure 71, a similar prediction trend is also observed for Material II at (10%, -5%) and (15%, -10%) applied strain.

Although the model can slightly over/under predict adhesion loss at certain applied strain conditions, the predictions agree relatively well with the experimental results considering the variation of the pull-off test data. It can be concluded that the numerical approach with an assumed virtual interface crack is capable of predicting the adhesion loss in complex forming process involving uniaxial tension, biaxial tension, and tension-compression deformation modes.

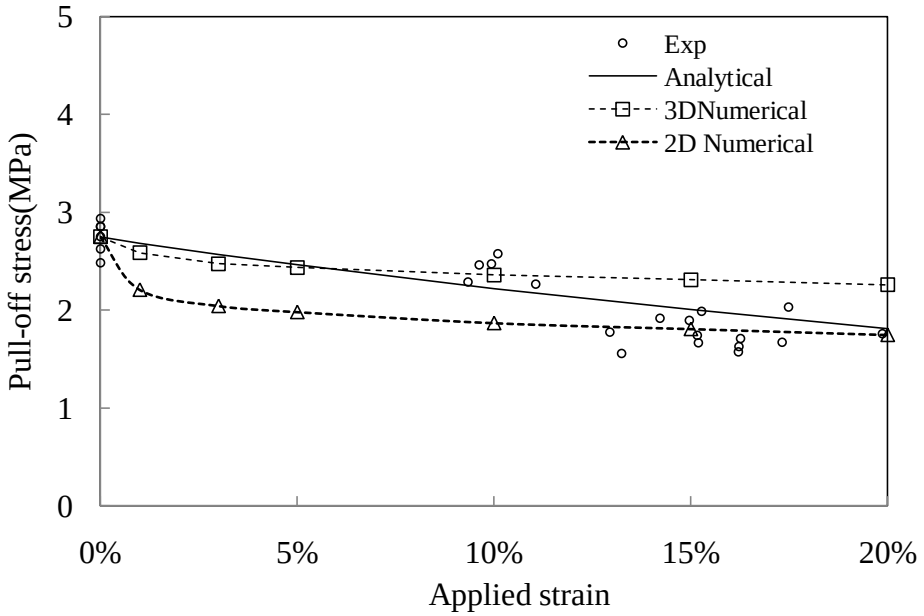

Figure 66 Experimental and prediction results in uniaxial tension modes for Material I (Gray) coated sheet

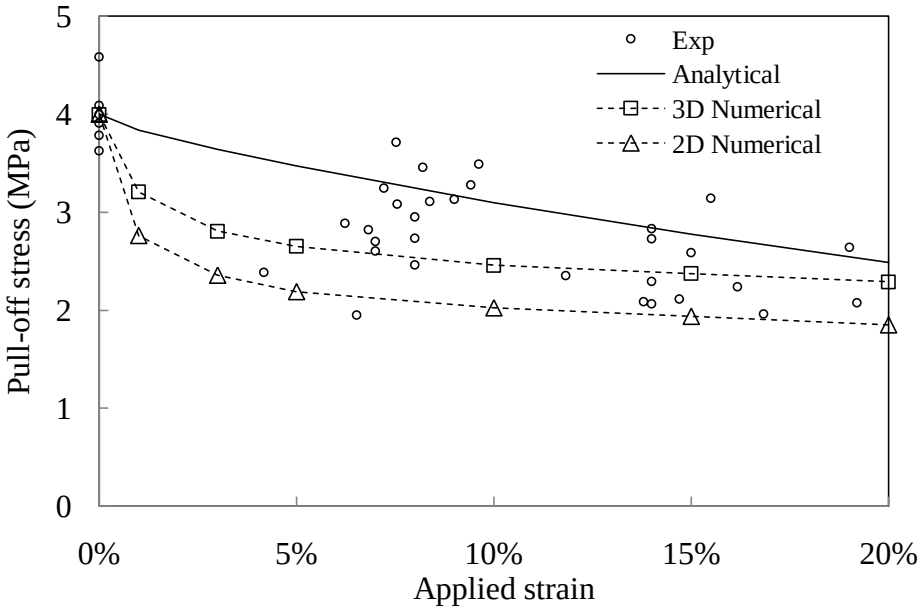

Figure 67 Experimental and prediction results in uniaxial tension modes for Material II (Brown) coated sheet

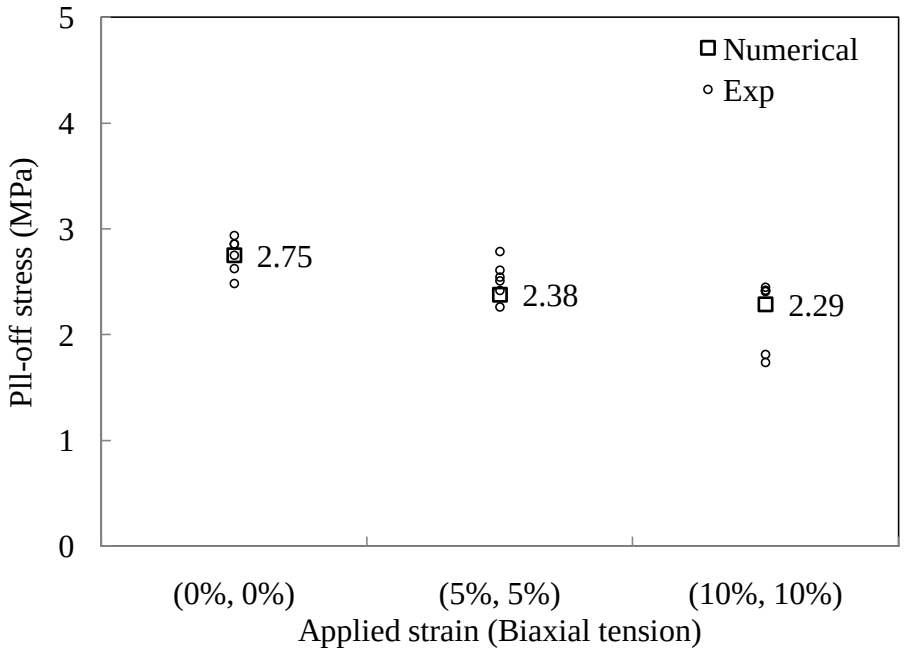

Figure 68 Experimental and prediction results in biaxial tension modes for Material I (Gray) coated-sheet

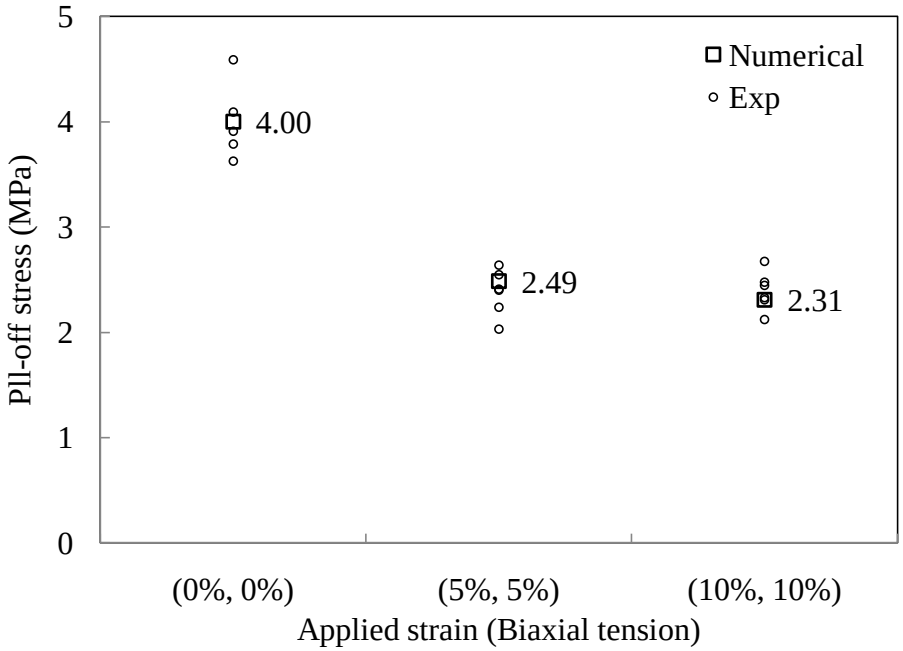

Figure 69 Experimental and prediction results in biaxial tension modes for Material II (Brown) coated-sheet

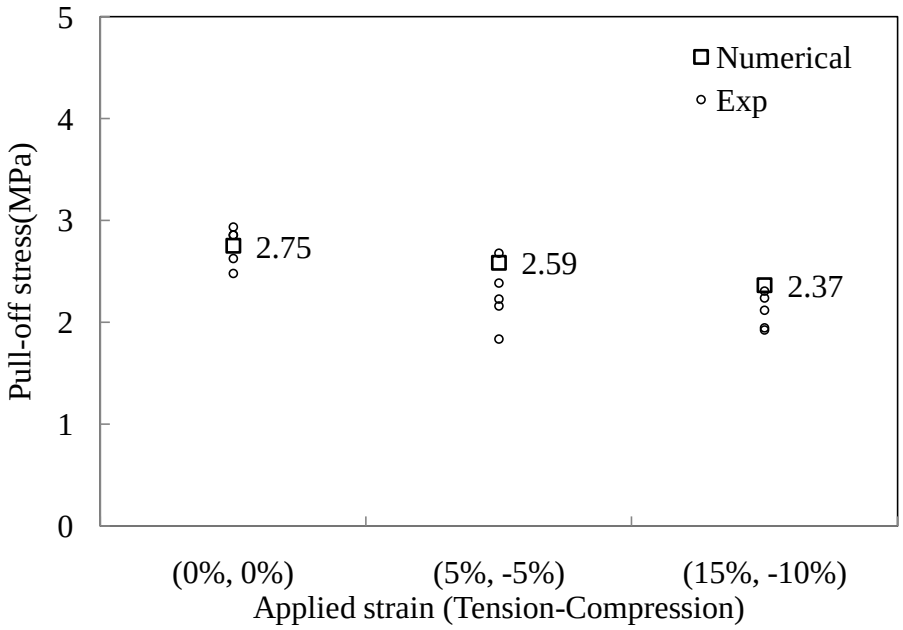

Figure 70 Experimental and prediction results in tension-compression modes for Material I (Gray) coated-sheet

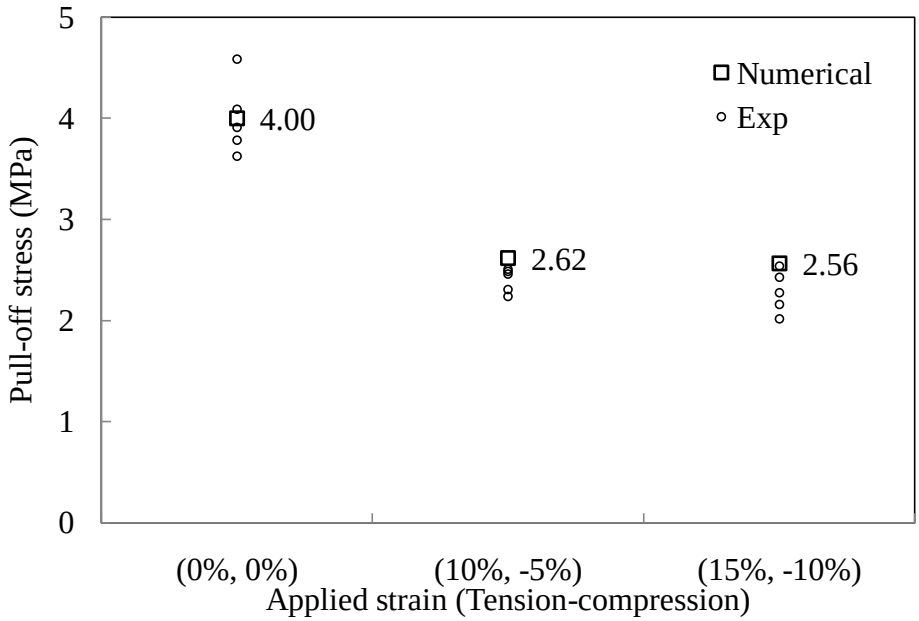

Figure 71 Experimental and prediction results in tension-compression modes for Material II (Brown) coated-sheet

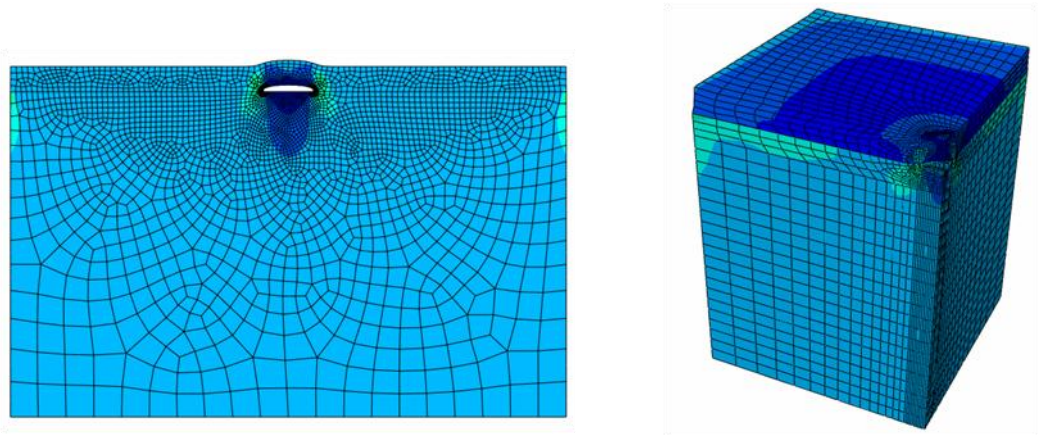

Figure 72 Single virtual crack model (2D) and round shape interface crack model (3D)

6. CONCLUSIONS AND SUGGESTIONS FOR FUTURE WORKS

This Section summarizes the finding and contribution of the research presented in this dissertation. Suggestions for future works are also discussed.

6.1 Conclusions

The application of polymer coated sheet metal in stamping has resulted in the need for a better understanding of coating adhesion after sheet metal forming process. In this dissertation, a methodology for predicting coating adhesion loss was developed and validated.

Through experiments, the research first investigated if the coating adhesion can be affected by plastic deformation induced during sheet metal forming process. The pull-off test was chosen to measure the adhesion strength of polymer coating quantitatively. The pull-off stresses of two PVDF coatings with different primers (polyester and polyurethane) on sheet steel substrates were tested. The experimental work included various deformation modes. Special specimens and testing procedures such as sequential stretching and modified Yoshida tests were developed to obtain the desired deformation modes such as uniaxial tension, biaxial tension, and tension-compression. It was found that, prior to any straining; the coating with polyurethane primer exhibited a higher initial adhesion strength than the coating with polyester primer. It was also observed that, for both materials and in all deformation modes, the coating adhesion strength is reduced after plastic deformation.

In the present research, the coating's bonding/fracture energy is considered as the adhesion potential defined by a virtual interface crack and a pull-off stress. Thus, the initial pull-off test result can serve as an input for the calculation of the adhesion potential that represents the property of the coating-substrate interface. Based on the concept of adhesion potential and the assumption of virtual crack, the second part of the dissertation presents the development of an analytical model for adhesion loss prediction. In the model, it is assumed that debonding would occur when the applied load and the up-lifting stress lead to a fracture energy exceeding the known adhesion potential (calculated from the initial pull-off test). The mathematical model is derived from semi-infinite interface fracture mechanics formula. Adhesion loss prediction was made for specimens loaded in uniaxial tension deformation mode. It was found that the analytical results are in good agreement with experimental measurements for both tested materials. A parametric study was also conducted to investigate the effects of virtual crack size selection, the coating-substrate thickness ratio, and the mechanical property of the coating material.

The scope of the analytical model is limited to predicting adhesion loss of specimens subjected to uniaxial tension only. The capability of the model has to be extended to cover various deformation modes to become useful. The last part of the research attempted to address this issue. A numerical approach was proposed to combine mathematical models and finite element analysis to predict the pull-off stress of the coating after various deformation conditions. A circular virtual interface crack was used in three-dimensional finite element model. Based on the stress field calculated in the

finite element simulation and the mathematical model describing the pull-off load, adhesive potential can be calculated to predict adhesion loss. The proposed approach was evaluated for uniaxial tension, biaxial tension, and tension compression deformation modes. Compare to experimental results, it was found that the methodology is capable of achieving very good predictions of coating adhesion loss.

The present investigation has contributed to a better understanding of the effects of plastic deformation on coating adhesion. From the study, it can be concluded that plastic deformation can be detrimental to coating adhesion. However, a complete separation of coating from substrate can hardly occur through sheet forming alone. This finding agrees well with the observation in coated sheet stamping practice where metal fracture almost always precedes coating delamination. Therefore, prediction of complete debonding of coating is not of primary interest. Extending prior results in interface fracture mechanics, the present work allow quantitative evaluation of coating adhesion loss due to sheet forming processes. It is clear that the applicability of the methodology is not limited to the materials used in the present study. The proposed approach can also be adopted to facilitate the development of coating systems.

6.2 Suggestions for future works

Although the present work demonstrated that a good prediction of coating adhesion loss can be achieved, a number of issues are worthy of further investigation.

- Currently, pull-off tests are conducted to evaluate coating adhesion before and after deformation. As adhesion can be evaluated via other means such as lap

shear test, further exploration in the experimental evaluation of adhesion is suggested.

- Although the deformation of the sheet metal work-piece is typically characterized by the major and minor strains, the sheet metal commonly experiences bending during the deformation process. Therefore, the effect of bending on coating adhesion deserves further investigation.
- While the numerical approach can handle more complex problems and can lead to more accurate analysis results, analytical models allow a more in depth understanding of the interaction among material parameters and loading conditions. The current analytical model is limited to uniaxial tension deformation. Future efforts can be made to extend the existing analytical model into other deformation modes.
- Polymer coated sheet metal is essentially a layered material system. With increasing interests in the application of metal-polymer-metal sandwich material in industry, development of multi-layered model to study the issues in forming sandwich material warrants further exploration.

REFERENCES

[1] R. Vayeda and J. Wang, Adhesion of coatings to sheet metal under plastic deformation, International Journal of Adhesion and Adhesives, 2007; 27: 480-492.

[2] R. Drufke, An introduction to coil coating, Metal Finishing, 2006; 104: 35-37.

[3] F. Graziano, Coil and sheet coating, Metal Finishing, 2000; 98: 175-179.

[4] R. Seija, Bottom-line benefits of prepainted metal, Finishing Today, 2007; 83: 20-23.

[5] J. DeVries, Prepainted metal offers 10 advantages, Industrial Paint and Powder, 2006; 82: 22.

[6] ASTM-D3359, Test methods for measuring adhesion by tape test, ASTM International, 2009.

[7] T. Chang, E. A. Sproat, Y.-H. Lai, N. E. Shephard and D. A. Dillard, Test method for accelerated humidity conditioning and estimation of adhesive bond durability, Journal of Adhesion, 1997; 60: 153-162.

[8] C. Sun, M. D. Thouless, A. M. Waas, J. A. Schroeder and P. D. Zavattieri, Ductile-brittle transitions in the fracture of plastically-deforming, adhesively-bonded structures. Part I: Experimental studies, International Journal of Solids and Structures, 2008; 45: 3059-3073.

[9] R. C. Ostergaard, B. F. Sorensen and P. Brondsted, Measurement of interface fracture toughness of sandwich structurees under mixed mode loading, Journal of Sandwich Structure and Materials, 2007; 9: 445-466.

[10] P. G. Charalambides, J. Lund, A. G. Evans and R. M. McMeeking, A test specimen for determing the fracture resistance of bimaterial interface, Journal of Applied Mechanics, Transactions ASME, 1989; 56: 77-82.

[11] Y. Guan, Y. Xia and F. Xu, Interface fracture property of PEO ceramic coatings on aluminum alloy, Surface and Coatings Technology, 2008; 202: 4204-4209.

[12] M. D. Thouless, The effects of transverse shear on the delamination of edge-notch flexure and 3-point bend geometries, Composites Part B: Engineering, 2009; 40: 305-312.

[13] Q. D. Yang, M. D. Thouless and S. M. Ward, Elastic-plastic mode-II fracture of adhesive joints, International Journal of Solids and Structures, 2001; 38: 3251-3262.

[14] C. Sun, M. D. Thouless, A. M. Waas, J. A. Schroeder and P. D. Zavattieri, Rate effects in mode-II fracture of plastically deforming, adhesively bonded structures, International Journal of Fracture, 2009; 156: 111-128.

[15] M. R. Begley, D. R. Mumm, A. G. Evans and J. W. Hutchinson, Analysis of a wedge impression test for measuring the interface toughness between films/coatings and ductile substrate, Acta mater., 2000; 48: 3211-3220.

[16] J. J. Vlassak, M. D. Drory and W. D. Nix, A simple technique for measuring the adhesion of brittle films to ductile substrates with application to diamond-coated titanium, J. Mater. Res., 1997; 12: 1900-1910.

[17] J. J.-A. Wang, I. G. Wright, M. J. Lance and K. C. Liu, A new approach for bimaterial interface fracture toughness evalution, Journal of Pressure Vessel Technology, 2008; 130: 1-9.

[18] J.-A. J. Wang and K. C. Liu, An innovative technique for evaluating fracture toughness of graphite materials, Journal of Nuclear Materials, 2008; 381: 177-184.

[19] S. S. V. Kandula, C. D. Hartfield, P. H. Geubelle and N. R. Sottos, Adhesion strength measurement of polymer dielectric interfaces using laser spallation technique, Thin Solid Films, 2008; 516: 7627-7635.

[20] A. V. Pocius, Adhesion and adhesives technology: an introduction, 1997.

[21] ASTM-D1002, Apparent shear strength of single-lap-joint adhsively bonded metal specimens by tension loading (metal-to-metal), ASTM International, 2005.

[22] M. Takiguchi and F. Yoshida, Deformation characteristics and delamination strength of adhesively bonded aluminum alloy sheet under plastic bending, JSME International Journal, Series A (Solid Mechanics and Material Engineering), 2003; 46: 68-75.

[23] ASTM-D2095, Tensile strength of adhesive by means of bar and rod specimens, ASTM International, 2008.

[24] ASTM-C633, Adhesion or cohesion strength of thermal spray coatings, ASTM International, 2008.

[25] M. Watanabe, S. Kuroda, K. Yokoyama, T. Inoue and Y. Gotoh, Modified tensile adhesion test for evaluation of interfacial toughness of HVOF sprayed coatings, Surface & Coatings Technology, 2008; 202: 1746-1752.

[26] M. V. Babu, R. K. Kumar, O. Prabhakar and N. G. Shankar, Fracture mechanics approaches to coating strength evaluation, Engineering Fracture Mechanics, 1995; 55: 235-248.

[27] ASTM-D4541-09, Pull-off strength of coatings using portable adhesion testers, ASTM International, 2009.

[28] DeFelsko, Positest adhesion tester, 2006.

[29] D. G. Lee and B. C. Kim, Investigation of coating failure on the surface of a water ballast tank of an oil tanker, Journal of Adhesion Science and Technology, 2005; 19: 879-908.

[30] B. J. Chisholm, D. C. Webster, J. C. Bennett, M. Berry, D. Christianson, J. Kim, B. Mayo and N. Gubbins, Combinatorial materials research applied to the development of new surface coatings VII: an automated system for adhesion testing, Review of Scientific Instruments, 2007; 78.

[31] R. Lacombe, Adhesion measurement methods: theory and practice, CRC Press, Boca Raton FL, 2006.

[32] E. E. Gdoutos, Fracture mechaincs: an introduction, 2005.

[33] W. F. Hosford and R. M. Caddell, Metal forming mechanics and metallurgy ,Cambridge University Press, 2007.

[34] AutoSteel-Partnership, Different forming modes can be simulated by different simulative tests, http://www.a-sp.org/database/viewsec.asp?sec=246, Accessed February 2010.

[35] D. A. Dillard, B. Chen, T. Chang and L. Yeh-Hung, Analysis of the notched coating adhesion test, J Adhesion, 1999; 69: 99-120.

[36] J. Schaufler, K. Durst, O. Massler and M. Goken, In-situ investigation on the deformation and damage behaviour of diamond-like carbon coated thin films under unaxial loading, Thin Solid Films, 2009; 517: 1681-1685.

[37] M. Brieu, J. Diani and N. Bhatnagar, A new biaxial tension test fixture for uniaxial testing machine - a validation for hyperelastic behavior of rubber-like materials, Journal of Testing and Evaluation, 2007; 35: 364-372.

[38] N. Bhatnagar, R. Bhardwaj, P. Selvakumar and M. Brieu, Development of a biaxial tensile test fixture for reinforced thermoplastic composites, Polymer Testing, 2007; 26: 154-161.

[39] J. Cao, X. Wang and F. J. Mills, Characterization of sheet buckling subjected to controlled boundary constraints, Journal of Manufacturing Science and Engineering, 2002; 124: 493-501.

[40] D. R. Shouler and J. M. Allwood, A novel sample design for formability testing in pure shear, ICTP 2008 (The 9th international conference on technology of plasticity), 2008; 1246-1251.

[41] K. Yosida, J. Hayashi and M. Hirata, Yosida buckling test, IDDRG, 1981; Kyoto, Japan.

[42] X. Wang and J. Cao, On the prediction of side-wall wrinkling in sheet metal forming process, International Journal of Mechanical Sciences, 2000; 42: 2369-2394.

[43] J.-K. Kim and T.-X. Yu, Forming and failure behavior of coated, laminated and sandwiched sheet metals: a review, Journal of Materials Processing Technology, 1997; 63: 33-42.

[44] H. F. Nied, Mechanics of interface fracture with applications in electronic packaging, IEEE Transactions on Device and Materials Reliability, 2003; 3: 129-143.

[45] M. L. Williams, The stress around a Fault or Crack in Dissimilar Media, Bulletin of the Seismological Society of America, 1959; 49: 199-204.

[46] F. Erdogan, Stress distribution in bonded dissimilar materials with cracks, Journal of Applied Mechanics, 1965; June: 403-410.

[47] J. R. Rice, Elastic fracture mechanics concepts for interfacial cracks, Transactions of the ASME. Journal of Applied Mechanics, 1988; 55: 98-103.

[48] J. Dundurs, Edge-bonded dissimilar orthogonal elastic wedges, Journal of Applied Mechanics, 1969; 36: 650-652.

[49] J. R. Rice and G. C. Sih, Plane problems of cracks in dissimilar media, Transactions of the ASME. Journal of Applied Mechanics, 1965; June: 418-423.

[50] S. Zhigang and J. W. Hutchinson, Interface crack between two elastic layers, International Journal of Fracture, 1990; 43: 1-18.

[51] J. W. Hutchinson and Z. Suo, Mixed Mode cracking in layered materials, Advance in Applied Mechanics, 1992; 29: 63-191.

[52] C. H. Wang, Fracture of interface cracks under combined loading, Engineering Fracture Mechanics, 1997; 56: 77-86.

[53] L. Banks-Sills and D. Ashkenzai, A note on fracture criteria for interface fracture, International Journal of Fracture, 2000; 103: 177-188.

[54] L. Banks-Sills, N. Travitzky, D. Ashkenazi and R. Eliasi, A methodology for measuring interface fracture properties of composite materials, International Journal of Fracture, 1999; 99: 143-160.

[55] V. Tvergaard, Resistance curves for mixed mode interface crack growth between dissimilar elastic-plastic solids, Journal of the Mechanics and Physics of Solids, 2001; 49: 2689-2703.

[56] V. Tvergaard and J. W. Hutchinson, The influence of plasticity on mixed mode interface toughness, Journal of the Mechanics and Physics of Solids, 1993; 41: 1119-1135.

[57] V. Tvergaard and J. W. Hutchinson, The relation between crack growth resistance and fracture process parameters in elastic-plastic solids, Journal of the Mechanics and Physics of Solids, 1992; 40: 1377-1397.

[58] R. v. Tijum, W. P. Vellinga and J. T. M. D. Hosson, Adhesion along metal-polymer interfaces during plastic deformation, Journal of Material Science, 2007; 42: 3529-3536.

[59] M. J. van den Bosch, P. J. G. Schreurs and M. G. D. Geers, On the prediction of delamination during deep-drawing of polymer coated metal sheet, Journal of Materials Processing Technology, 2009; 209: 297-302.

[60] M. J. van den Bosch, P. J. G. Schreurs and M. G. D. Geers, Identification and characterization of delamination in polymer coated metal sheet, Journal of the Mechanics and Physics of Solids, 2008; 56: 3259-3276.

[61] A. G. Evans, J. W. Hutchinson and Y. Wei, Interface adhesion: effects of plasticity and segregation, Acta materialia, 1999; 47: 4093-4113.

[62] H. H. J. Rösler, M. Bäker, Mechanical behaviour of engineering materials: metals, ceramics, polymers, and composites, 2007.

[63] J. S. I. M. Ward, The mechanical properties of solid polymers, 2004.

[64] Matweb, www.Matweb.com, 2009.

[65] SIMULIA, Abaqus 6.6, 2006.

[66] D. M. Barnett and R. J. Asaro, Fracture mechanics of slit-like cracks in anisotropic elastic media, Journal of the Mechanics and Physics of Solids, 1972; 20: 353-366.

[67] H. Gao, M. Abbudi and D. M. Barnett, Interfacial crack-tip field in anisotropic elastic solids, Journal of the Mechanics and Physics of Solids, 1992; 40: 393-416.

[68] C. F. Shih and R. J. Asaro, Elastic-Plastic analysis of cracks on bimaterial interfaces:Part I-Small scale yielding, Journal of Applied Mechanics, Transactions ASME, 1988; 55: 299-316.

[69] Z. Suo, Singularities, interfaces and cracks in dissimilar anisotropic media, Proceedings of the Royal Society London, 1990; A427: 331-358.

VITA

Name: Yu-Hsuan Huang

Address: Department of Mechanical Engineering, 3123 TAMU, College Station TX 77843-3123

Email Address: yhhuang26@neo.tamu.com

Education: B.S., Naval Architecture and Marine Engineering, National Cheng Kung University, Taiwan, 1998
M.S., Power mechanical engineering, National Tsing Hua University, Taiwan, 2000
Ph.D., Mechanical Engineering, Texas A&M University, 2010